Cdc37's C Terminal Platform Stabilized by Hectd3 in Complex with Raf1 and Hsp90, Visualized by Cryo-EM

by

Carlos Nowotny

DISSERTATION

Submitted in partial satisfaction of the requirements for degree of

DOCTOR OF PHILOSOPHY

in

Biochemistry and Molecular Biology

in the

GRADUATE DIVISION

of the

UNIVERSITY OF CALIFORNIA, SAN FRANCISCO

Approved:

DocuSigned by:
Carol Gross
F2413DA7F84F46A...

Carol Gross

Chair

DocuSigned by:
David A. Agard

David A. Agard

DocuSigned by:
John D Gross
C876331A93DC4B1...

John D Gross

Committee Members

Dedication

For my grandmother, my mother and my wife.

Acknowledgements

I would like to thank Dr. David Agard for his continuous patience & support throughout this project. I would like to also thank the members of my committee Dr. John Gross and Dr. Carol Gross for their support and stimulating discussions which assisted in guiding this project.

I would like to thank all members of the Agard lab. Their continual support when both scientific, technical, and emotional allowed me to grow as scientist and as a person throughout my tenure. I wish to thank friends and colleges outside of the lab for their fresh perspective on scientific problems as well as hurdles that test us outside of science.

I would like to thank my friends outside of UCSF who continually supported my scientific ambitions while enriching my growth in my identity outside of being a scientist.

I thank my family who supported me throughout changes in countries, languages, and schools.

I would like to thank my grandmother, my mother and my wife. They all have given me prime examples of strength, competitiveness, and never wavering love. Your example of strength is what allows me to find it within myself.

Contributions

I would like to thank Klim Verba, Maru Jaime-Garza, Mario Tabios, and Daniel Coutandin for their insight and their collaboration in performing experiments.

Epigraph

One of the things I learned the hard way was that it doesn't pay to get discouraged.

Keeping busy and making optimism a way of life can restore your faith in yourself.

-Lucille Ball

Abstract

Hsp90 is a well conserved and highly expressed molecular chaperone that interacts with 10% of the proteome to facilitate folding and activation. These interacting partners, dubbed clients, interact with Hsp90 throughout their entire lifetime and not just in the stages of initial folding. This continual interaction with this clientele makes Hsp90 a hub of proteostasis regulation which includes folding, activation, and degradation triage decisions. The E3 ubiquitin ligase Hectd3 has been shown to degrade Raf1 in an Hsp90 dependent manner. Here we show Hectd3 in complex with Hsp90:Cdc37:Raf1 in a closed Hsp90 state. Hectd3 reveals a C-terminal platform on Cdc37 providing a potential scaffold for Hectd3 ubiquitination. We show Hectd3 can mono ubiquitinate the kinase domain of Raf at multiple lysine positions, when Hsp90 is not in a molybdate trapped closed protective state. This mono ubiquitination of Raf1 upon Hsp90 opening could potentially bias the kinase toward a degradative end with other E3 ligases performing polyubiquitination needed for Raf to be processed by the Ubiquitin Proteasome System (UPS).

Table of Contents

List of Figures

Introduction

Proteins & Proteostasis

At the heart of every complex physiological process lie proteins that must interact and work together to better accomplish a goal. Proteins are chains of amino acids whose folding into a three dimensional shape is under kinetic and thermodynamic control [1]. A protein's three-dimensional shape gives rise to the protein's function. Protein can serve as structures of support such as collagen or actin, enzyme protein which catalyzes specific reaction, or receptors and signal transduces in cellular signaling pathways. This goal could be to support structure such a collagen which makes up our connective tissue. Bind to a molecule of capsaicin which allows your body to recognize that something is spicy. Other proteins are important in cellular signaling pathways that allow cells to grow and differentiate.

With proteins responsible for so much in the body it is very important to have a system to ensure that proteins are healthy and functioning correctly. Our body's complete collection of proteins is known as our proteome. Proteostasis is our body's process of maintaining proper balance and function of every single protein[2]. This balance ensures that specialized proteins such as receptor proteins are only made and maintained in cells that need them, while proteins that are responsible for more basic function, such as cellular respiration, cell division, cell metabolism and cell signaling are made and maintained in all cells. Proteostasis ensures proteins are synthesized in the right place, at the right concentration, at the right time depending on external stimuli or challenges.

Proteostasis also ensures that proteins that are no longer needed by the cell or have been damaged past the point of refolding are removed. One way to do this is via the Ubiquitin Proteasome System (UPS). Proteostasis can mark proteins for degradation by adding a chain of small proteins called ubiquitin[3].

Prosteostasis's ability to maintain proper balance and function is driven by a complex network of interconnected chaperones that make up the protein triage system. It is this triage system that allows proper partitioning of proteins down a pathway that is beneficial to the cell. Be it initial folding, refolding of a denature or semi-denatured intermediate, or the degradation of other proteins.At the crux of this protein triage system lies Hsp90

Hsp90

While the molecular mechanism of Hsp90 triage is incompletely understood, we appreciate that Hsp90 is a hub for regulation[4]. Hps90 can be regulated by a diverse set of co-chaperones, and post translations modifications.

In the cell Hsp90 exists as a dimer. It's ability to bind and hydrolyze ATP allows it to cycle and sample through a wide array of conformational states. These conformational and nucleotide states can be modulated by an array of cochaperones like Aha1 and p23[5].

Hsp90's clientele is not only vast, it interacts with 10% of the proteome but it is enriched for very important signaling molecules that have roles in steroid signaling, the heat shock response and signal transduction and tumorigenesis[6] (Fig 1).

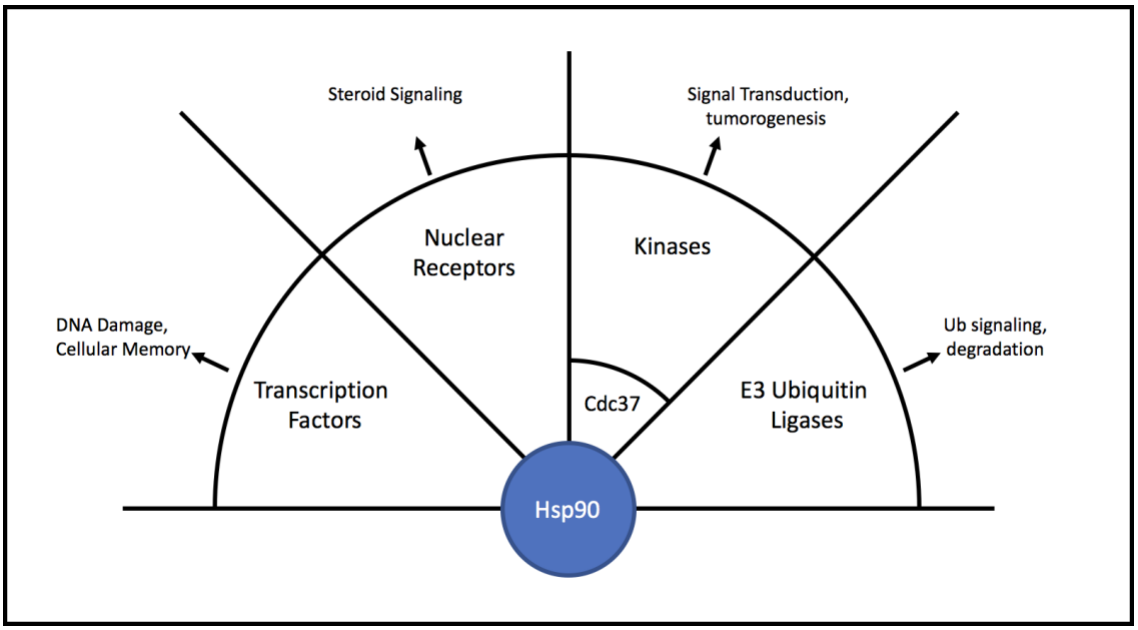

Figure 1 Hsp90 is a Hub for the Regulation of Important Signaling Factors
Adapted from (Taipale, M., Jarosz, D. F., & Lindquist, S. (2010).. *Nature reviews Molecular cell biology*.)

The class of clients that are important nodes in cellular signal transductions are kinases. Kinases are a class of enzymes that catalyze the transfer of a phosphate group from ATP to proteins. This modification can alter protein activity, interaction or localization. This impacts cell growth, metabolism and signal transduction and proper function going awry can lead to disease[7]. We cannot understand Hsp90's relationship with kinases without introducing Cdc37.

Cdc37

Cdc37 is an adaptor-like protein that allows all of Hsp90's kinase clients to be properly chaperoned. Several studies have shown the important role of Cdc37 in Kinase loading onto Hsp90[8]. Studies have shown that Cd37 can stabilize kinases by a mechanism that is not dependent on its interaction with Hsp90 but can not compensate for the loss of Hsp90 activity[9].

The N-terminus of Cdc37 is responsible for the recognition of the C-lobe of kinases and is the most conserved across evolution. S13 and 20HPN22 are responsible for interacting with the C-terminal lobe of kinases including Cdk4, EGFR, Her2, bRaf and Raf1 Phosphorylation of S13 by casein kinase II (CKII) is required for kinase recognition and loading onto Hsp90[10]. Dephosphorylation of S13 by PP5 allows for kinase release[11]. Cryo EM structures of Cdc37 with Hsp90 and a kinase have shown the kinase binding domain of Cdc37 is followed by a coiled coil that extends away from the complex and then with a beta sheet strap that interacts with Hsp90[12–14]. NSAID-mediated de-phosphorylation of Cdc37's coiled coil at S97 inhibits Cdc37-Hsp90 interactions and leads to the eventual degradation of the kinase AXL via the E3 ligase CHIP and UPS (Pan et al 2008).

In EM structures in complex with a "closed" Hsp90, the Cdc37 the middle domain appears as a globular alpha helical bundle that interacts with Hsp90 and stabilizes the n terminus of the kinase that is threaded through the Hsp90 lumen. This interaction can provide Cdc37 with kinase binding specificity. Antibody binding to the aC-helix of Cdk2

has been shown to disrupt Cdc37 and Hsp90 interaction[15]. Dimerization of Cdc37 has been shown to occur via the middle domain of Cdc37[16,17].

The middle domain which has structural homology to the co-chaperone Cdc7L1[18] can bind to Hsp90 in different places depending on Hsp90 conformational state (Eckl 2013[19]). In an "open" Hsp90 state the middle domain has been shown to bind to the N-terminal ATP binding domain of Hsp90[16].

Far less structurally is known about the C-terminus of Cdc37. NMR work has shown it to assemble as a 4 helical bundle and that the C-terminus is responsible for assisting the N-terminus in stabilizing kinases. This portion is also necessary for Cdc37 to sample a transiently closed state that allows for the proper loading of kinases onto Hsp90[8]. Work in the Gelis and Neckers labs show that phosphorylation at Y298 results in the partial unfolding of the C-terminal domain. This unfolding facilitates the docking of tyrosine kinases via their SH2 domains. This docking site facilitates the phosphorylation of Hsp90 on Y197 which results in the dissociation of Cdc37, which affects the chaperoning of kinase clients. They show Cdc37 serves not simply as client recruiter but also as a modulator of Hsp90 post translational modifications and chaperoning in a client class specific manner[20,21].

Interestingly in all current structures that include Hsp90, kinases and Cdc37 this C-terminal portion of Cdc37 is too heterogeneous to be visualized via cryo-EM and has been limited to NMR structures. The remaining c-terminal sequence beyond the 4

helical bundle shown in NMR exists as an unstructured tail according to the AlphaFold predicted model. One of Cdc37's most studied kinase bidding partners if cRaf or Raf1.

Raf1

Raf1 is a very important module in the RAS/MAP kinase pathway[22].This pathway is responsible for bridging growth signals from outside of the cell to effectors in the nucleus that control cellular growth, differentiation, migration, and survival[23] The signal begins with receptor tyrosine kinases (RTKs) at the cell surface that then activate RAS proteins , which in turn activate the MAP kinase cascade, which is made of three protein kinases, Raf, Mek, and Erk[24–26]. There are three RAF proteins in vertebrates, aRaf, bRaf and cRaf or Raf1.

All Rafs share a common domain structure that includes the Rad binding domain (RBD) and a cysteine-rich domain (CRD) in their N-terminal region and a C-terminal protein kinase domain. The RBD binds GTP-bound Ras and is critical for recruitment and activation. The CRD is critical for membrane binding to phosphatidylserine[27]. Dysregulation of the Raf pathway is observed in developmental disorders and cancers [28–31].

Hsp90 and Cdc37 are required for all Raf functions[32,33] with Raf1 particularly dependent on Hsp90 and Cdc37[6]. Structures of bRaf complexes in both an autoinhibited as well as active state have been resolved [34–37].Structures of Raf bound to Hsp90 and Cdc37 have given us a look into Raf regulation by hsp90 and its co-chaperones [13,38,39].

Raf1's greater dependence on the Hsp90-Cdc37 chaperone system arises from its instability as opposed to a specific recognition motif that Cdc37 or Hsp90 recognize with more fidelity than bRaf or aRaf. A study using hydrogen deuterium exchange showed breathing motions of the N-lobe of the kinase partially expose the kinase segment that will be threaded through the Hsp90 lumen. It is these client dynamics that poise the kinase for chaperone dependence.

14-3-3 are scaffolding proteins that bind to pS259 and pS621 on Raf1, keeping it in an inactive protected state in the cytosol. Hsp90 and Cdc37 promotes S621 phosphorylation. One group surprisingly found in cells Raf phosphorylated at s621 remained insensitive to Hsp90 and Cdc37 inhibition. They conclude that S621 is a maker for Raf1 maturity. This "mature" version of Raf1 remains insensitive to Hsp90 mediated degradation[40]. Li and colleagues soon after identified Hectd3 the ubiquitin ligase responsible for Hsp90 mediated degradation of Raf1. They verified a 4 component complex formed in cells via the use of a proximity ligase assay, and by making stable cell lines of Hectd3 and performing pull downs showed that Hectd3 pulled down with Hsp90, Raf and Cdc37[41]. We set out to better understand how Hectd3 could interact with the Hsp90 Cdc37 Raf system.

Hectd3

We have an incomplete understanding of how Hsp90 client kinases are degraded. Previous work has elucidated some of the major players responsible. It has been known

for a while that if Hsp90 is inhibited its clients will be degraded[32] Previous work in our lab showed that inhibitors enrich an open state of Hsp90.

Hectd3 is part of a larger ubiquitin modification system that encapsulates E1 E2 and E3 enzymes. E1s are ubiquitin activating enzymes, E2s are ubiquitin conjugating enzymes and E3s are molecules that really substrate specificity. E3 ligases can be further broken down into RING U-box, RBR and Hect E3 ligases[42]. HECT E3 ligase strand apart from other E3's in their ability to form a thioester intermediate and directly ubiquitylate their substrates. All HECT E3 ligases contain the same catalytic domain, their substrate specificity is determined by their N-terminal recognition domain. Though small in their number compared to other E3 ligases HECT ligases have been implicated in several diseases[43]. The 15 members of the HECT E3 family can further be classified into the NEDD or HERC family. NEDD4 family members all contain a Ca2+ binding C2 domain filled by two to fours WW domains. The HERC family is characterized by the presence of at least one regulator of chromosome condensation 1 (RCC1) domains at their n-termini. The remaining 13 members are more diverse in their recognition domain architecture and are classified as "other HECTs". HECTD3 falls into this "other" family, the only domain it has outside of its catalytic HECT domain is a DOC domain that contains homology to APC10, a processivity factor of the anaphase promoting complex[44]. There are multiple processes that regulate Hectd3 activity including PTMs, inter and intramolecular interactions, adaptor protein binding and DUB interactions[45].

Laurence Pearl's lab identified Hectd3 as the E3 ubiquitin ligase responsible for the Hsp90 mediated degradation of Raf1[41]. In addition, it also showed that Hectd3 also was responsible for the degradation of LBK1 and MASTL to a lesser degree. Hectd3 has several known substates for ubiquitination, these include Raf1 and Tara[46] who are then degraded. It ubiquitinated several other substrates in a non degradative fashion including Syntaxin 8, MALT1, Caspase 8 & 9, TRAF3 and stat3[47–52].

Hectd3 can be broken up into two portions. A catalytic domain and a recognition domain. It is unknown how Hectd3 recognizes its substrates, as Hectd3 substrates do not share a common recognition motif of degron. Hectd3 pulldown and ubiquitination of both Raf and Tara are eliminated with the deletion of its N-terminal recognition domain.

The recognition domain architecture is made up of Linker-DOC-Linker. The DOC domain has homology to APC10, a processivity factor of the anaphase promoting complex. In the anaphase promoting complex APC10 prevents the dissociation of substrates so they may be poly ubiquitinated[44].It is our hypothesis that Hsp90 presents Raf1 to Hectd3 for ubiquitination and subsequent degradation. Alpha fold co-folding experiments paint an incomplete picture as to what could potentially be being recognized by Hectd3 (Fig 2).

Project Aims

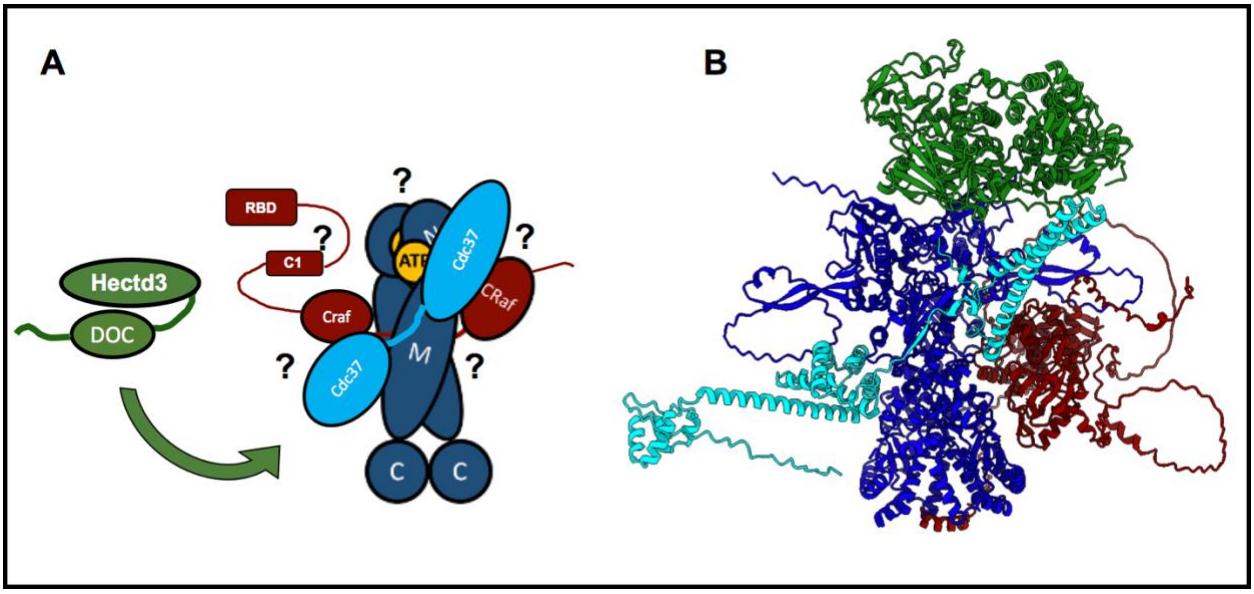

Figure 2 Alphafold Co-folding of Hsp90:cdc37:Raf1 and Hectd3

A. Schematic Cartoon showing potential Hectd3 Binding Sites
B. Alpha-Fold 3 co-folding of full length Cc37(cyan) Hsp90 dimers (blue) Raf1(red) and Hectd3 (green) fail to reveal one robust binding module

At the onset of this project I set out three goals. The first was to optimize the purification of Hsp90:Cdc37:Kinase complexes. The second was to optimize conditions to stabilize a 4 component complex with Hectd3. Thirdly I wanted to establish an in vitro ubiquitination assay to understand mechanistically how Hectd3 ubiquitinates Raf1 in an Hsp90 mediate manner. Broadly this project aspires to leverage Cryo-EM and *in vitro* biochemistry to better understand how these four proteins are interacting and give us insight into how Hsp90 triage decisions can be biased toward a degradative end. This has tremendous implications from a basic science standpoint as well as a therapeutic standpoint as a better understanding into how kinases are chaperoned gives us insight

into what goes awry in maladies such as cancer where kinases such Raf1 are unchecked and overly active.

Plasmid Construction & Rational

Implementation of a polycistronic expression vector was utilized to achieve stoichiometric expression of all proteins in an expression cassette[53]. This vector utilizes a P2A peptide between proteins of interest in a single mRNA transcript. 2A peptides act as “self-cleaving” causing ribosomes to skip a peptide bind in translation effectively separating the proteins (Fig3). The mechanism of 2A mediated cleavage stems from ribosomal skipping the formation of the glycl-propyl peptide bond at the C-terminus of the 2A sequence. The conserved sequence of GDVEZNPGP is responsible for the steric hindrance that prevents peptide bond formation and ribosomal skipping. Though this ribosomal skipping is highly efficient it does not occur at every single 2A site. Unsuccessful skipping leads to the formation of a fusion protein. There are also instances where there is successful ribosome skipping but the ribosome falls off and there is discontinued translation, resulting in only the expression of the protein upstream of the 2A sequence. Variation in expression temperature, inducer concentration, cell density, did not seem to make a difference in the amount of P2A read throughs that were observed. All read-throughs represented less than 10% of the total protein expressed. The manipulation of all expression cassettes was done with Gibson molecular cloning utilizing NEB Gibson Assembly Protocol[54](citation). Primers were

designed utilizing their NEBuilder online interface and checked for correctness manually using Snapgene(from Dotmatics; available at snapgene.com).

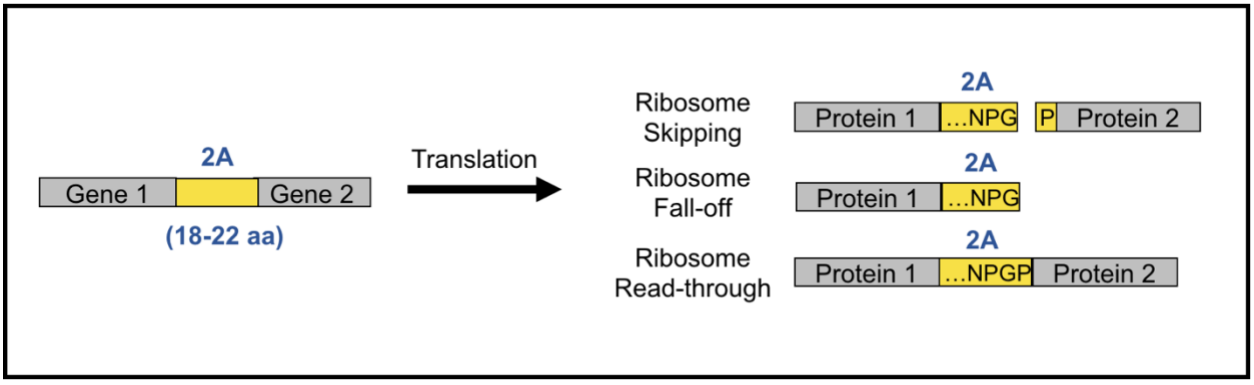

Figure 3 Schematic of Possible 2A Gene Outcomes

2A Expression cassettes results in stoichiometric expression of all genes in the cassette through ribosome skipping. Ribosome fall-off and ribosome read-throughs lead to a small percentage of polypeptide chimeras

Biochemical Characterization of Kinase complexes and Hectd3

A previously used protocol for the purification of Hectd3 was adapted for the materials available in the lab[2,3]. The main differences were the use of Nickel resin instead of TALON resin and change in dialysis and cleavage conditions.. Dialysis and cleavage overnight into a 150 mM NaCl buffer lead to a lot of visible protein aggregation. TEV cleavage at 500 mM NaCl overnight led to complete cleavage and considerably reduced protein aggregation.

Association between Hectd3 and the Cdc37-cRaf-Hsp90 complex is very transient. Previously established methods in the lab utilized a yeast system to purify Hsp90-kinase complexes. Kilm Verba had previously used these to purify and solve the structure of Hsp90 Cdc37 and CDK4[12]. This structure was novel in that it showed Hsp90 splitting the two lobes of a kinase, threading a partially unfolded bit of the n terminus through the lumen. While it was uncertain at the beginning of the project, if this was the state of Hsp90 that is responsible for presentation of Hectd3 it is where we began our inquiry.

Utilizing a yeast polycistronic 83-nu expression vector the kinase domain of Raf1 was expressed and purified utilizing the same protocol Klim was able to use for CDK4.

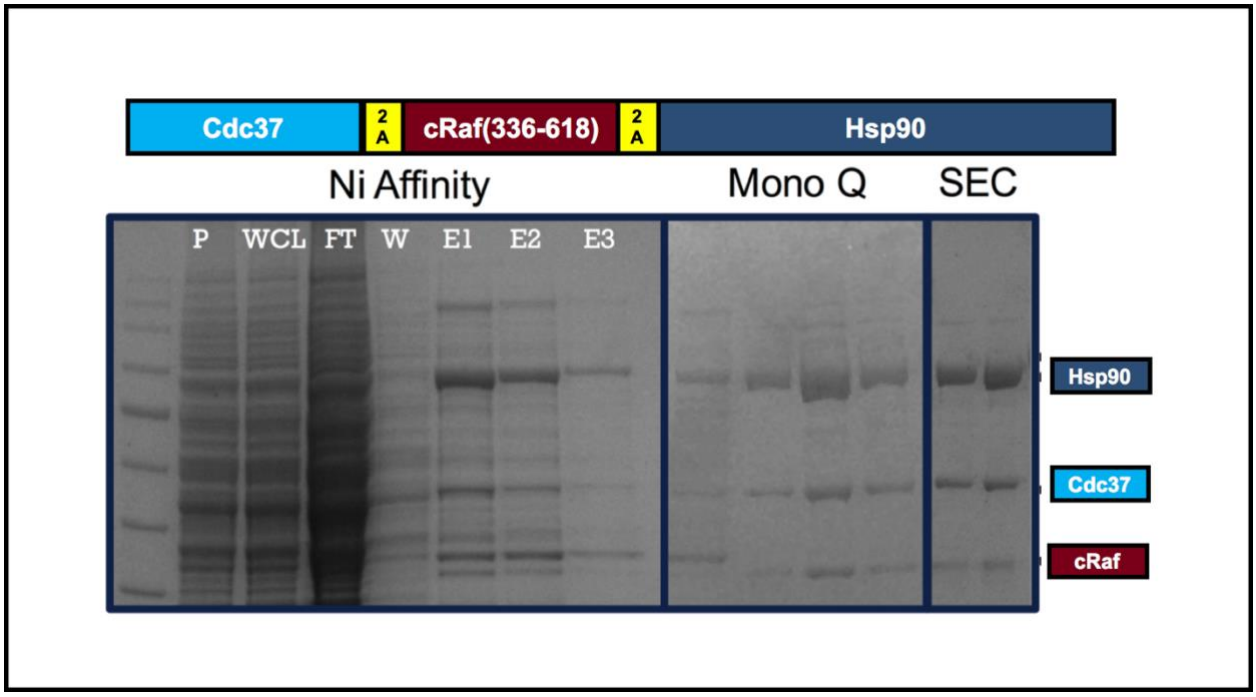

Figure 4 Purification of Hsp90:Raf1$_{KD}$:Cdc37

Hsp90β, Cdc37 Raf1$_{KD}$ complexes were purified from yeast in both a Hsp90 open state and an Hsp90 closed state. Molybdate, a phosphate analog, stabilizes an ATP-like closed state of Hsp90. Open state Hsp90 complex are purifies sans Molybdate.

Raf1 is a more thermally unstable kinase that added some difficulty to the prep especially for preps that did not include molybdate in the purification process. Purifications without molybdate allowed Hsp90 to open and we would always see increasingly lower yields compared to an Hsp90 that closed and protected the kinase throughout the purification steps.

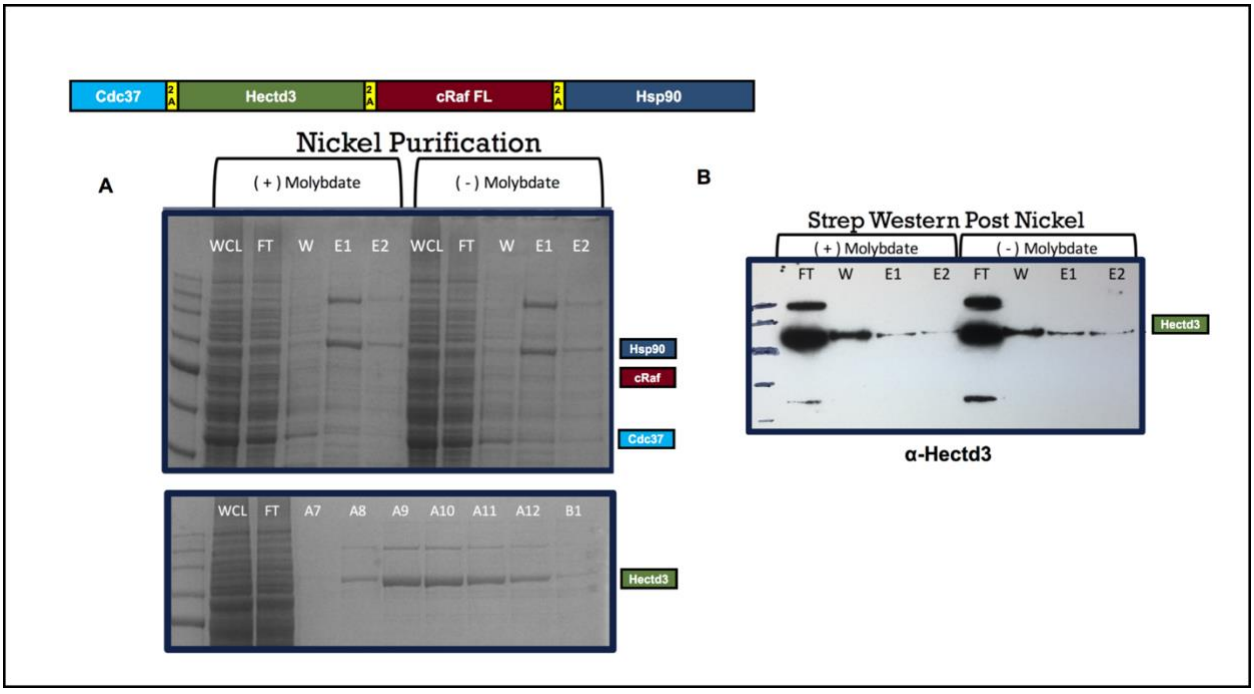

Figure 5 Hectd3 Transiently Interacts with Hsp90:Raf1$_{KD}$:Cdc37

A. Hsp90β, Cdc37, and cRAf (KD) can be expressed and purified, while full length (FL) Raf1 has proven too transient purify in complex with Hsp90 and Cdc37 with or without molybdate. Pulling on a catalytically dead HECTD3 (C823A), did nothing to increase 4 protein complex stability.
B. Western blot analysis revealing the Hectd3 transiently interacts with Hsp90:Raf1$_{KD}$:Cdc37, but its interactions are not strong enough to survive bulk purification

Yeast cells were transfected with Cdc37:Raf1:Hectd3:Hsp90. Pull downs were performed on Hsp90 and Hectd3 in an attempt to capture a quaternary complex containing all 4 components. Pulling on Hsp90 yielded a three-component complex while pulling on Hectd3 only resulted in Hectd3 being isolated. Western blotting on the hsp90 pull downs revealed minute amounts of Hectd3 (Fig 5). We concluded that Hectd3 binds transiently to the Cdc37:Raf1:Hsp90 complex.

Attempting in vitro binding of Cdc37:Raf1:Hsp90 did not yield a stable complex over an analytical column. The analytical column revealed that Hectd3 forms higher order complexes in high enough concentrations. Hectd3's DOC domain does not dimerize at concentrations at or below 30μM, it by itself also does not form a stable complex with Cdc37:Raf1:Hsp90 (Fig 6,7).

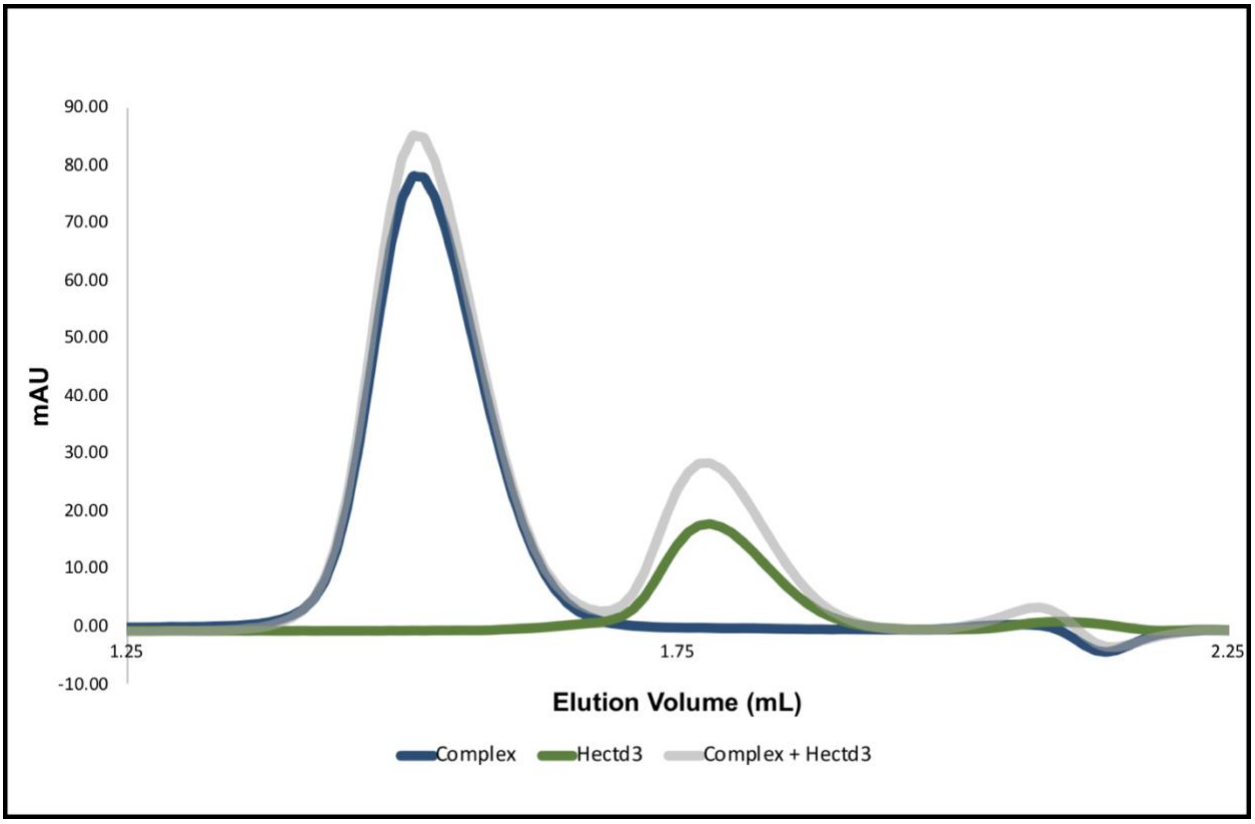

Figure 6 Hectd3 Fails to Associated with Hsp90:Raf1$_{KD}$:Cdc37 in vitro

A. Size exclusion chromatography of Hsp90:Raf1$_{KD}$:Cdc37 after being incubated with the DOC domain of Hectd3 at 20 μM Tris 7.5, 70 mM NaCl, 10 mM $MgCl_2$, $MaMo_4$, 1mM DTT

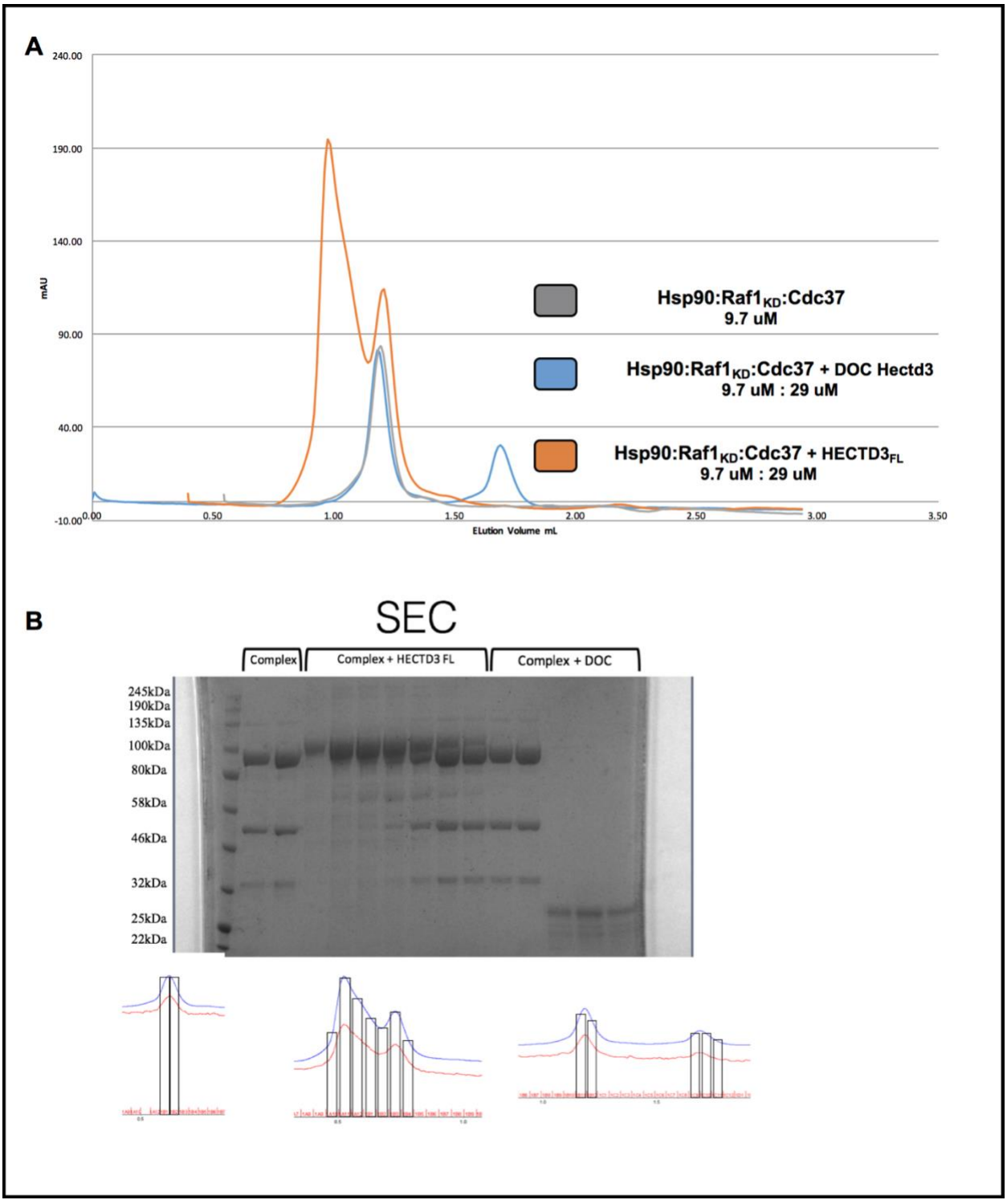

Figure 7 Hectd3 DOC Domain Fails to Form Complex with Hsp90:Raf1$_{KD}$:Cdc37 in vitro

(figure caption continued on next page)

(figure caption continued on previous page)

A. Size exclusion chromatography of Hsp90:Raf1$_{KD}$:Cdc37 after being incubated with the DOC domain of Hectd3 and Hectd3$_{FL}$ at 20μM Tris 7.5, 70 mM NaCl, 10 mM $MgCl_2$, $MaMo_4$, 1mM DTT
B. SDS-PAGE gel stained with colloidal blue showing peaks of analytical runs.

It was unclear whether with dimerization of full length Hectd3 was preventing association to Hsp90:Raf1$_{KD}$:Cdc37 complex. Within the HECT family ligases use methods of autoinhibition to prevent non-specific ubiquitination. Hectd3's dimerization is concentration dependent as dimer peaks in SEC that are reinjected run as monomers. The catalytic Hect domain when purified also has a strong propensity to dimerize. These dimers can also be stabilized by BS3 crosslinking (Fig 8). Though tangential to the association with Hsp90 these dimers were used for structural analysis.

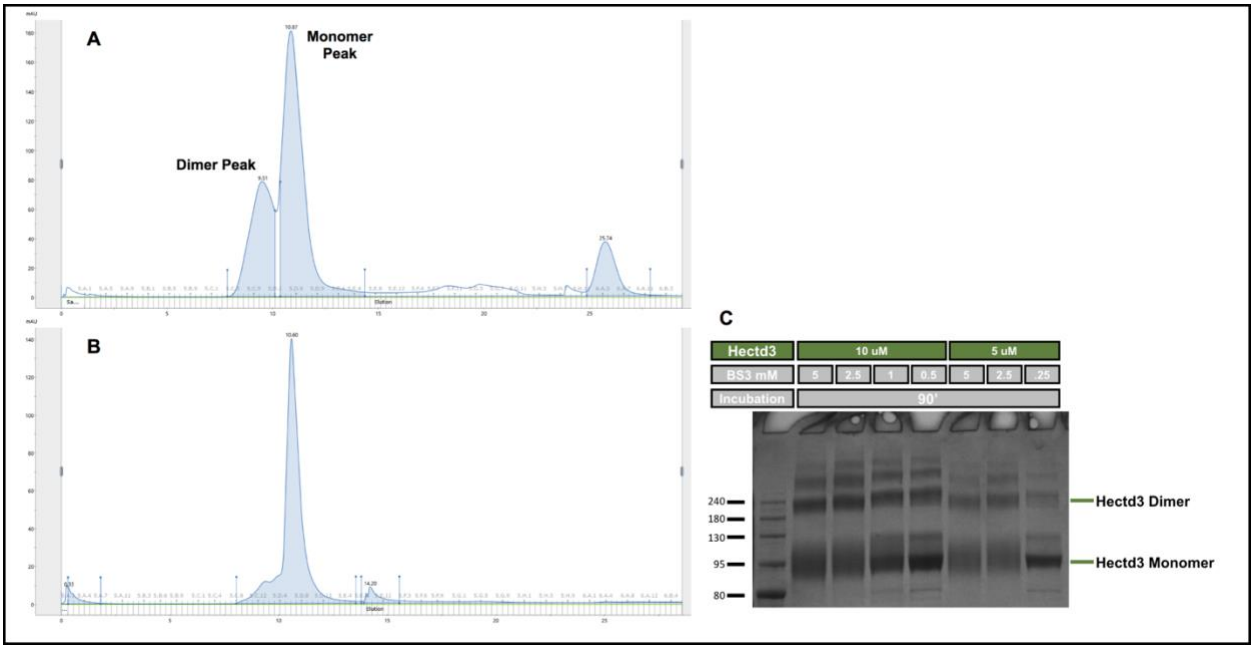

Figure 8 Hectd3 dimers can be stabilized by BS3

A. SEC chromatography of Hectd3 shows a monomer and dimer peak
B. SEC chromatography of rerun Hectd3 dimer peak that returns to the monomer peak during the dilution of subsequent runs
C. BS3 Crosslinking Reveals Hectd3 dimerization and oligomerization

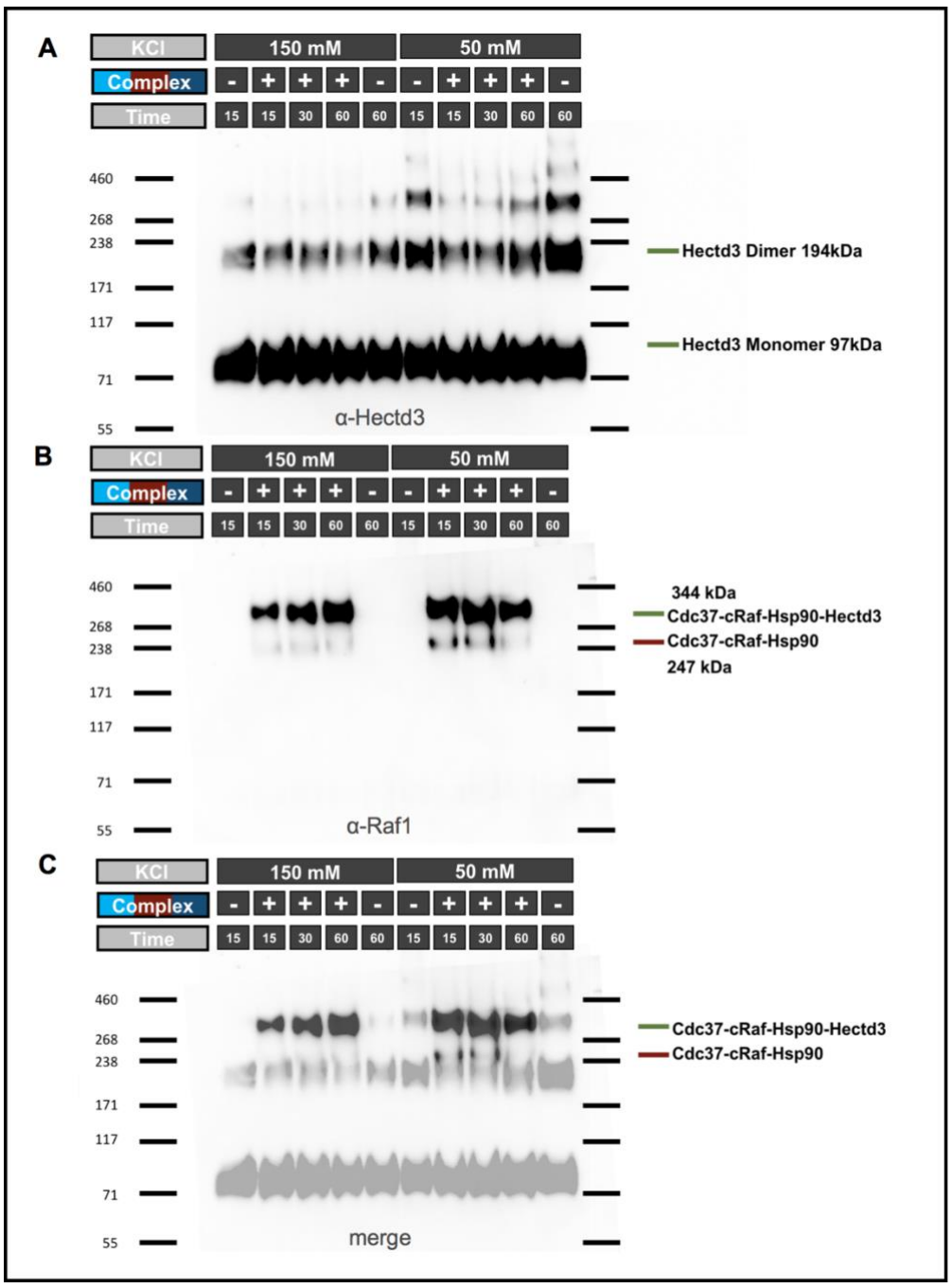

Figure 9 Hectd3 Crosslinks with Hsp90:Raf1$_{KD}$:Cdc37 as a Monomer

A. Western Blot Analysis of Crosslinking of Hsp90:Raf1$_{KD}$:Cdc37 with Hectd3. 2.85μM Hsp90:Raf1$_{KD}$:Cdc37 complex was incubated with Hectd3 at various salt concentrations and then incubated with 1.42 mM BS3 at 24 C. Blot visualizes Hectd3
B. Western Blot Analysis of Crosslinking of Hsp90:Raf1$_{KD}$:Cdc37 with Hectd3. Original blot was mildly stripped and re-probed for Raf1
C. Overlay of both blots

Crosslinking of purified Hsp90:Raf1$_{KD}$:Cdc37 with Hectd3 reveals that Hectd3 binds to the tertiary kinase module as monomer (Fig 9). The laddering of these crosslinks were verified utilizing mass photometry (Fig 10), a biophysical technique that uses light scattering to give an accurate molecular weight of particles in solution[55]

In these crosslinking experiments it became apparent that our quaternary Hsp90:Raf1$_{KD}$:Cdc37:Hectd3 crosslinked sample even after run through SEC was "contaminated" with tertiary Hsp90:Raf1$_{KD}$:Cdc37 and HEctd3 dimers and monomers.

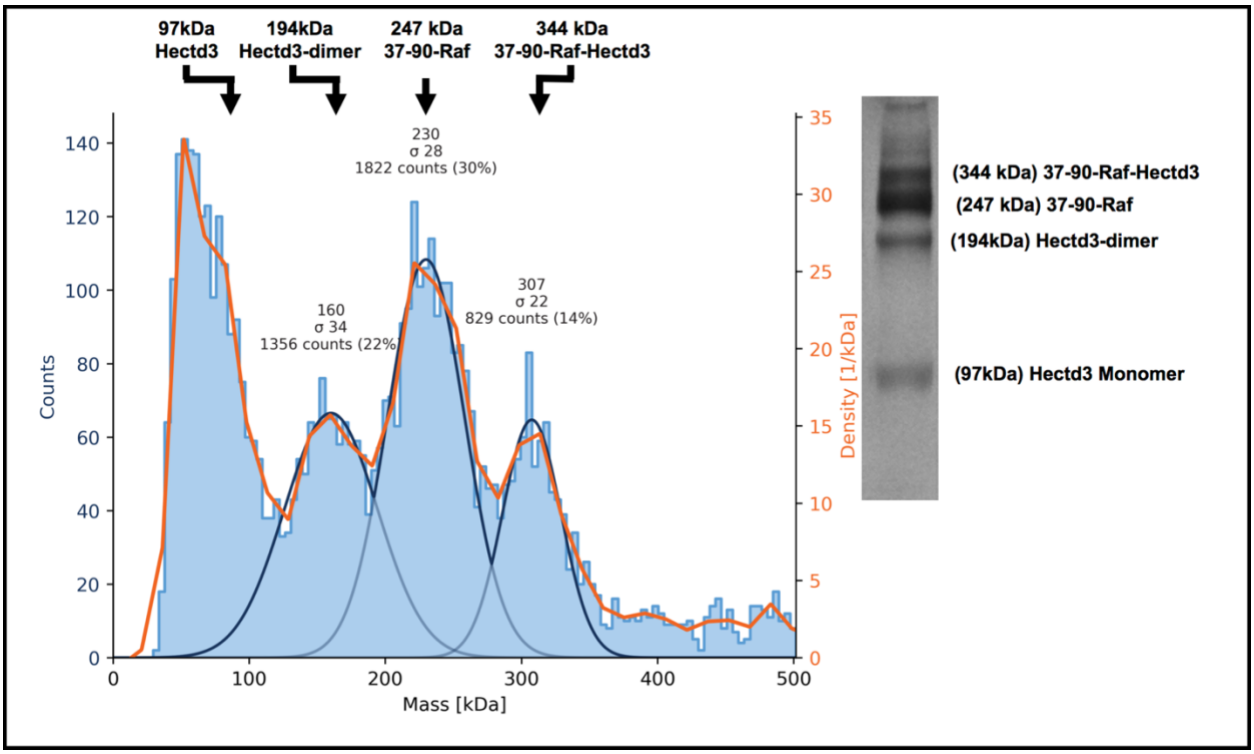

Figure 10 Mass photometry Verifies Mass of Crosslinked Hsp90:Cd37:Raf1$_{KD}$:Hectd3

A. Plot of Hsp90:Raf1$_{KD}$:Cdc37:Hectd3 crosslinked species obtained via mass photometry. Samples were crosslinked as described above and run on an S200 columns with Tris 7.5, 150 mM KCl, 1 mM DTT

Hectd3's transient association was seen though pulldowns as well as crosslinking. This gave an initial foothold from which optimization could take place. It was a distinct possibility that pulldown of Hectd3 required the full length version of the kinase. Bulk purification of a full length version was not possible in yeast as 99% of the kinase ended up in aggregates in the pullet fraction after lysis. Hectd3 binding to the Cdc37:Raf1:Hsp90 complex could also benefit from post translational modifications (PTMs) provided by expression in a mammalian system. Protein yield could also be improved utilizing a mammalian cell line that is used specifically for protein expression. We also wanted to incorporate more efficient versions of affinity tags in order to better pullout complexes of interest. With all these goals in mind I moved to optimize expression of kinase containing complexes in the Expi293 System.

Transient expression of a Clover-Raf1$_{FL}$ construct yielded visible puncta within the cells even at lower expression times and lower DNA concentrations. Although the Expi293 cells have endogenous chaperones that facilitate proper folding of overexpressed components 90% of expressed Raf1 remained in pelleted fraction post lysis (Fig 11). Addition of the Hsp90 inhibitor radicicol led to the polyubiquitination and degradation of the Raf1.

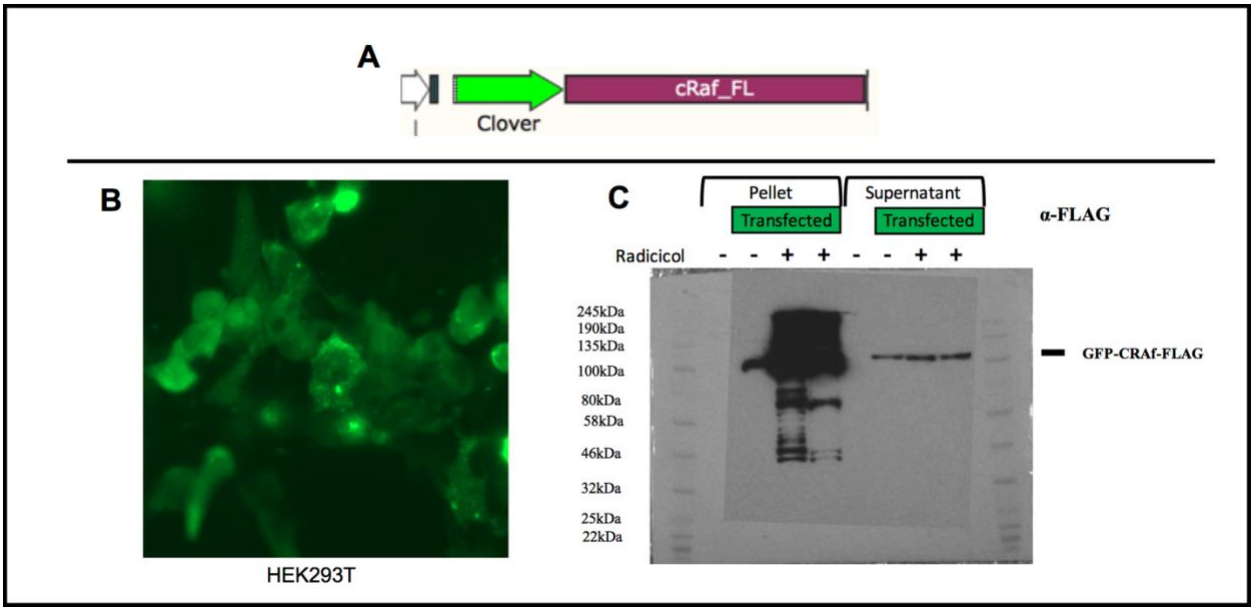

Figure 11 Transiently Over Expressed FL Raf1 Is Largely Insoluble

A. The schematic of the expression cassette used in Clover-Raf1$_{FL}$Expression. It is driven by a CMV promoter and there is a C terminal flag tag on Raf1.
B. Fluorescent imaging of Expi293 cells 24 after transfection
C. Western blot of soluble and insoluble fractions of lysed Expi293 cells treated with the Hsp90 inhibitor Radicicol

Addition of Cdc37 and Hsp90 to the expression cassette ameliorated the puncta and resulted in uniform cytoplasmic expression. Addition of a catalytically dead (823A) Hectd3 to the mammalian expression cassette yielded cells where half of the cells showed uniform expression and the other half showed severe puncta formation (Fig 12). Hectd'3 ability to oligomerize certainly contributes to this puncta formation. Overall any cells transfection with this 4 protein cassette exhibited very bad viability. After 24 hours post transfection viability was never above 60%.

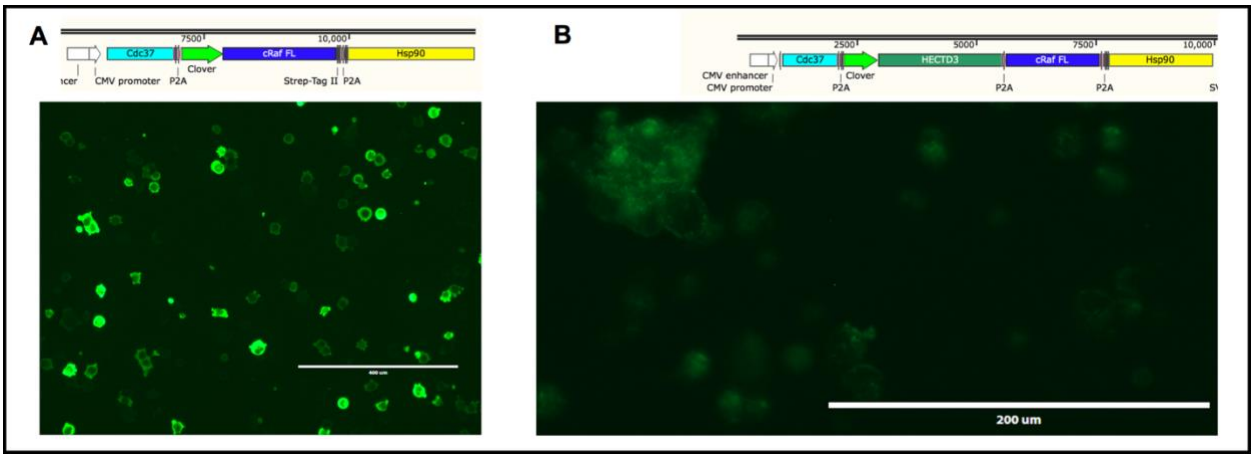

Figure 12 Hectd3 823A Overexpression with Cdc37:Hsp90:Raf1$_{FL}$ Results in Reduced Cell Viability and Expression

A. Expression cassette and fluorescent imaging of cells 24 hours post expression for Cdc37:Hsp90:Raf1$_{FL}$ construct
B. Expression cassette and fluorescent imaging of cells 24 hours post expression for Cdc37:Hectd3:Hsp90:Raf1$_{FL}$ construct

Both truncated and full-length kinase containing complexes can be purified out of Expi293 cells. A few key optimizations in the purification boosted yield and quality of complexes. The addition of a double strep tag on the Raf1 as well as the addition of 0.5% Tween during the purification gave us a huge increase in protein yield (Fig13). The non-ionic detergent served to better present the streptag of the kinase allowing better binding to the strep beads. The method of lysis was changed from emulsiflex homogenation to cryo-milling.

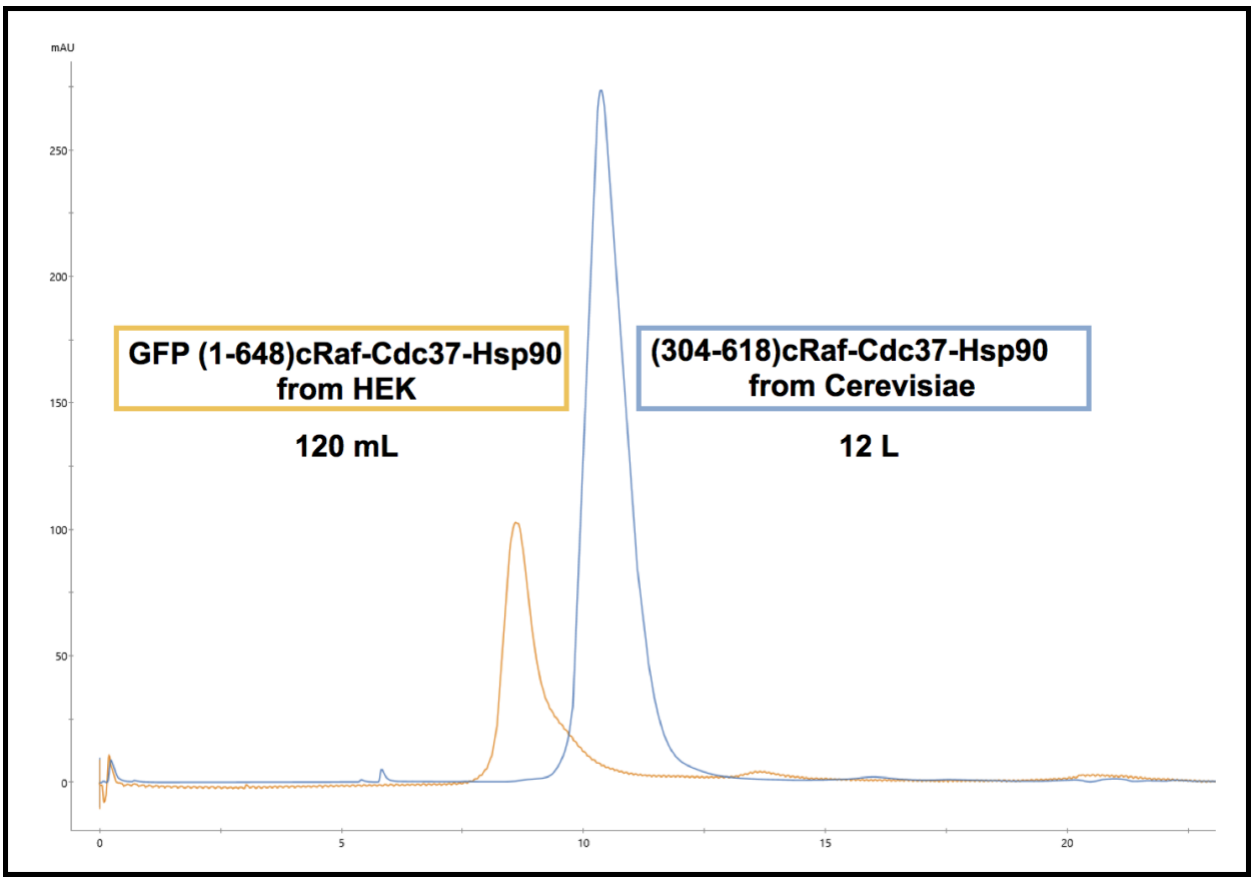

Figure 13 Expi 293 System Increase Protein Yields Compared to Yeast

Final size exclusion chromatography traces of purifications of kinase complexes in yeast (yellow) compared to Expi293 cells (blue) . Volume of media used in cell growth is denoted below the construct.

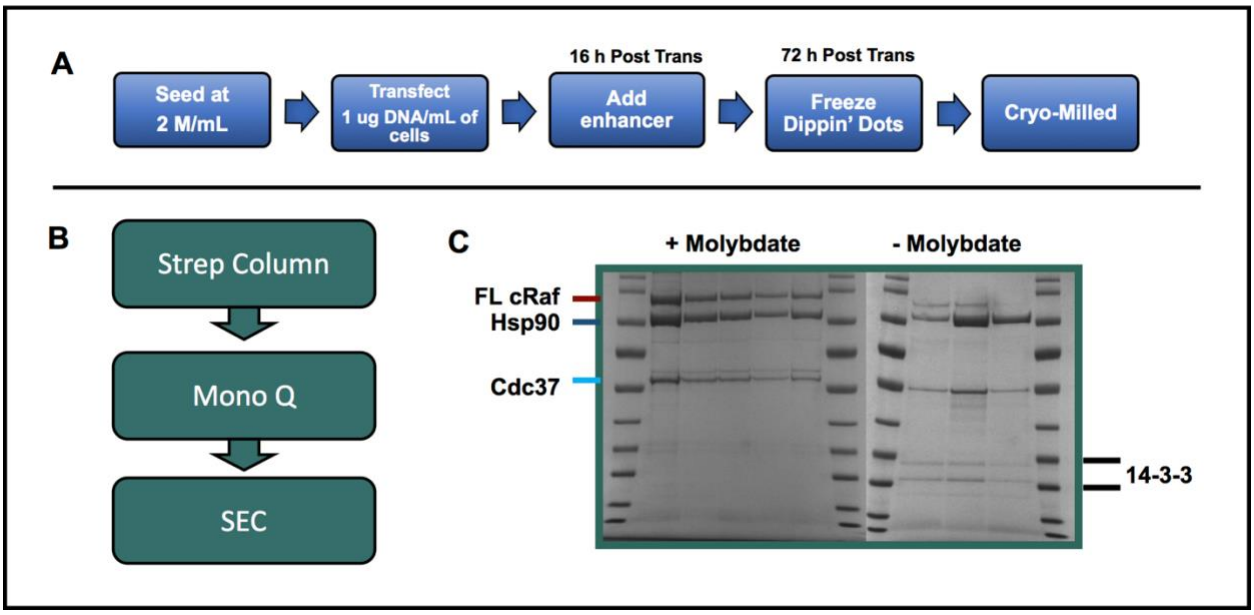

Figure 14 Cdc37:Hsp90:Raf1$_{FL}$ is purified from Expi293 Cells

A. Schematic Expi293 cell seeding and transfection protocol. Cell collection was optimized for 72 hours post transfection. Time points after 72 hours showed increase protein aggregation and decreased cell viability. After cells were pelleted they were resuspended in minimal media before being frozen dropwise into liquid nitrogen, creating cellular “Dippin’ Dots”. These “Dippin’ Dots were cryomilled before moving directly to purification.
B. Schematic of Purification for Hsp90 kinase complexes. Cell lysates wer eloaded onto a strep column using a peristaltic pump and eluted on the ettan. The purification was finished with a Mono Q and SEC step.
C. Initial Pulldown from Strep Column reveals our 3-component complex. Interestingly “Open” complexes purified without molybdate associated more with endogenous 14-3-3 proteins.

Full Length Raf1 complexes can be purified with and without molybdate (Fig 14). A small portion of 14-3-3 proteins were found in both samples but they were more present in the molybdate less purification. 14-3-3 are a group of scaffolding proteins that assist in the stabilization and activation of protein kinases. They have SH2 domains that bind to phosphorylation sites on the kinase. This differential binding of the SH2 domain

suggests that trapping Hsp90 closed with molybdate yields different states of Hsp90. These 14-3-3 proteins disappear with subsequent rounds of purification but it is possible that these varying states could yield different binding affinities to Hectd3. It was our hypothesis that Hsp90's ability to open could potentially yield varying binding interfaces potentially more amenable to HECTD3. The following sections detail how we biochemically prepared our samples for our EM dataset.

Cryo-EM Sample Preparation and Data Analysis

Cryo-EM is a powerful structural biology tool that is a major aspect of the Agard lab. Cryo-EM allows for the visualization of macromolecular complexes in their native state. After isolation and purification complexes of interest are vitrified on a cryo EM grid. The vitrification is vital as it allows for the preservation of complexes in their native solution state without being broken apart by the formation of ice crystals. Where early microscopists were limited to using natural light to visualize their samples, the invention of electrons gums have allowed us to use a more powerful radiation source to visualize our samples. The wavelength of accelerated electrons in a 300 kV microscope has a theoretical wavelength of 1.97 pM, we are no longer limited by the sampling frequency of the radiation source. Most of the deviation from the theoretical maximums that could be possible from an electron microscope come from radiation damage on the sample itself. The images collected from an electron microscope are known as micrographs. For high resolution collections several micrograph frames are collected as part of a movie. UCSF MotionCor2[56] is used here to correct anisotropic image motion across the

entire frame of the micrograph. Iterative patch-based motion detection is combined with dose weighting and these Motion corrected and dose weighted micrographs are used in subsequent analysis. This movie can then be corrected for electron beam induced motion and stage drifting. These dose-weighted micrographs contain projections of the particles frozen in the vitreous ice sheet in random orientations. In single particle electron microscopy these projections are picked from the micrograph and then extracted. These 2D projections are classified and averaged to increase the signal to noise ratio. These 2D class averages can then be used to create an ab-initio 3D reconstruction. In alternative approaches like RELION[57](REgularization LIkelihood OptimizatioN) the problem of particle reconstruction is formulated as finding the model that has the highest probability of being correct given both the observed data as well as available prior information. The available prior information here would be an existing model of a similar complex. Cryo-EM data processing is an iterative endeavor with the use of multiple programs whose algorithms are being constantly improved and refined. While a lot of time can be spent in the optimization of processing pipelines the most difficult portion of obtaining a cryo-EM sample is generally in the optimization and stabilization of the complex of interest and then the optimization of EM Grid type, buffer and blotting conditions.

Preliminary Data and Sample Optimization

Hectd3 Negative Stain and Cryo EM

Negative stain EM is used for a quick characterization of EM samples where a heavy metal stain like Uranyl Formate is applied to the sample. While this gives tremendous contrast for visualization it potentially perturbs the complexes native conformation. Because negative stain microscopy visualizes the stain as opposed to the actual protein complex resolution is limited to the grain size of the stain. Uranyl formate has a relatively fine grain size compared to other stains but the resolution of reconstructions are between 20-30 Angstroms. Negative stain EM of the ligase looked very promising post purification of Hectd3 (Fig 15).

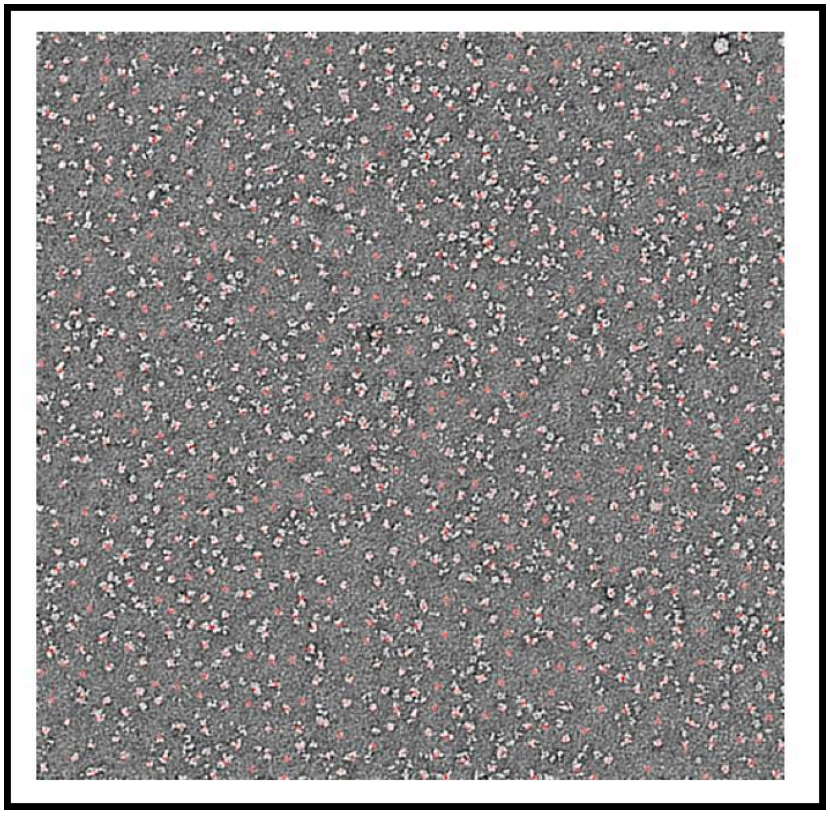

Figure 15 Negative Stain EM of Hectd3 Reveals Particles

Hectd3 diluted to 300 nM and negatively stained with uranyl formate. Red marks show where cryoSPARC's blob picker selected particles.

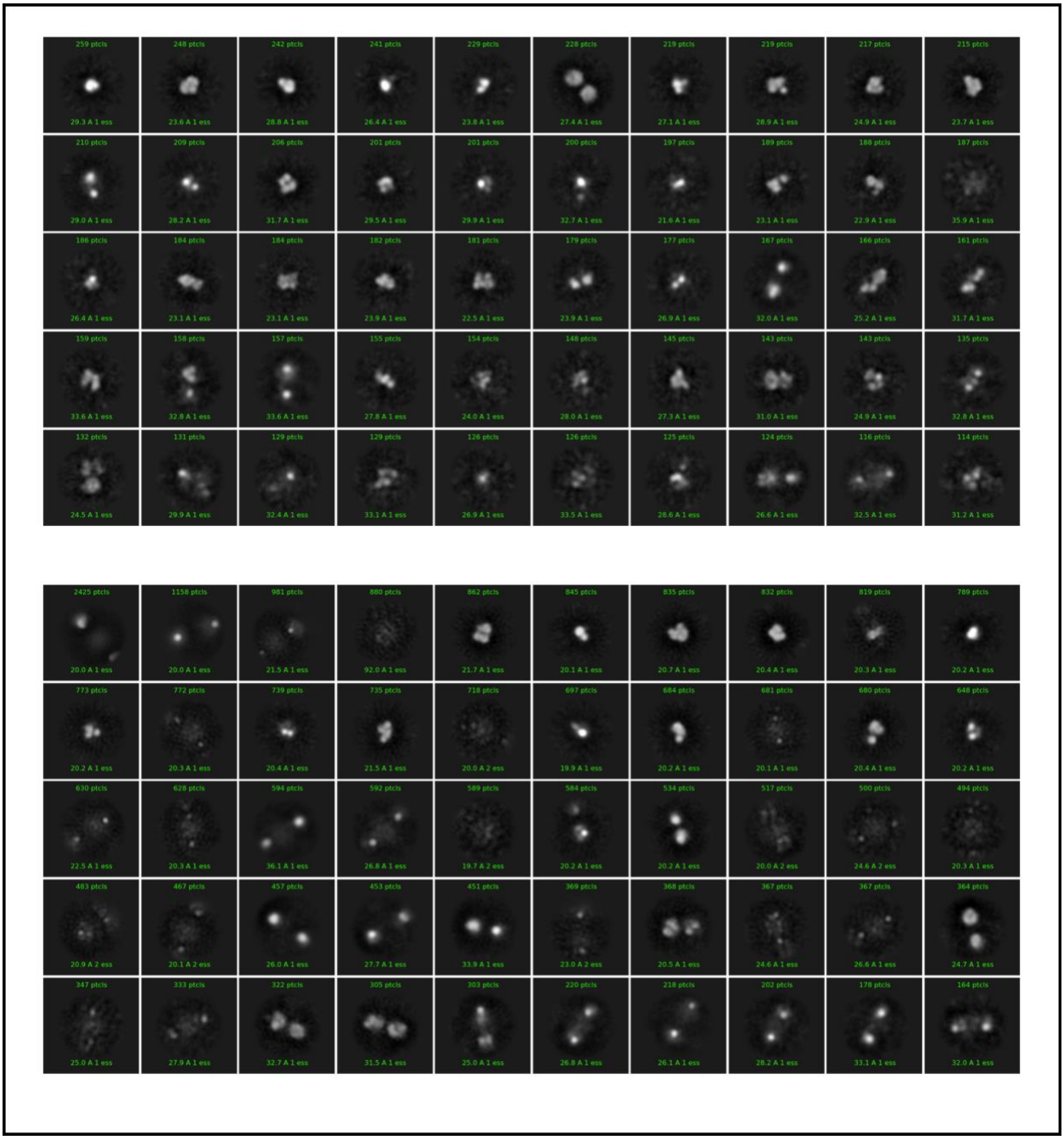

Figure 16 2D Class Averages of Negative Stain Hectd3 Particles Generated in cryoSPARC

A. Particles were picked conservatively using blob picking from negative stain micrographs. Particles were extracted and cryoSPARC was asked for 50 classes
B. Particles were less conservatively picked, extracted and averaged, asking cryoSPARC for 50 class averages.

There is still no structure of Hectd3. At the genesis of this project when these 2D classes averages were generated it was very exciting to see particles that could be averaged into 3D reconstructions utilizing croSPARC (Fig 16). When first looking at the size of the particles there were two distinct possibilities.

The purification of Hectd3 made it apparent that its HECT domain dimerizes at high concentrations. Previous work has also shown that other HECT ligases dimerize via their catalytic domain in solution and their activity can be activated via disrupting this dimer interface[58]. The X-Ray crystal structure of catalytic HECT domain of HUWE1 revealed the dimerization interface between the two HECT domains. The volume of the 3D reconstructions allows for the fitting as two HECT domains. This seemed to be the most valid possibility until an Alpha fold generated model of the full-length ligase was released. The 3D reconstruction density volume was also sufficiently large to fit the full-length ligase (Fig 17,18). Given the concentration of the ligase on the grid was 300 nM it is most likely that these are reconstructions not of dimers but full length Hectd3 monomers.

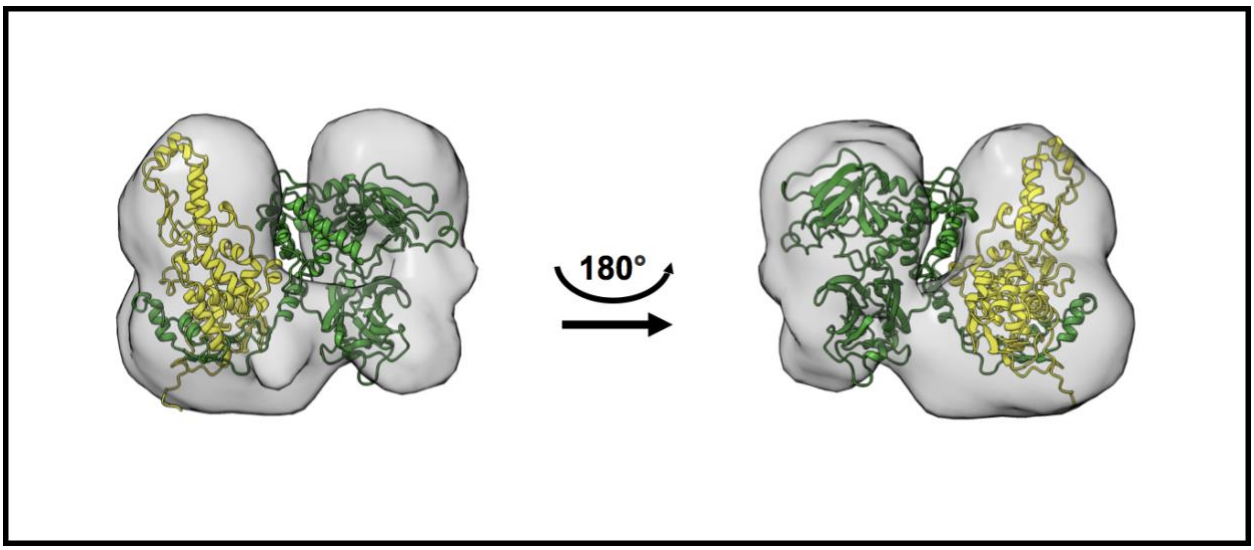

Figure 17 Alpha Fold Hectd3 Predictions fit into Negative Stain 3D Reconstruction

The top 10 non-empty class averages from the less conservative blob picking were used in the creation of an AB Initio 3D reconstruction. The AlphaFold generated model of Hectd3 was fitted into the negative stain density. The catalytic domain is colored gold and the recognition domain is colored green.

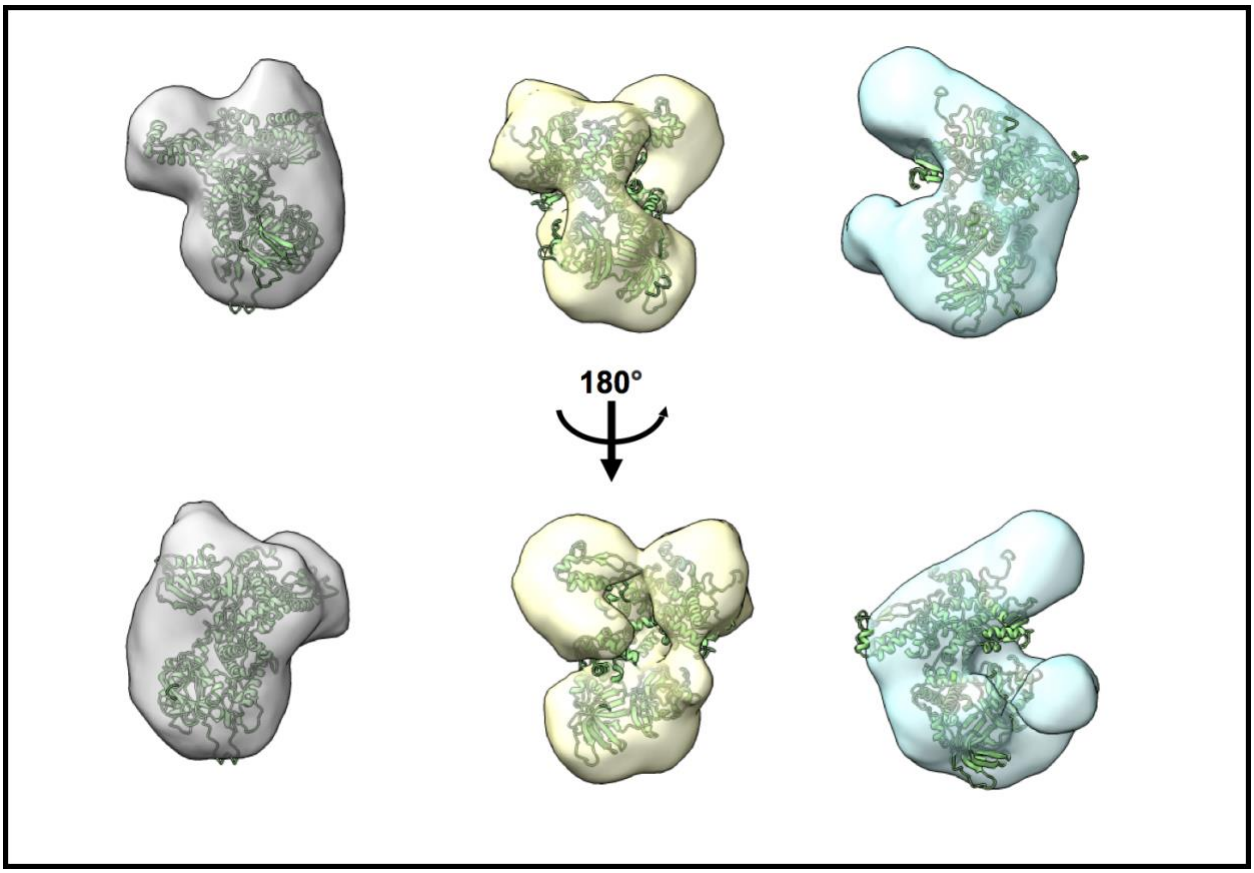

Figure 18 Hectd3 Alpha Fold model can be fit into various Negative Stain 3D Reconstructions

All class averages from the conservative blob picking were used in the creation of three Ab Initio 3D reconstruction. The AlphaFold generated model of Hectd3 was docked into the negative stain density.

Structural snapshots on various HECT catalytic domains as well as structural dynamic work has revealed that the HECT domain is composed of an N-Lobe and a C-lobe that is connected by a flexible hinge loop. This catalytic domain is very dynamic and must sample two conformational states both in order to form its thioester intermediate as well as ubiquitinate its substrate (Fig 19). These conformational rearrangements also lead to the formation of unanchored ubiquitin chains. The catalytic HECT domain can be

divided an N-lobe and C-Lobe. One side of the N lobe is responsible for E2 binding occurs while the other side is when substrate binding occurs. The C-lobe contains the catalytic cysteine where the thioester intermediate is formed. The C-lobe is very dynamic as it is responsible for posing the catalytic cysteine for both the transthioesterification needed to great the thioester intermediate as well as posing the catalytic cysteine for nucleophilic attack by the target lysine that results in isopeptide bond formation.

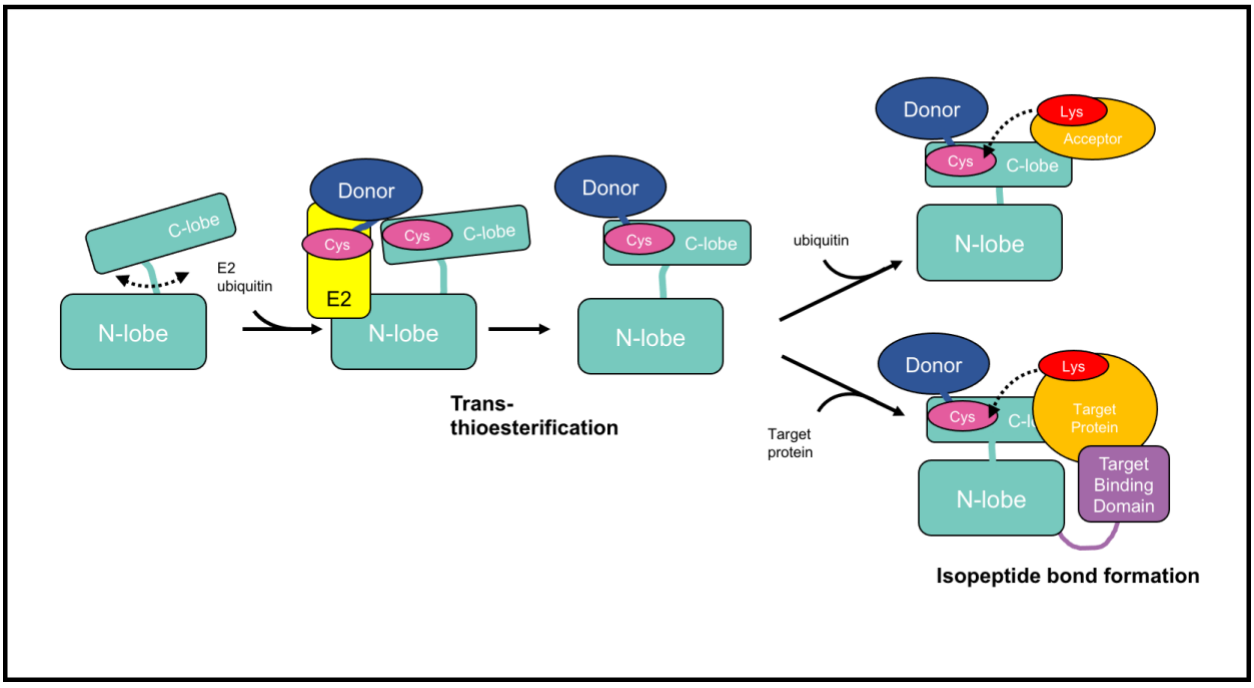

Figure 19 HECT Domains Exhibit Tremendous Structural Flexibility

Schematic of the HECT domain's flexibility that allow for the formation of its thio-ester intermediate that allows it to ubiquitinate its substrate.

With the tremendously encouraging negative stain results of Hectd3 we moved to Cryo-EM to attempt to visualize the ligase. Vitrification led to a lot of aggregation and it was very difficult to identify individual particles (Fig 20).

Over picking utilizing a blob picker yielded 2D classes that did not look proteinaceous. Optimization with functionalized grids and various detergents on just the ligase itself should be the next things attempted.

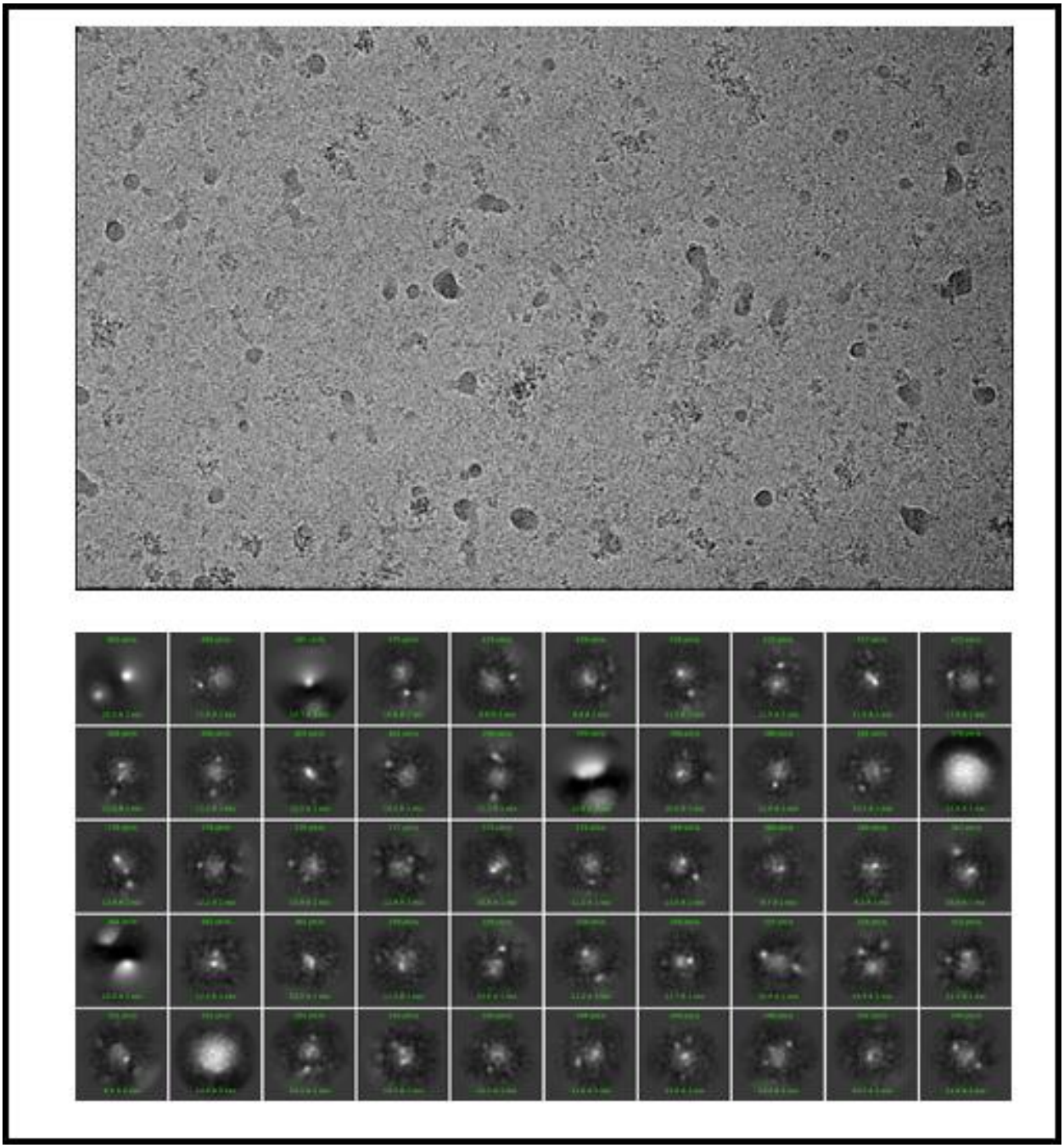

Figure 20 Hectd3 Vitrification Leads to Protein Aggregation

A. Representative micrograph of collection. Hectd3 was applied onto Cu Quantifoil 300 mesh grids at a concentration of 5μM. Data was collected at 200 KV a pixel size of 1.15 and the total dose was 60 e/A2
B. Micrographs were Motion corrected before blot picking and particle extraction. The top 60 2D Class Averages of Hectd3 are shown

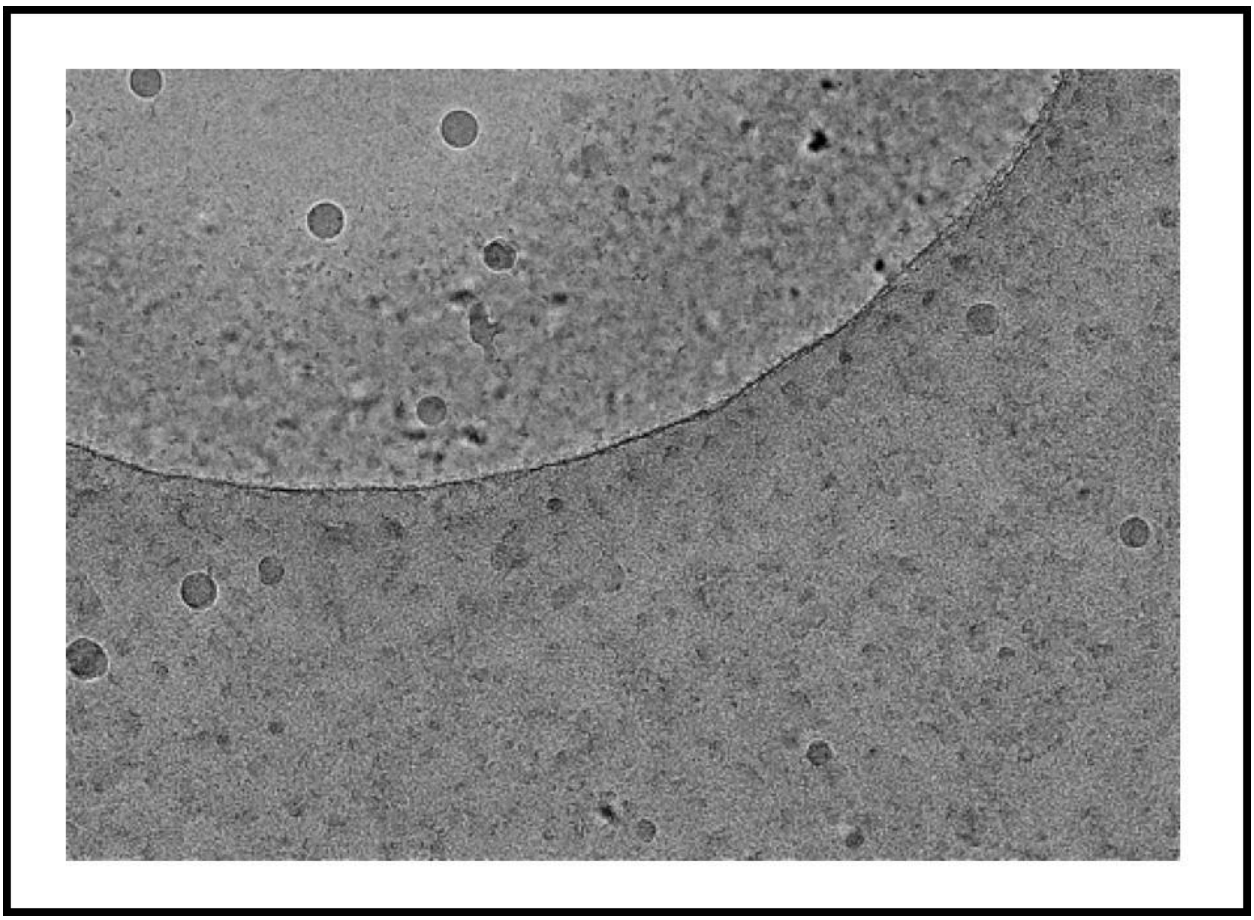

Figure 21 Hsp90 Raf1 Cdc37 Complexes are Squeezed out of Thinner Ice

A. After purification Cdc37:$Raf1_{KD}$:Hsp90 was applied to Cu Quantifoil grids at a concentration of 5μM.

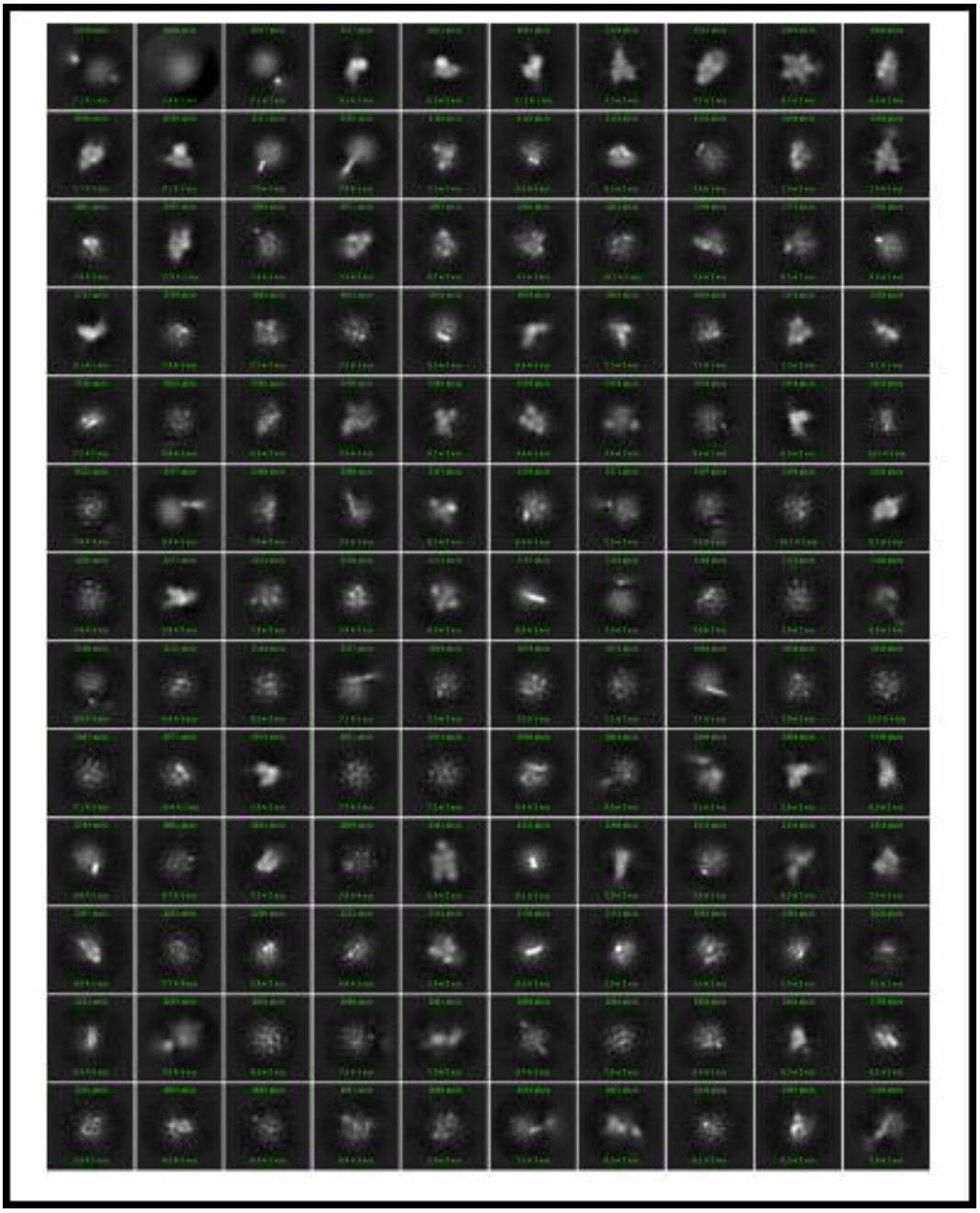

Figure 22 2D Class Averages of Hsp90:Cdc37 and Raf1 in complex with Hectd3

4 component complex of Cdc37:$Raf1_{KD}$:Cdc37:Hectd3 was applied onto Cu Quantifoil 300 mesh grids at a concentration of approximately 5μM. Data were collected at 200 KV a pixel size of .072 and the total dose was 57.5 e^{-}/A^{2}. Micrographs were motion corrected and particles selected using a blob picker before 150 2D class averages were created.

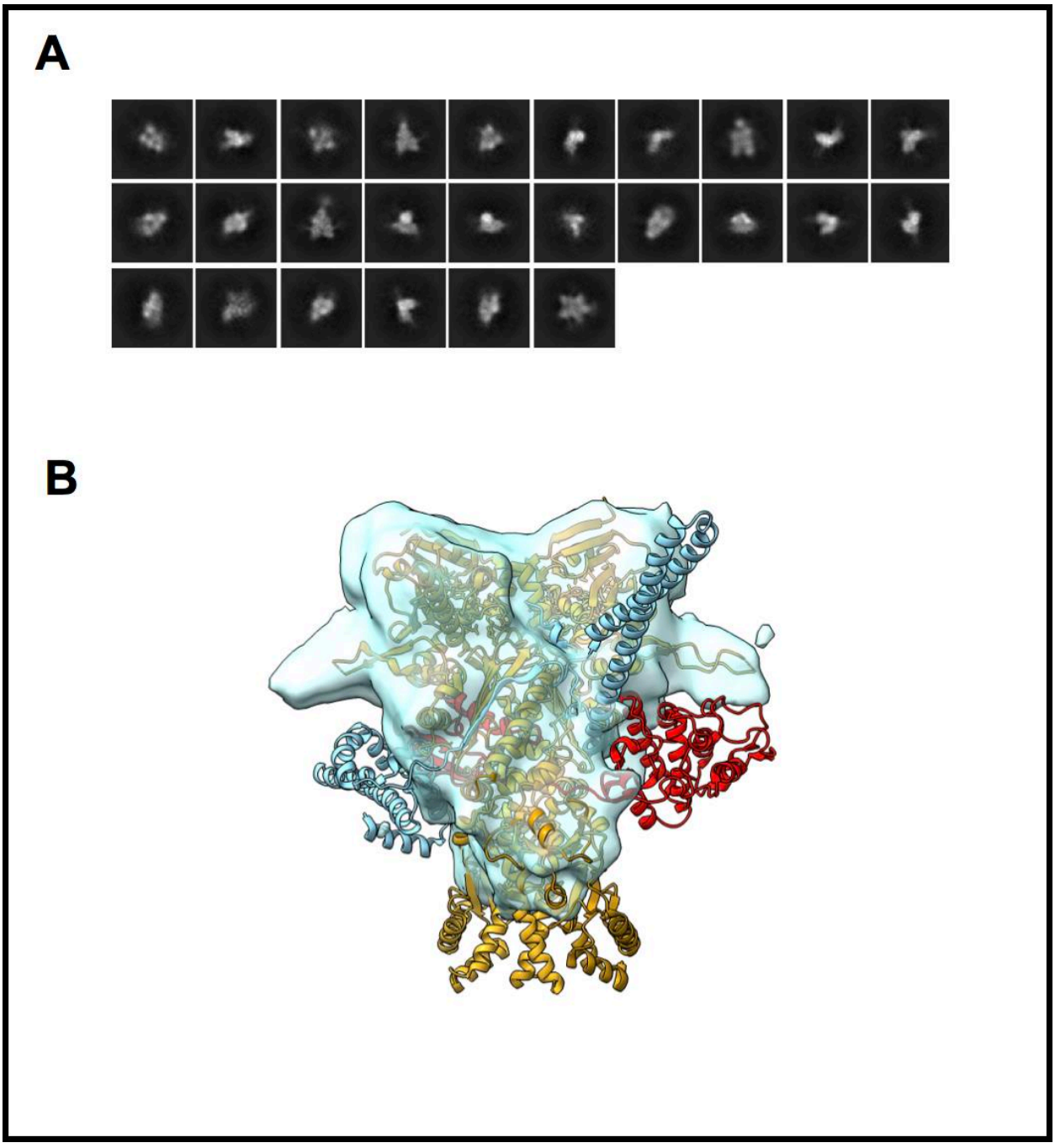

Figure 23 Ab Initio Reconstruction of Hsp90:Cdc37:Raf1 KD complex with Hectd3

A. Select 2D Class averages used in the ab Initio reconstruction.
B. 3D Ab initio reconstruction with the formerly solved structure of Hsp90 cdc37 and CDK4 (5FWL) docked into the density.

After a pulldown of the complex was established, a 4 component complex containing Hsp90 Cdc37 Raf and Hectd3 were frozen on Cu quantifoil grids. Particles preferred thicker ice and were squeezed out of holes that had thinner ice (Fig. 21).

The overnight collection Hsp90:Cdc37:Raf and Hectd3 taught a valuable lesson in the importance of saving our protein samples from the air water interface. We were unable to see any density corresponding to Hectd3. Even the normally robust C-terminal domain of Hsp90 was disrupted by the air/water interface to the point it did not appear in the 3D reconstruction (Fig. 23).

Cdc37:Hsp90:Raf1$_{FL}$:Hectd3 Complex

Incubating Cdc37:Hsp90:Raf$_{FL}$ with excess catalytically dead (C823A) Hectd3 and running over an analytical column showed the Hectd3 was too transient to bind to Cdc37:Hsp90:Raf$_{FL}$. A pulldown experiment was designed that allowed for a 4 component complex suitable for Cryo-EM (Fig 24). Incubation times and reaction volumes were inspired by Chari's Noddings previous work in the lab[59] .An excess of Hectd3 (C823A) was mixed with approximately 1.5μM Cdc37:Hsp90:Raf$_{FL}$ complex. This mixture was exchanged into a low salt buffer (50 mM KCl) and then incubated on Streptactin XT resin for 90 min at 4C. This incubation was then allowed to flow through and washed with two column volumes of 50 mM KCl twice. An elution solution containing desthibiotin was allowed to incubate on the strep resin for 30 min before it

was eluted. Elutate was 4 uL of eluate was put on PEG 2K amino grids and visualized via cryo-EM. Data was processed utilizing cryoSPARC (Fig 25).

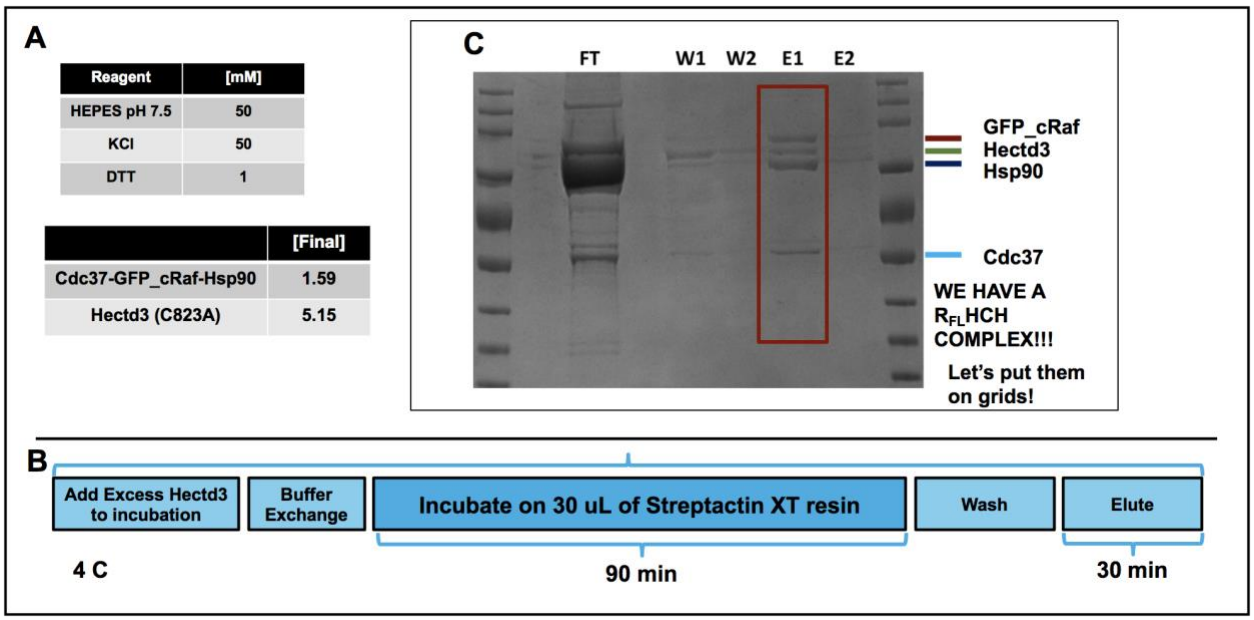

Figure 24 Sample Preparation of Cdc37:Hsp90:Raf1$_{FL}$:Hectd3 for Analysis via Cryo-EM

A. Protein concentration and incubation buffer composition for pulldown
B. Schematic of Complex incubation and elution from strep resin
C. Coomassie stained gel of Flowthrough, Washes and Elutions from strep resin

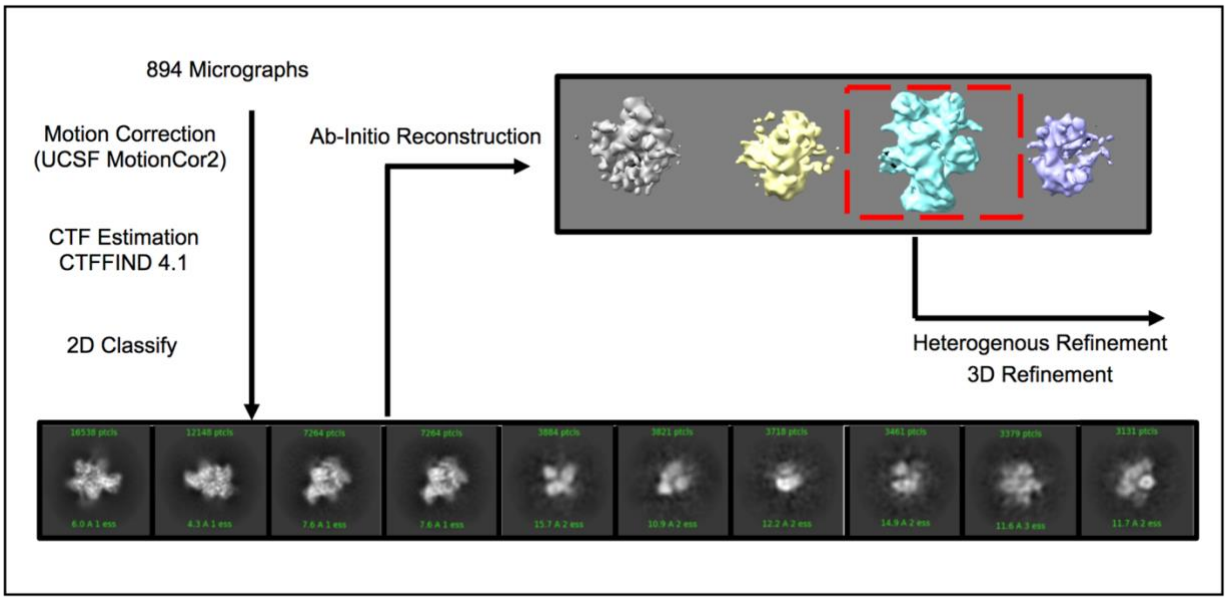

Figure 25 Initial Processing Pipeline for Cdc37:Hsp90:Raf1$_{FL}$:Hectd3

894 Micrographs were motion corrected on the fly using MotionCorr2. CTFFind 4.1 was used to eliminate any micrographs with a CTF estimation over 6 Angstroms. CryoSPARC's blob picker was used for particles section before 2D classification, followed by the ab initio reconstruction asking for 4 classes. The particles in the best ab initio class were used for 3D homogeneous refinement.

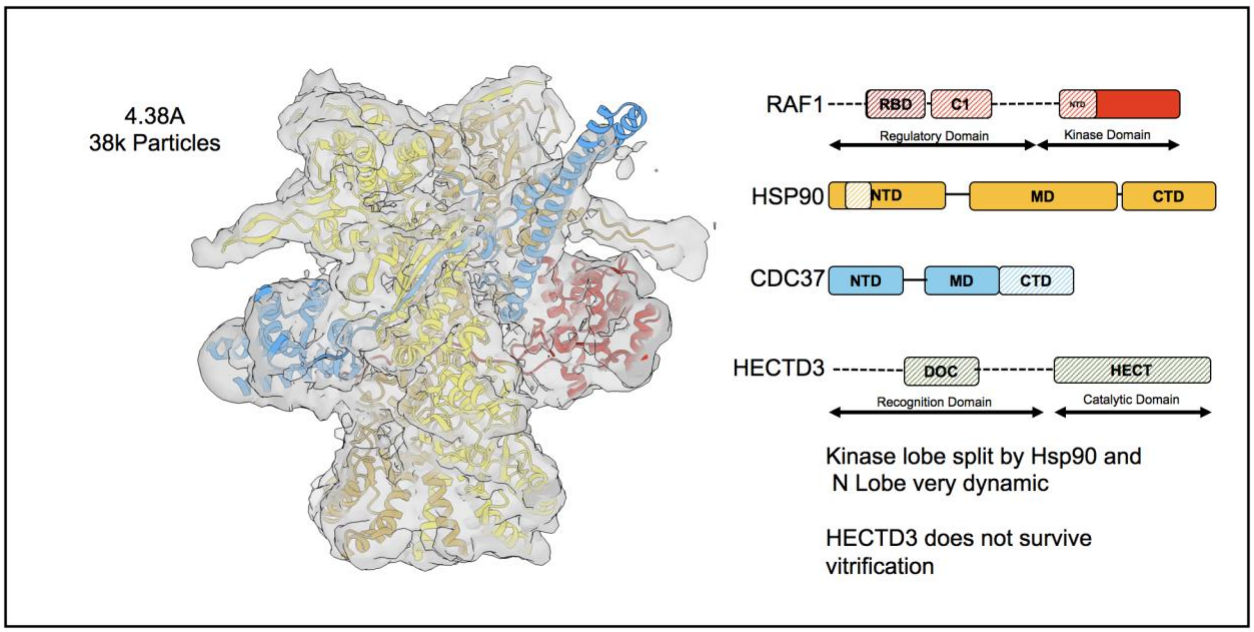

Figure 26 Cdc37:Hsp90:Raf1$_{FL}$:Hectd3 does not have any Hectd3 Density

A. Electron density with built in model of Hsp90 (Gold) Cdc37 (Blue) and Raf1 (red)
B. Domain of architecture of all proteins present in the EM sample. Solid colors denote the protein domains that were able to be built into the model

Hectd3, disappointingly, does not survive vitrification (Fig 26). Hsp90 adopts a strikingly similar closed conformation to molybdate closed Hsp90. With no gamma phosphate present we observe this complex to be in the ADP post hydrolysis state before Hsp90 opens. Hsp90 splits N-terminal and C-terminal kinase lobes. The N terminus of the kinase is unfolded and the beta4-beta5 strand is threaded through the Hsp90 lumen. This unfolded portion of the kinase N lobe is stabilized by Cdc37 on the other side of the HSp90 lumen. The N terminus of the kinase is very dynamic, lowering the thresholds reveals additional density on the back side of the Cdc37. Further 3D classification was unable to pull out any additional robust N-lobe density.

Although Hectd3 pulls down very nicely in the biochemical assays it is too heterogeneous to be visualized in the cryo-EM maps. Moving forward I forward I used crosslinking to stabilize the 4 components [60].

With the recognition domain of Raf not being visualized we wondered how much this portion of the kinase was responsible for the ability of Hectd3 to recognize the HCRAf complex. I expressed and purified two other kinase constructs, one that contained only the kinase domain of cRaf and the other that contained the kinase domain and an additional 30 amino acids at its N-terminus.

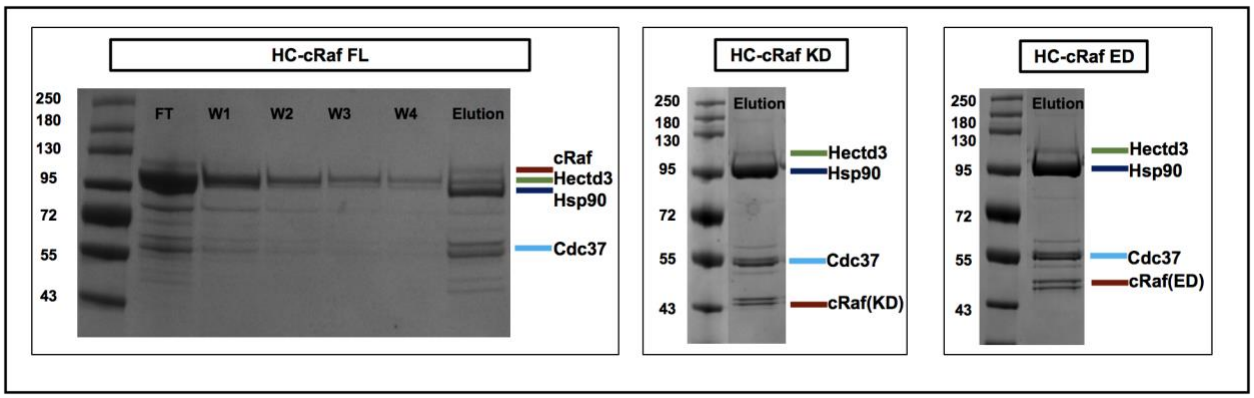

Figure 27 Comparative Pulldown of Hectd3 by 3 Raf Hsp90 Kinase Constructs

Three Raf1 constructs were purified in complex with Hsp90 and Cdc37. Raf_{FL} consisted of all of Raf1, Raf_{KD} of just the kinase domain Raf and Raf_{ED} consisted of the kinase domain with the inclusion of the 30 amino acids preceding the kinase N-lobe. All kinase constructs were incubated with Hectd3 and stringently washed to compare Hectd3 association.

Incubating a C823A Hectd3 and including a very stringent detergent wash validated the interaction with Hectd3 was real. Hectd3 can pulldown with an Hsp90 Cdc37 Raf complex that only contains the kinase domain of Raf1 (Fig 27). To better assign the additional density brought about by a stabilized Hectd3 I decided to move forward with the kinase domain Raf complex.

Cdc37:Hsp90:Raf1$_{KD}$:Hectd3$_{X}$ Complex

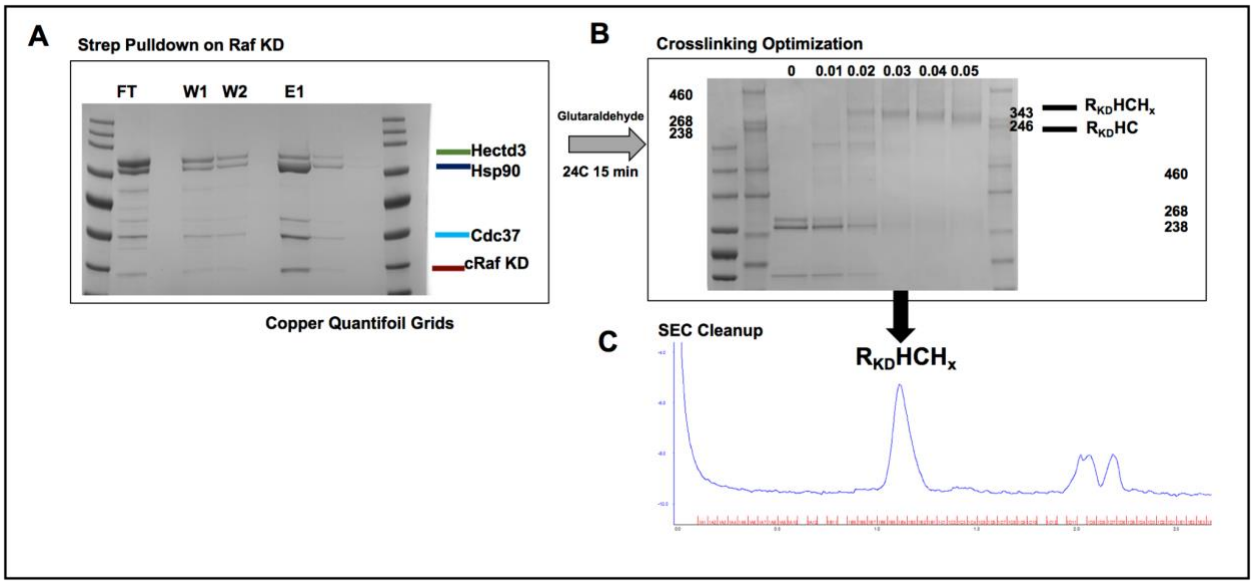

Figure 28 Cdc37:Hsp90:Raf1$_{KD}$:Hectd3$_{X}$ Sample Preparation for Cryo-EM

A. Coomassie stained gel of Strep Pulldown of Hectd3 with Cdc37:Hsp90:Raf1$_{KD}$, showing the flowthrough (FT) Wash 1 (W1) Wash 2 (W2) and Elution (E). 2.3μM Cdc37:Hsp90:Raf1$_{KD}$ was incubated with 4μM Hectd3 and buffer exchanged into 50 HEPES ph 7.5, 50 mM KCl and 1 mM TCEP. The 4 components were incubated on strep resin for 90 min at 4C before being washed and eluted.
B. Coomassie Stained gel of 4 component complex elution crosslink optimization. Samples for EM were crosslinked with 0.03% glutaraldehyde at 24C for 15 m.
C. Size Exclusion Chromatography Trace of 4 component, crosslinked complex that is put on grids

Glutaraldehyde crosslinking was tested for optimal concentration at 24C for 15 min. 0.03% was the lowest amount of crosslinker used where the 4 components coalesced into a single band. After crosslinking the sample was cleaned by running over an analytical column and then put on Cu Quantifoil grids (Fig 28). Early 2D classification in cryoSPARC revealed a cloud of new density surrounding both the C-terminus of cRAf as well as the middle domain of Cdc37. In other views (marked in red) showed an extension emanating from the Cdc37 middle domain (Fig 29).

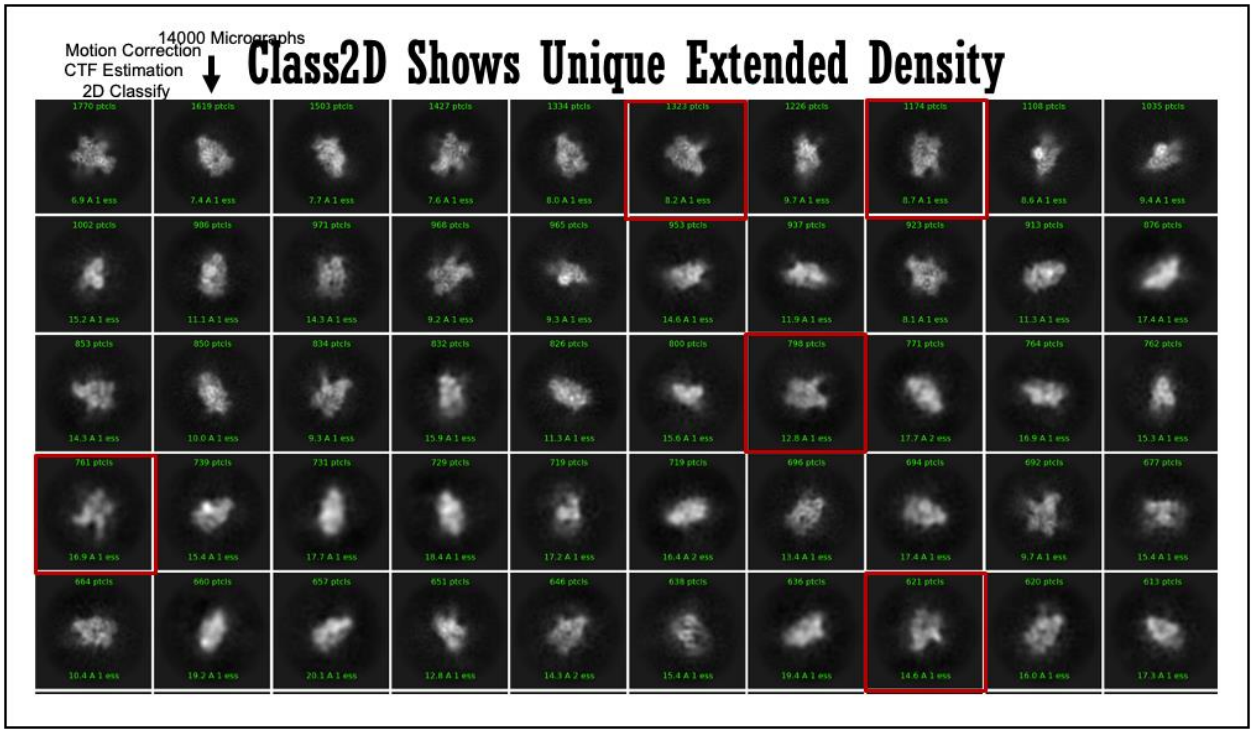

Figure 29 2D Class Averages of Cdc37:Hsp90:Raf1$_{KD}$:Hectd3$_{X}$ Reveal Novel Density

1400 Micrographs were motion corrected on the fly using MotionCorr2. CTFFind 4.1 was used to eliminate any micrographs with a CTF estimation over 6 Angstroms. CryoSPARC's blob picker was used for particles section before 2D classification to assess the quality of the data.

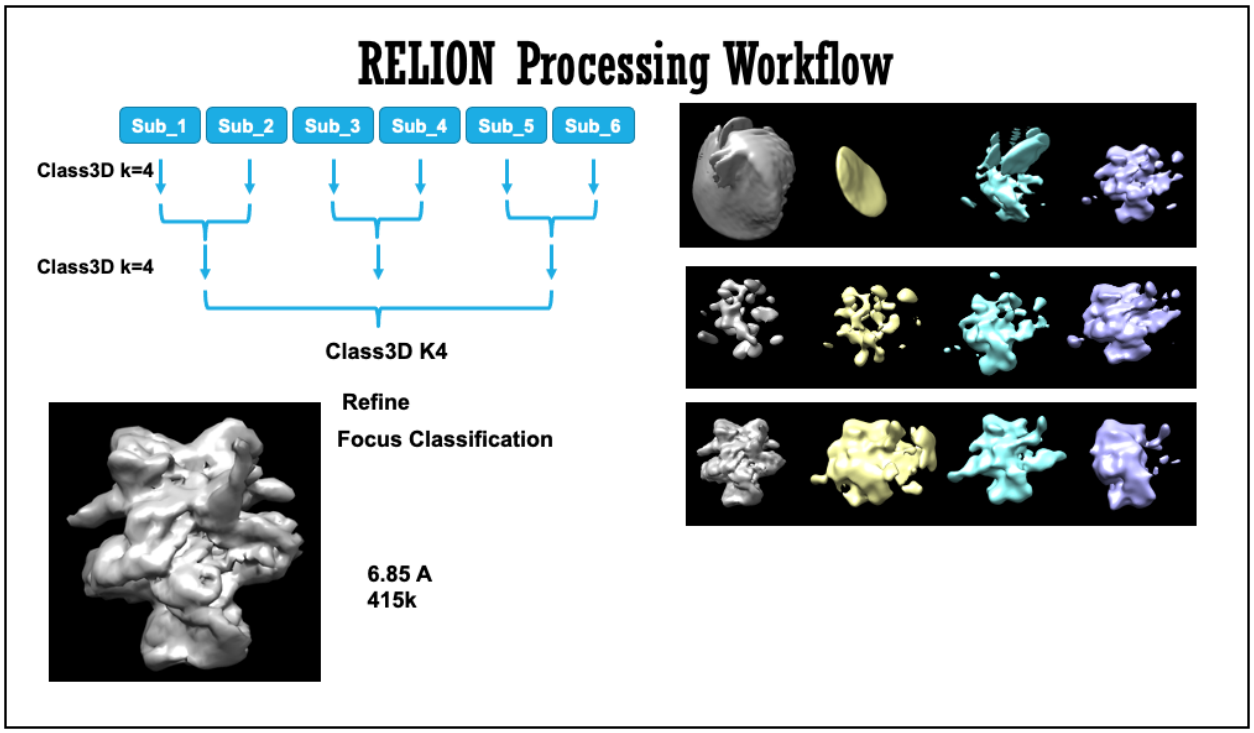

Figure 30 RELION Processing Pipeline for Cdc37:Hsp90:Raf1$_{KD}$:Hectd3$_{X}$
The location of particles belonging to good 2D class averages were imported to RELION and extracted. 3 round of 3D classification asking for 4 classes were performed using (5FWL) as an initial model. The 415k particles that gave the highest resolution were unbinned and refined.

After particles were cleaned up via 2D classification in cryoSPARC particles were subjected to 3 rounds of focus classification in RELION. Refinement yielded a structure that reached close to the theoretical Nyquist frequency resolution limit (Fig 30). Focused classification using a large spherical mask focusing on the middle and C-terminal domain of Cdc37 was then done on unbinned particle stacks, revealing heterogeneity of the Cdc37 C-terminal and Middle domain (Fig 33). Focused classification

refinements were used to build the best composite map. A model was built using PHOENIX[61] (Fig 34).

Cdc37 C-terminal domain seems to be stabilized by Hectd3, lowering the threshold of maps reveals density around the Cdc37 4 helical bundle as well as between the C-lobe of cRaf and the two extended helixes of Cdc37 (Fig 31). This extra density appears to make the two helixes of Cdc37 kink.

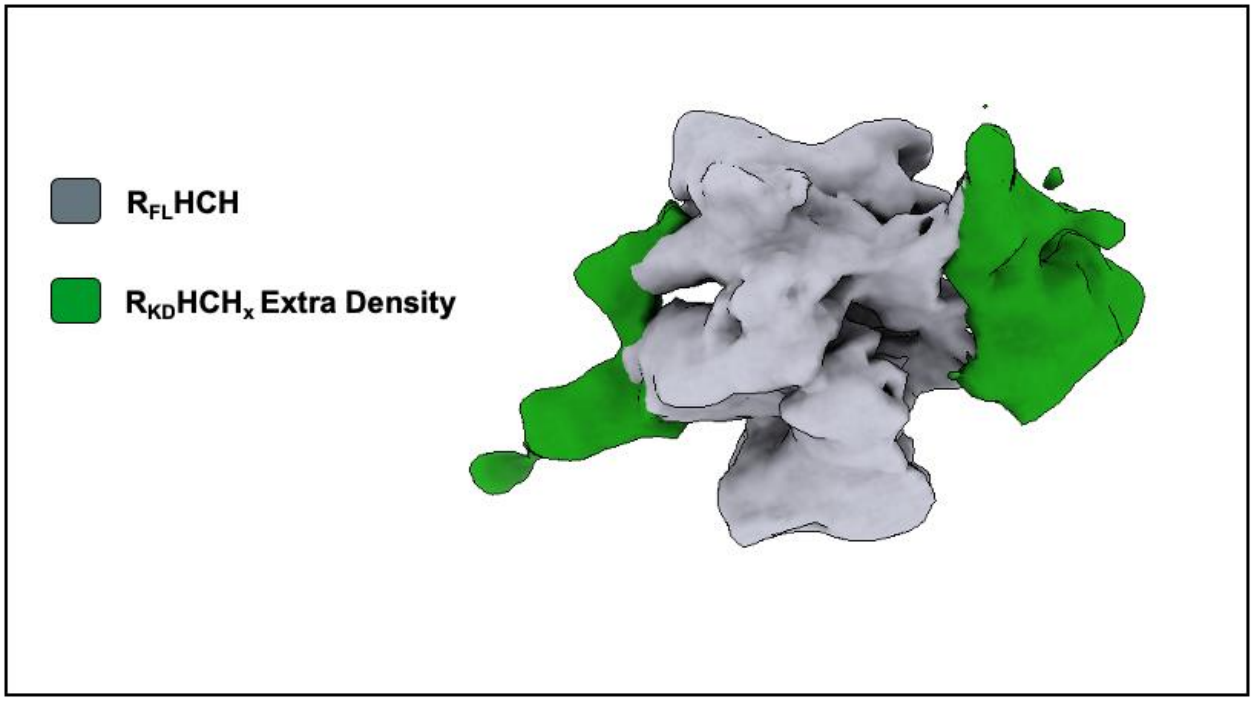

Figure 31 Cdc37:Hsp90:$Raf1_{KD}$:$Hectd3_X$ Reveals New Density

Overlap of EM densities for Cdc37:Hsp90:$Raf1_{FL}$:Hectd3 (grey) and Cdc37:Hsp90:Raf_{KD}:Hectd3x (green)

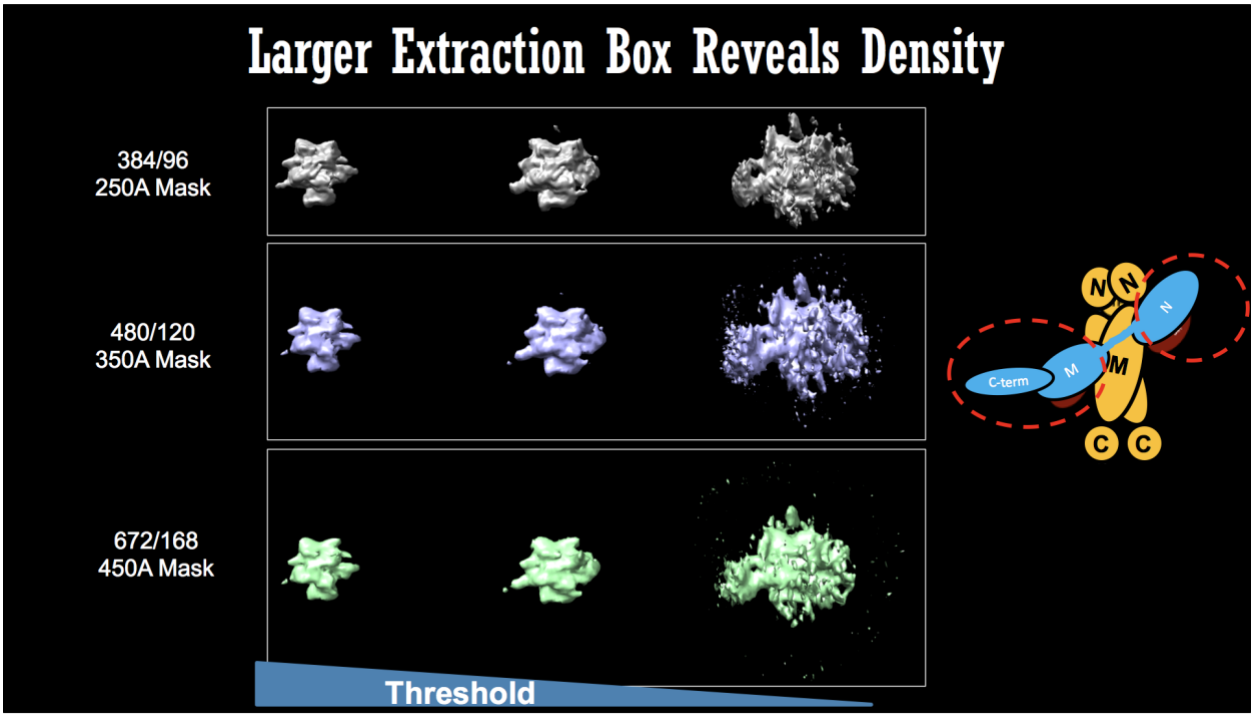

Figure 32 Extraction at larger Box size Reveals Additional Peripheral Density

EM density after 3 rounds of 3D classification. Particles were extracted at increasingly large box sizes and 3D classified with 5FWL as a starting model.

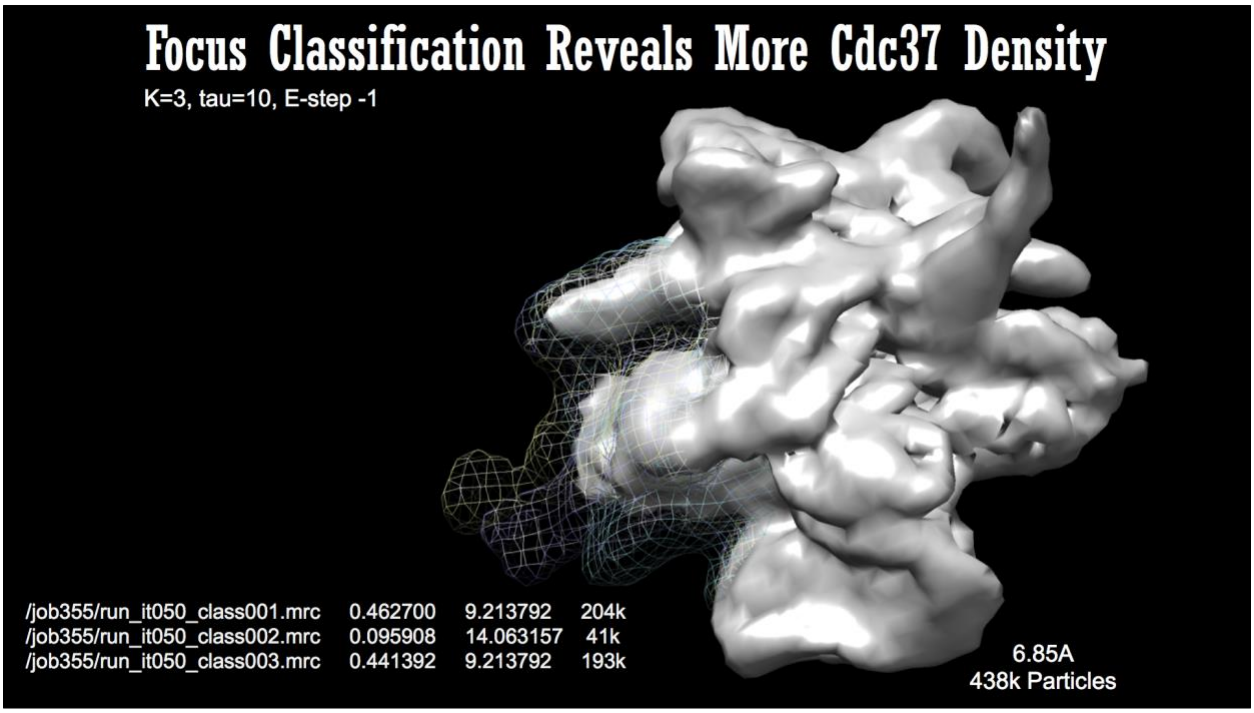

Figure 33 Focused Classification Reveals Movement of Cdc37 Middle and C Terminal Domain

Refined EM density of Cdc37:Hsp90:Raf_{KD}:$Hectd3_x$ with 3D focused classification jobs of the superimpose on top. Focused classification was performed without subtraction with a Tau of 10 an E-step of -1 and a spherical mask. Percentage of refined particles, resolution, and number of particles is reports for class 1 (purple), 2 (teal) and 3 (yellow).

The Cdc37 C-terminus has been implicated in kinase activation. The mutation W342C has been shown to impair sevenless tyrosine kinase and cause lethality in flies[62]. Additional NMR work specifically on the Cdc37 C-terminal bundle showed that W342 is mostly solvent exposed. Its mutation to a cysteine does not cause gross misfolding defects but reduces the hydrophobic interaction Cdc37 can have with a kinase client. Additionally W342C prevents sampling of a transient Cdc37 closed state where Cdc37 helps stabilize the partially unfolded kinase state of the aC-b4-b4/5 loop segment[8].

The transition of the chaperone complex from open to closed state is characterized by a major remodeling of interfaces between chaperone-co-chaperone-client interfaces. Previous NMR and structural data shows that loading of a kinase client onto Hsp90 is facilitated by dynamic sampling of low-populated closed states of Cdc37. This Cdc37 closure stabilizes metastable portion of the kinase client. The partially unfolded substrate is passed from a closed state of Cdc37 to a closed state of Hsp90 where the kinase domain is split between two lobes and threaded between the Hsp90 dimer lumen. This would occur in the presence of phosphorylated Cdc37 and ATP[63]. Continual chaperoning by Hsp90 and Cdc37 allow Raf1 to reach maturity. Intramolecular phosphorylation of Ser-621 is required to keep cRaf stable and active and enhanced recruitment of Hsp90 is observed for unstable CRAF mutants[64,65].

These phosphosites are binding sites for 14-3-3 proteins that are critical cofactors for Raf-1 activation, which maintain the protein in a state that is competent for both ATP binding and MEK phosphorylation.

Inhibition of Hsp90 hinders Ser-621 phosphorylation of immature CRAF, reducing its intrinsic kinase activity. Interestingly, association of CRAF to Hsp90 increases when Hsp90 is inhibited, suggesting Hsp90 has a role in presenting CRAF for degradation[66].

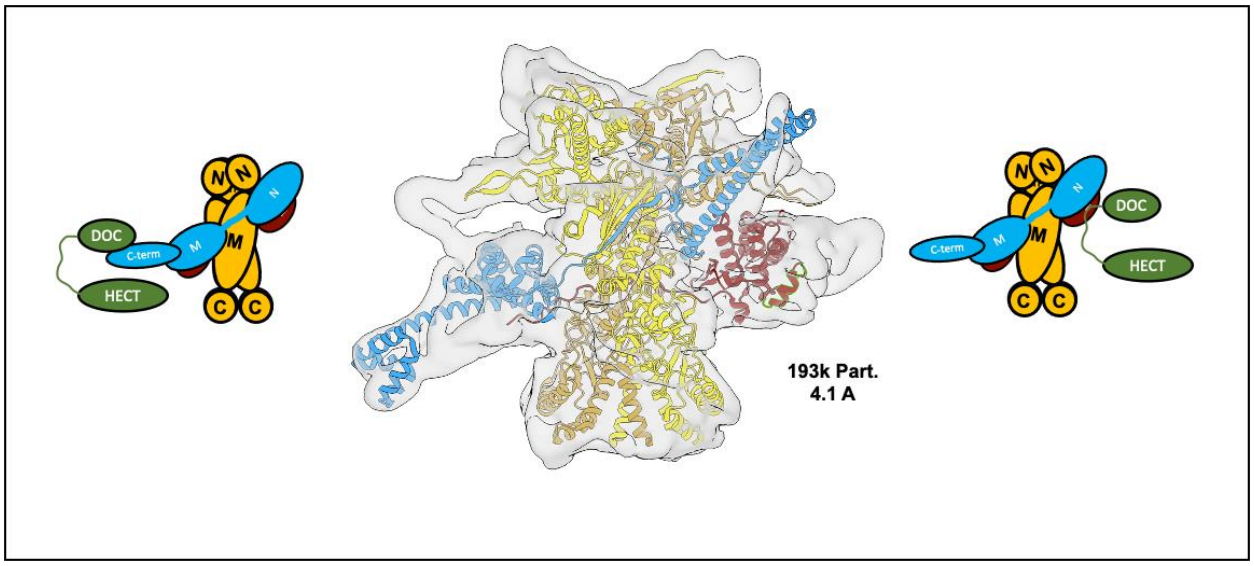

Figure 34 Stabilization by Hectd3 Reveals Cdc37 Platform

Model fit into the experimental density for Cdc37:Hsp90:Raf_{KD}:$Hectd3_{x}$ along with cartoon schematic of potential Hectd3 binding modes.

In Vitro Ubiquitination Assays

Although we saw robust ubiquitination *in vivo* of our transiently transfected $Raf1_{FL}$ it was my goal to establish an *in vitro* ubiquitination system in order to better probe and mechanistically understand how Hectd3 ubiquitinates Raf1 in an Hsp90 dependent manner. Hectd3 is one of 600 Es in the proteome. They are responsible for bestowing specificity to ubiquitin. In addition to marking proteins for degradation via K48 linkages, mono ubiquitination and varying other ubiquitin chain types have been shown to regulate function and translocation in the cell. Hectd3 is part of a family of ligases that have an atypical mechanism. While Ring and U-Box E3 ligases serve as a scaffold to

bring E2 enzymes to their substrates, Hect ligases are able to directly ubiquitinate their substrates via the formation of a thiol-ester intermediate (Fig 35).

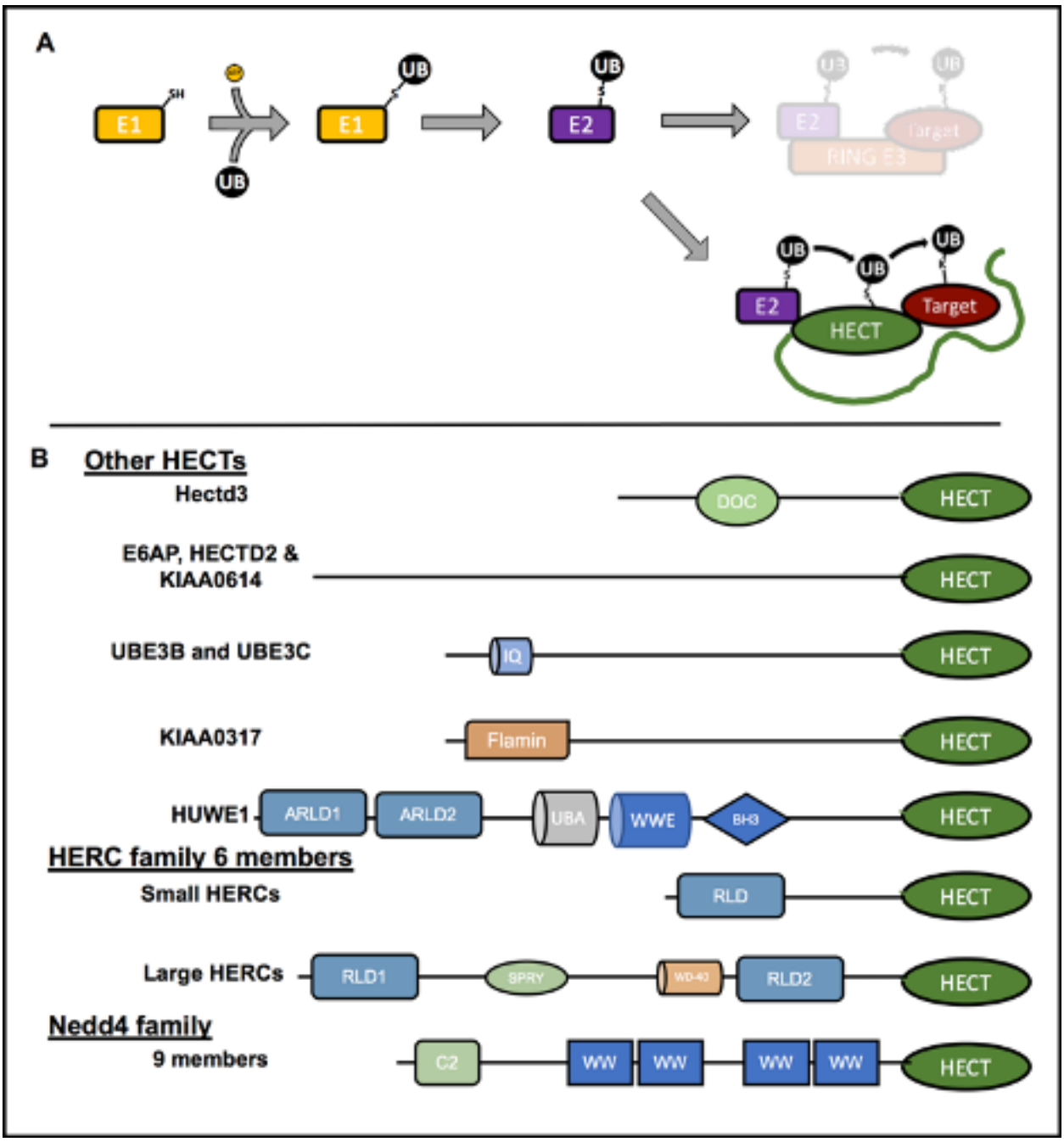

Figure 35 HECT ligases have an atypical mechanism

A. Schematic showing how HECT ligases ubiquitinate their substrates via the formation of a thioester intermediate and recognize their substrate via their N-terminal recognition domain.
B. Schematic showing the diversity of the N-Terminal domain within HECT family ligases

Their substrate specificity is determined by HECT ligase N-terminal recognition domain. This recognition domain varies not only in length but also domain architecture and composition. Before checking the ubiquitination of any substrates, we verified our purified components for purity as well as activity. In verifying the activity of E1 and E2 enzymes we saw a tremendous amount of auto ubiquitination on Hectd3 (Fig 36).

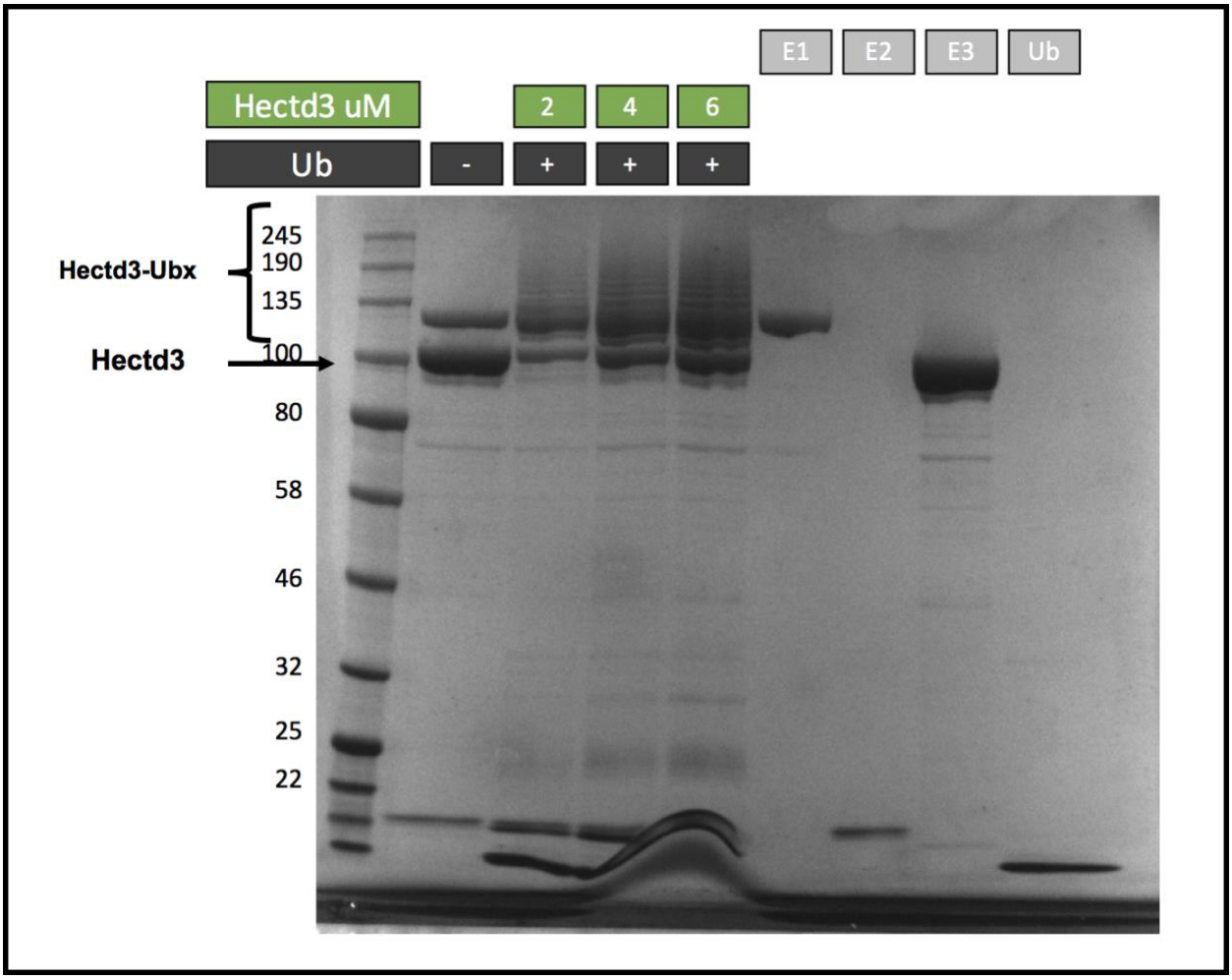

Figure 36 Hectd3 Exhibits High Autoubiquitination

Coomassie stained SDS PAGE of in vitro ubiquitination assays. Lanes 2,3 and 4 various Hectd3 concentrations incubated with 3 E1, 1μM E2, 10μM Ubiquitin and 5 mM ATP. Lane one contains no ATP. Lanes 5 - 8 are protein purity controls.

During purification it was observed that Hecd3's catalytic domain dimerizes in a concentration dependent manner. Incubating the catalytic domain with E1 E2 ubiquitin and ATP did not yield autoubiquitination. With no ubiquitination occurring with just the catalytic domain of the protein it was possible that either dimerization inhibits the formation of a thio-ester intermediate, and/or the recognition domain of the enzyme is the portion that is being ubiquitinated. We titrated down the concentration to see if reducing the dimer population resulted in formation of a thioester intermediate or resulted in autoubiquitination. Titrating down the concentration to 1 μM of the catalytic HECT domain allowed approximately 50% of the enzyme to form a thioester intermediate (Fig. 37). In this concentration regime no auto ubiquitination was observed.

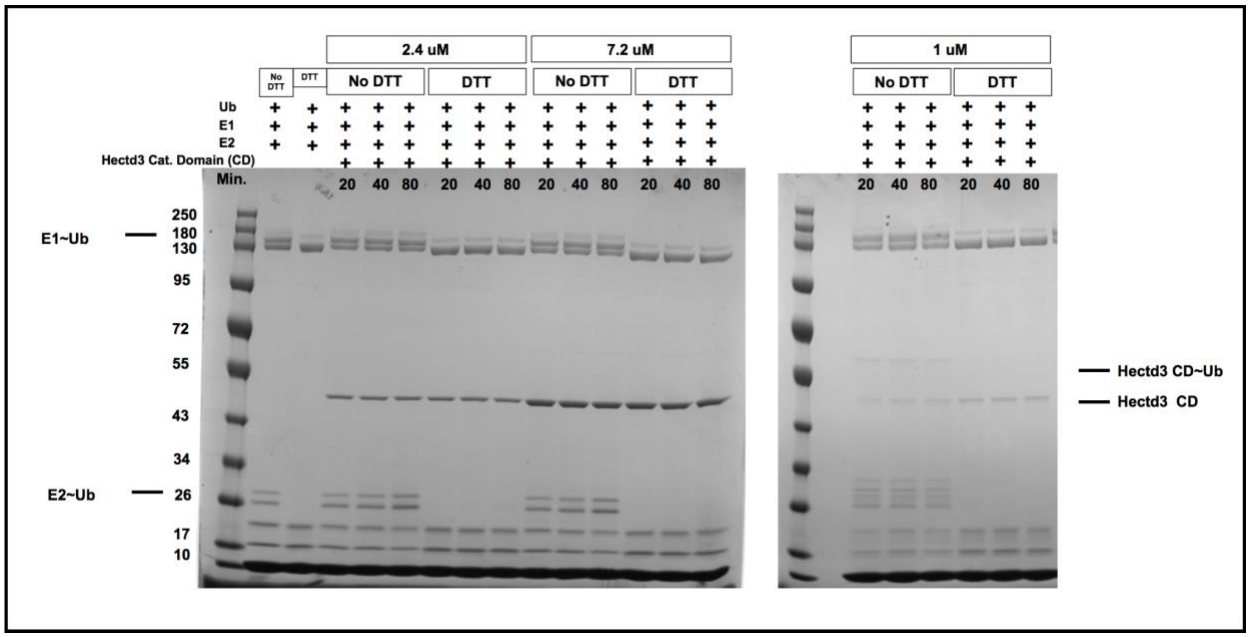

Figure 37 Hectd3 dimerization via its catalytic domain prevents thio ester intermediate formation.

Coomassie stained SDS-PAGE gels run in reduced and non-reduced conditions to show the formation of thio-ester intermediates.

In addition to the autoinhibition brought by HECT dimerization is there is evidence that many HECT enzymes are autoinhibited by their N-terminal recognition domain. This autoinhibition is relieved when the enzyme encounters a substrate. Such a mechanism is seen with the Hsp90 chaperone PP5. Wanting to test if the addition of Hsp90 or Cdc37 by themselves could enrich Hectd3's thio-ester intermediate state we added Hsp90 and or Cdc37 to Hectd3 priming reaction to see if they enriched for the thioester intermediate state. Though less auto ubiquitination was seen just by the band intensity of Hectd3 running at 97 kDa it was inconclusive whether Hsp90 or Cdc37 by themselves assisted in priming Hectd3 (Fig 38).

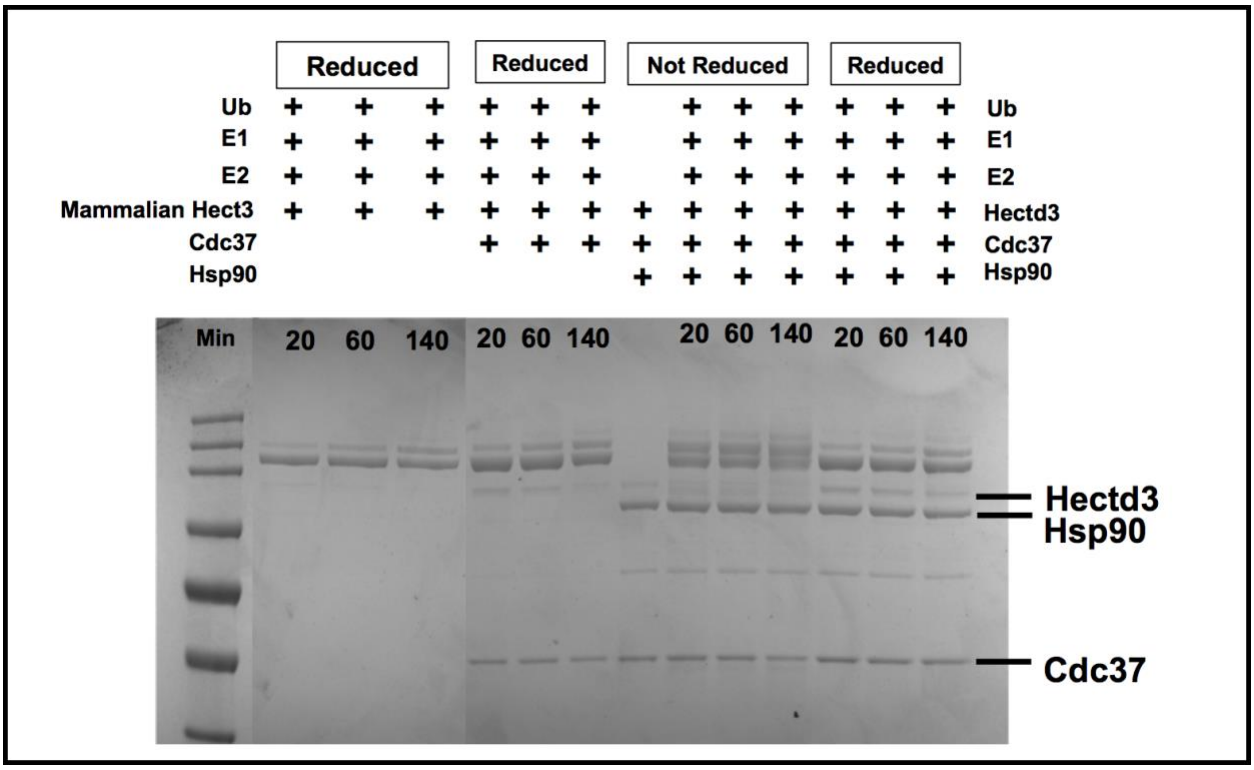

Figure 38 Hsp90 and Cdc37 Do Not Drastically Increase the Formation of HECTD3's thioester intermediate

Coomassie Stain SDS-PAGE gel of 0.5μM Hectd3$_{FL}$ incubated with 3μM E1, 1μM E2, 10μM Ubiquitin and 5 mM ATP. The addition of 3μM Hsp90 and/or 3μM Cdc37 did not robustly increase the amount of thiol-ester present. All reactions were incubated at 24C for noted time.

When a purified open complex of Hsp90:Cdc37:Raf1 was incubated with Hectd3 and the required E1 and E2 ubiquitination enzymes, three main things were observed. First proper priming of Hectd3, secondly a small amount of mono ubiquitination of Raf1, and a tremendous amount of auto ubiquitination of Hectd3 (Fig 39). A Western blot of Cdc37 and Hsp90 revealed that Hectd3 did not ubiquitinate either.

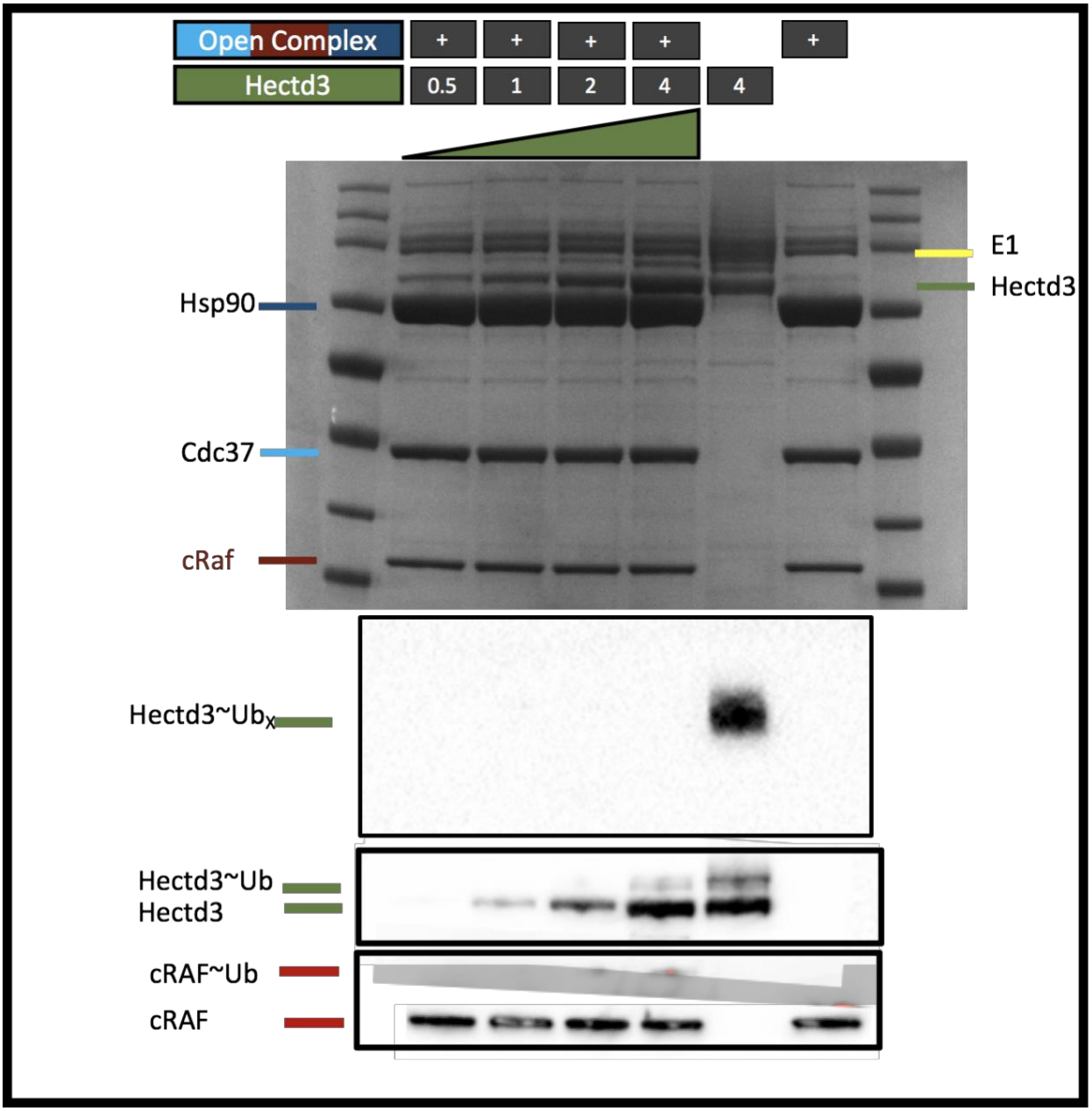

Figure 39 Hectd3 Mono Ubiquitinates Raf1 kinase domain

Coomassie stained SDS-PAGE gel of Cdc37:Raf1$_{KD}$:Hsp90 ubiquitination assay. 8.45μM of Cdc37:Raf1$_{KD}$:Hsp90 is incubated with 3μM E1, 1μM E2, 20μM Ubiquitin, 5 mM ATP and varying amount of Hectd3 for 2 hours at 24 C.

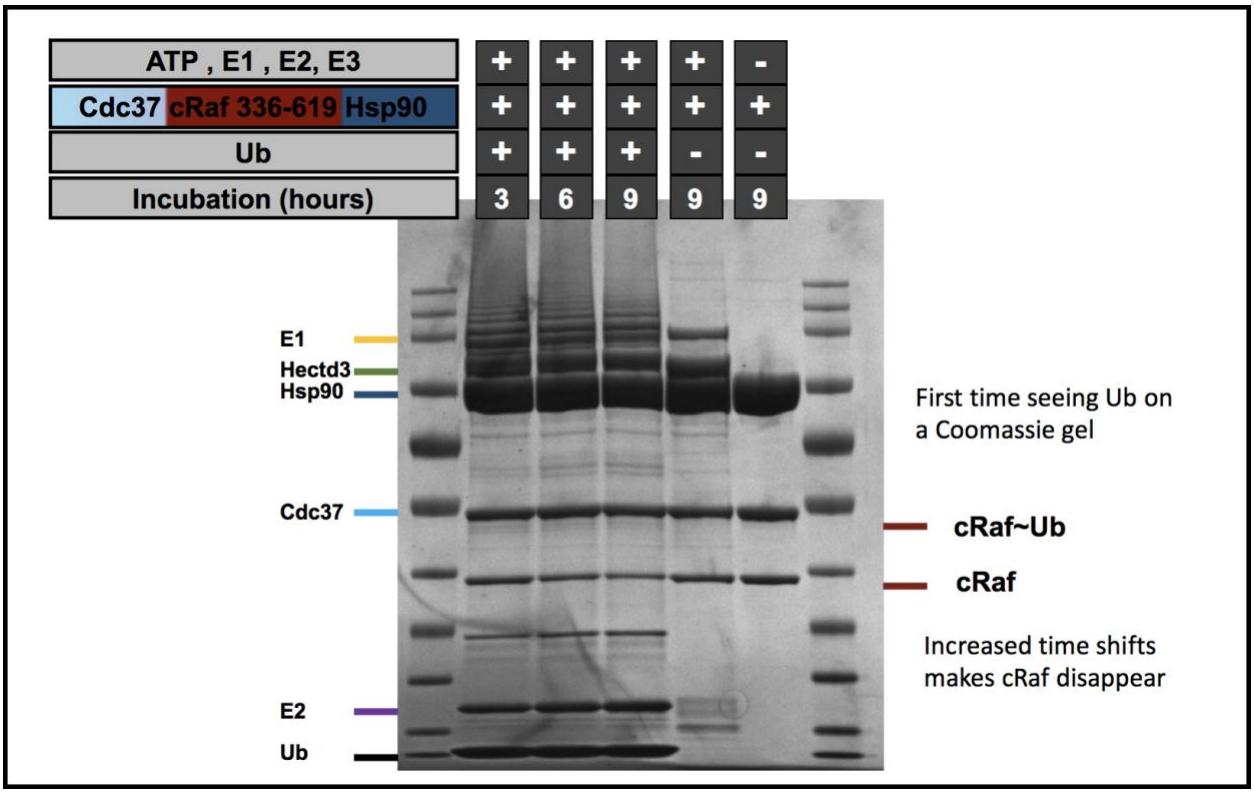

Figure 40 Hectd3 Autoubiquitination Predominates Over Raf1 Ubiquitination

Coomassie Stained SDS-PAGE gel of extreme time course of Cdc37:Raf1$_{KD}$:Hsp90 ubiquitination assay. 5μMμM of Cdc37:Raf1$_{KD}$:Hsp90 is incubated with 1μM E1, 1μM E2, 20μM Ubiquitin, 5 mM ATP and 2μM Hectd3 at varying time points at 24 C.

Attempting to change conditions to optimize Hectd3 ubiquitination led me to increase incubation time and temperature. Incubating up to 9 hours revealed the disappearance of Raf1 but did not reveal the distinct bands of a ubiquitination ladder. Once again, the ubiquitination on Hectd3 itself was incredibly strong. Increasing the temperature of the reaction gave us the greatest increase in Raf1 ubiquitination. Temperatures at or above 27C gave a distinct mono ubiquitination band as observed by anti Raf1 Western Blot.

When increased the exposure of the blot additional banding was observed correlated with the addition of 2, 3, and 4 ubiquitins (Fig 41,42).

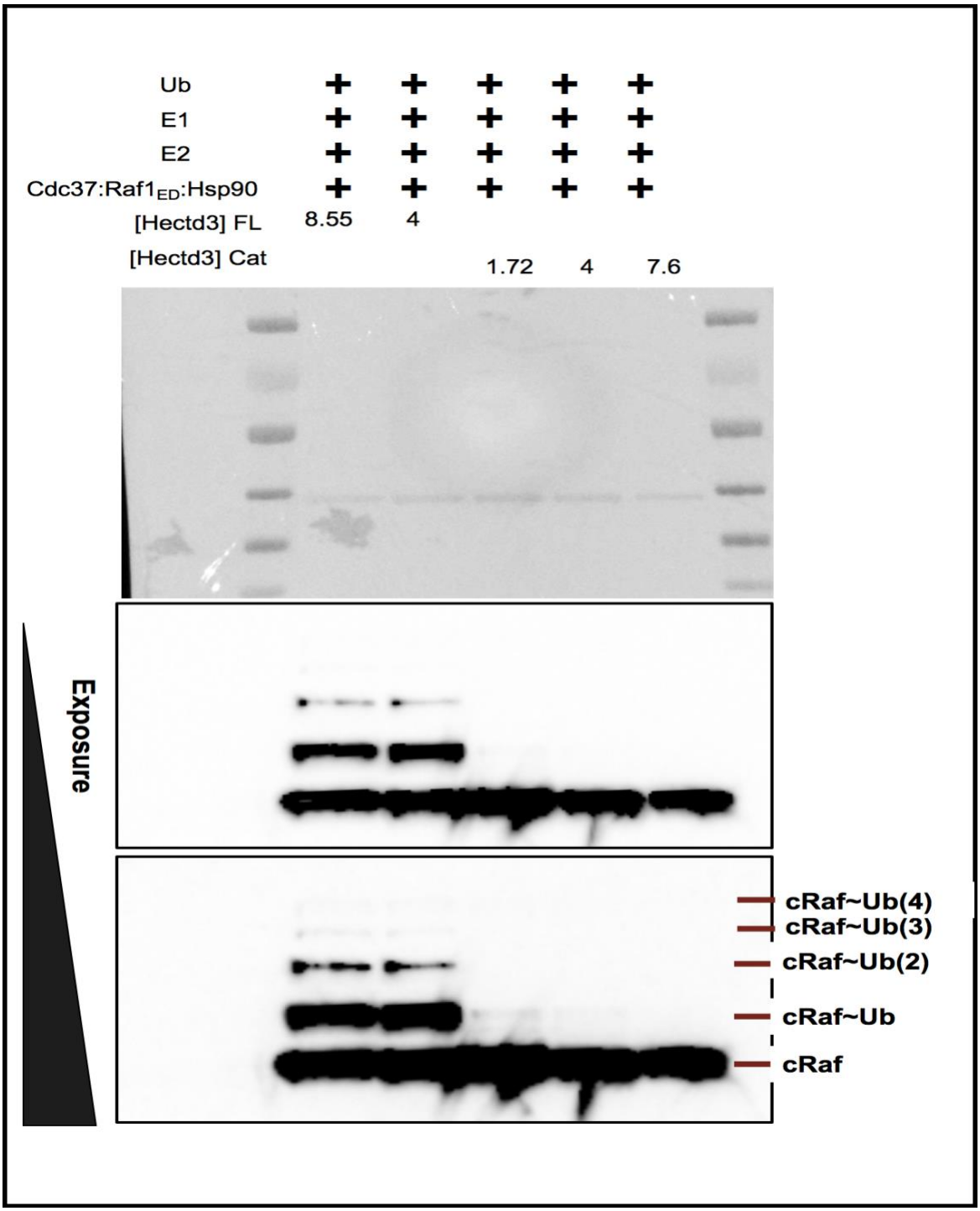

Figure 41 Hectd3 with Recognition Domain Ubiquitinates $Raf1_{KD}$ more than just the catalytic domain by itself

Western Blot Analysis of yeast expressed human Cdc37:$Raf1_{KD}$:Hsp90 ubiquitination assay. 5μM of Cdc37:$Raf1_{KD}$:Hsp90 is incubated with 1μM E1, 1μM E2, 20μM Ubiquitin, 5 mM ATP and Hectd3 at 24 C for 1 hour.

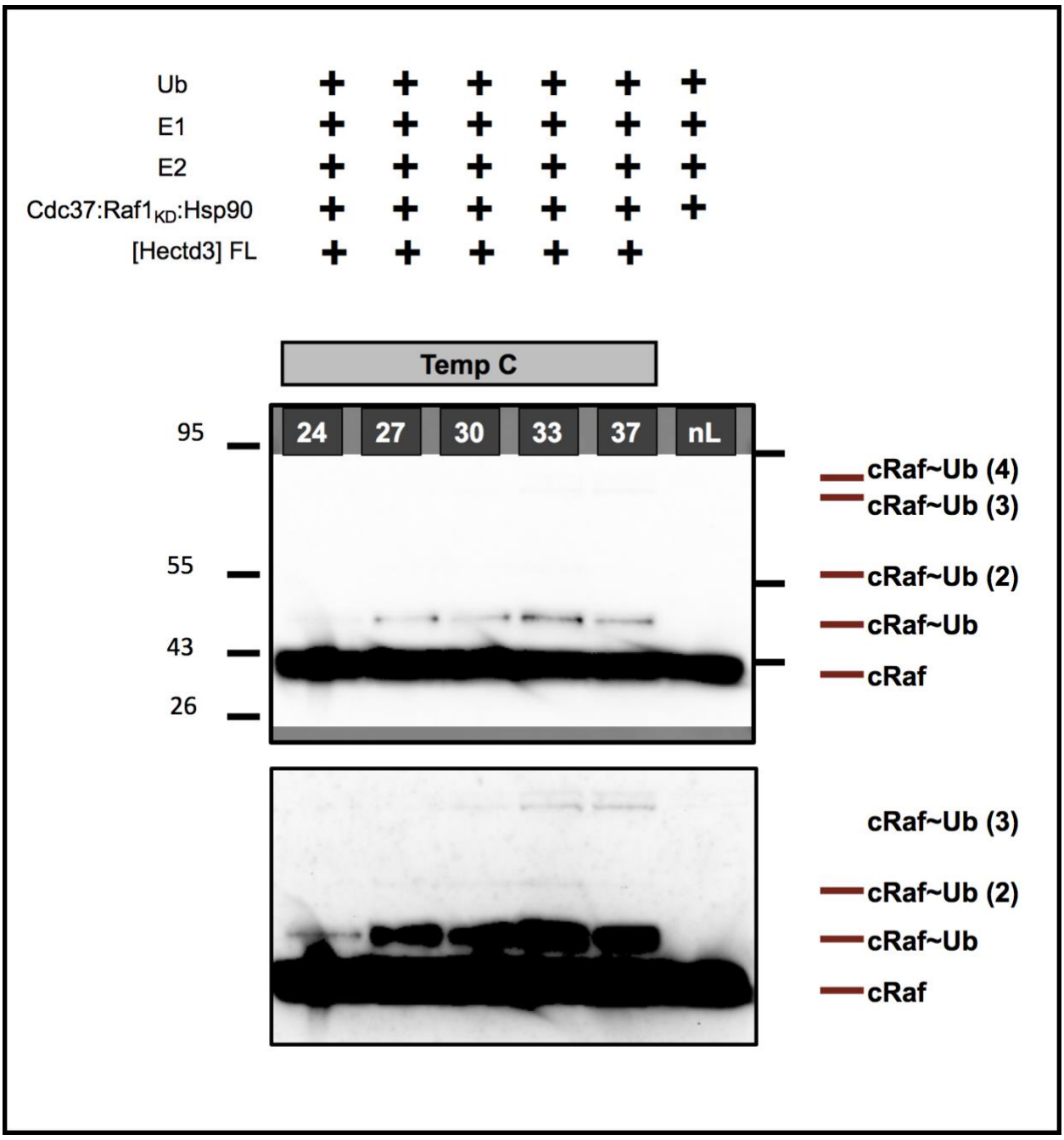

Figure 42 $Raf1_{KD}$ Ubiquitylation is Temperature Dependent

Western Blot Analysis of Cdc37:$Raf1_{KD}$:Hsp90 ubiquitination assay. 5μM of Cdc37:$Raf1_{KD}$:Hsp90 is incubated with 1μM E1, 1μM E2, 20μM Ubiquitin, 5 mM ATP and 2μM Hectd3 for 1 hour at varying incubation temperatures.

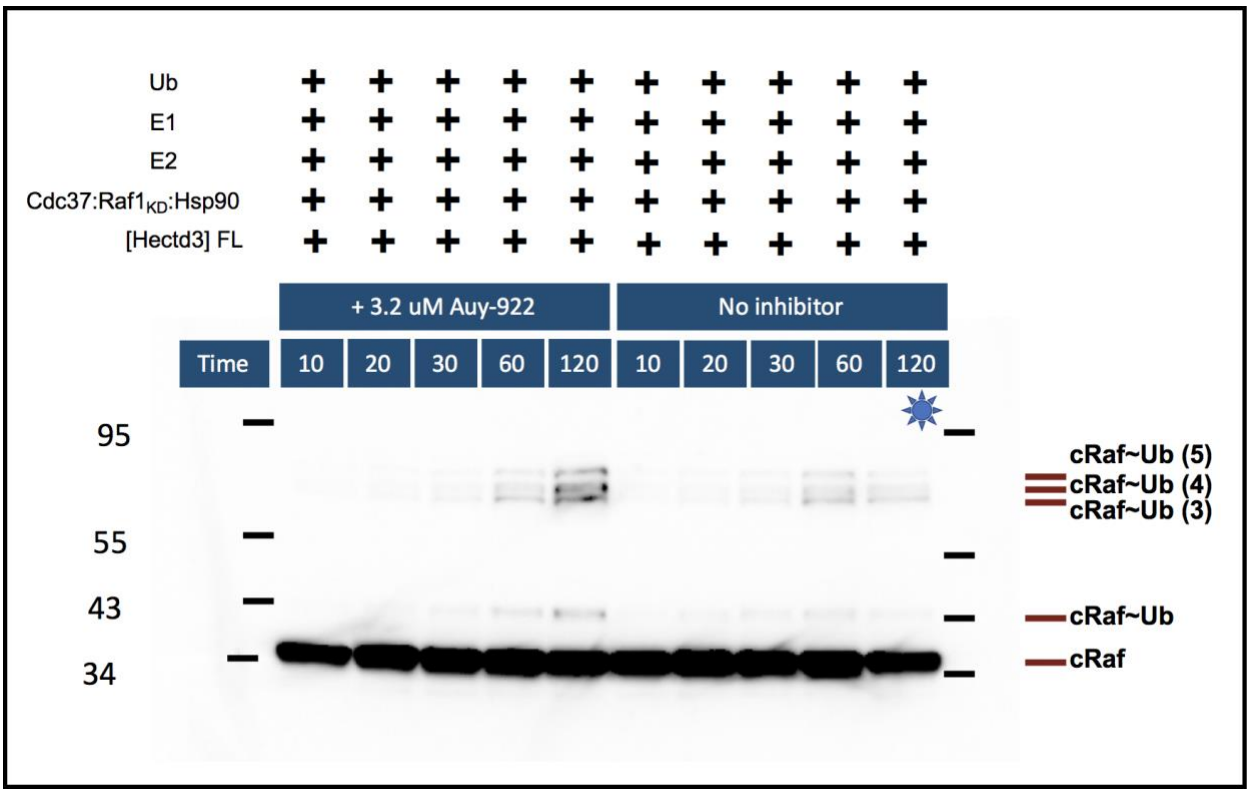

Figure 43 Hsp90 Inhibition Increases Ubiquitination

Western Blot Analysis of Cdc37:Raf1$_{KD}$:Hsp90 ubiquitination assay. 5μM of Cdc37:Raf1$_{KD}$:Hsp90 is incubated with 1μM E1, 1μM E2, 20μM Ubiquitin, 5 mM ATP and 2μM Hectd3 in the presence and absence of the Hsp90 inhibitor AUY-922 at 27 C.

Testing if incubating our complex with an Hsp90 inhibitor prior to addition of a primed Hectd3 would yield increased ubiquitination was inconclusive. Preincubation of co chaperones, either to the Hsp90:Cdc37:Raf1 Complex or to the Hectd3, E1, E2 solutions did nothing to increase the amount of Raf1 ubiquitination. In the case of HOP, the chaperone shielded Raf from ubiquitination (Fig 44).

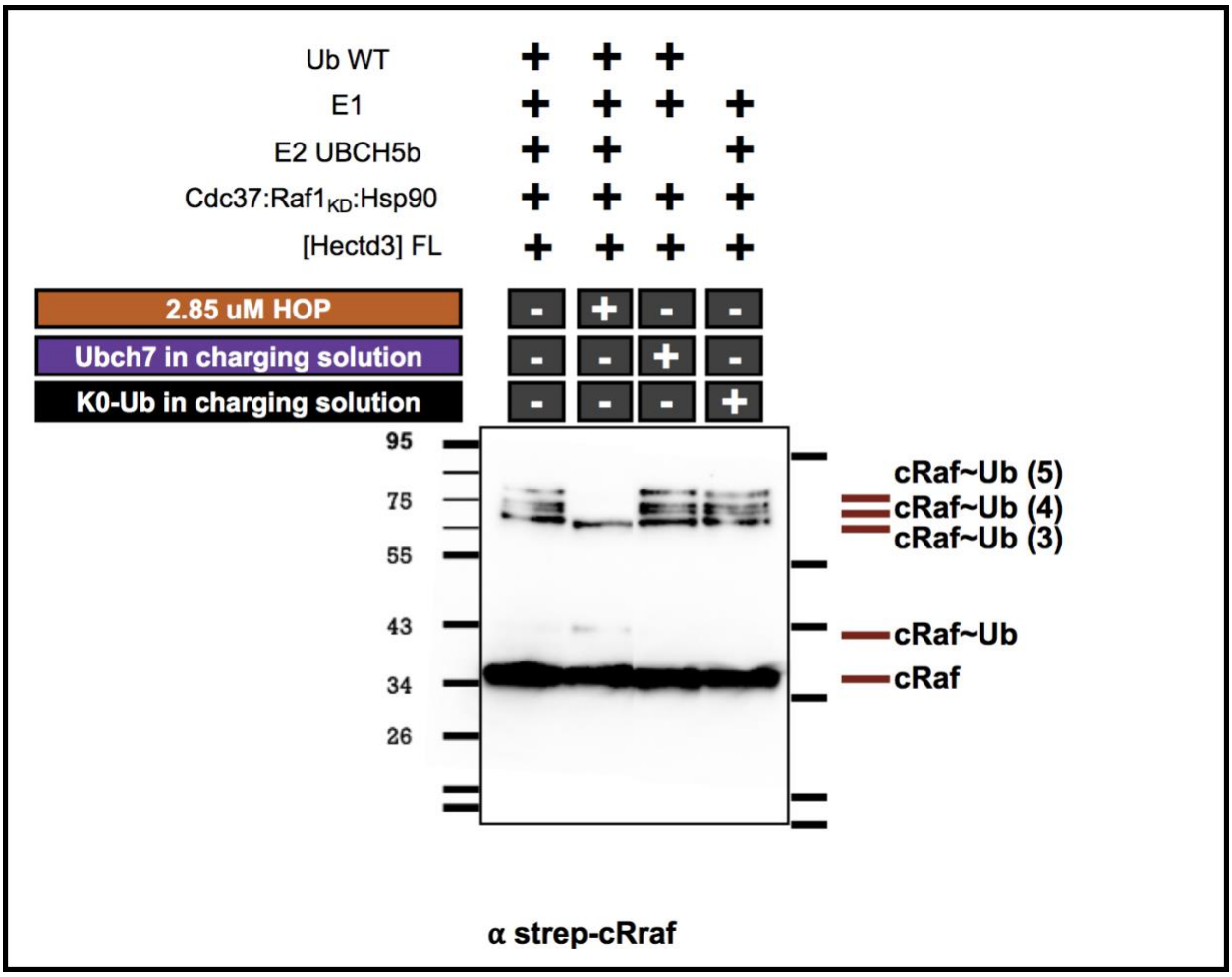

Figure 44 Hectd3 is mono ubiquitinating Raf at multiple positions

Western Blot Analysis of Cdc37:Raf1$_{KD}$:Hsp90 ubiquitination assay. 5μM of Cdc37:Raf1$_{KD}$:Hsp90 is incubated with 1μM E1, 1μM E2, 20μM Ubiquitin, 5 mM ATP and 2μM Hectd3 for 2 hours at 27C.

Utilizing Ub-K0 a mutant form of ubiquitin that prevents the formation of branched chains revealed that Hectd3 mono-ubiquitinated Raf1 at multiple positions instead of adding ubiquitin sequentially to elongate ubiquitin chains (Fig 44).

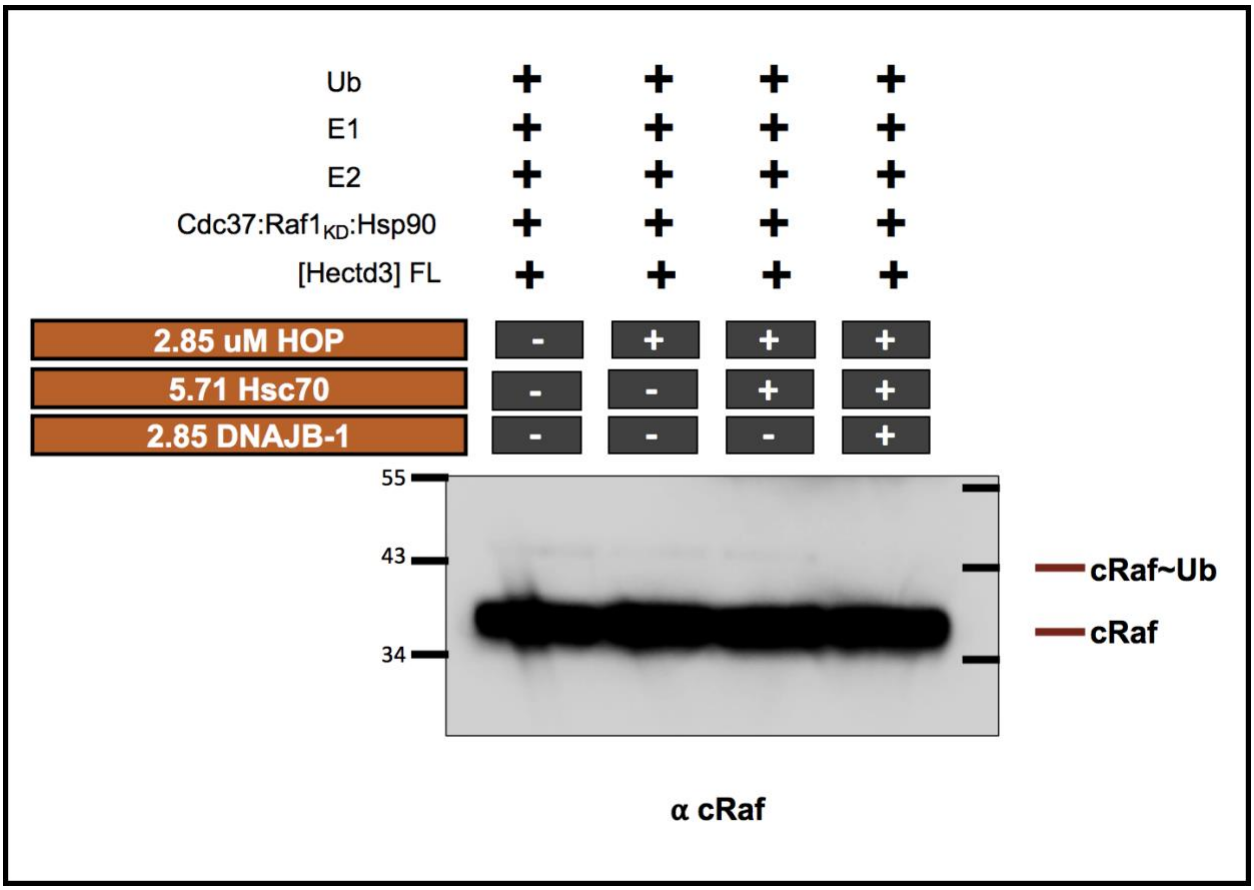

Figure 45 HOP, Hsp40 and Hsp70 do not increase mono ubiquitination

Western Blot Analysis of Cdc37:Raf1$_{KD}$:Hsp90 ubiquitination assay. 5μM of Cdc37:Raf1$_{KD}$:Hsp90 is incubated with 1μM E1, 1μM E2, 20μM Ubiquitin, 5 mM ATP and 2μM Hectd3 for 1 hour at 27C.

With our biggest gain in ubiquitination coming from the increase in temperature we hypothesized that Hsp90 opening was the limiting factor of our ubiquitin. We compared the ubiquitination of Raf1 kinase domain in complex with Hsp90 and Cdc37 with an extended kinase construct in complex with Hsp90 and Cdc37. This extended construct contained an additional 30 amino acids on its N-terminus. Surprisingly the Extended Kinase Complex was more stable than just he Kinase domain of Raf, resulting in less

ubiquitination (Fig 46). Despite my best efforts the ubiquitination observed was always a low percentage of the total kinase in the test tube. Control experiments and the sheer amount of ubiquitination that occurs on Hectd3 tells us that our components are capable of ubiquitinating but we are potentially missing a factor that drives that ubiquitination towards Raf1. Kinase maturity in the cell is often times measured by auto phosphorylation. A mature Raf is known to be phosphorylated at positions S259 S621. Once phosphorylated these positions become anchor points for 14-3-3's where they can be held in positions before activation. Even though this construct lacks these stabilizing phosphor-sites it was possible that other phosphor-sites gave stability that prevented Hectd3 from properly ubiquitinating Raf1. Treatment the Hsp90:Cdc37:Raf1 complex with a general phosphatase did nothing to increase ubiquitination.

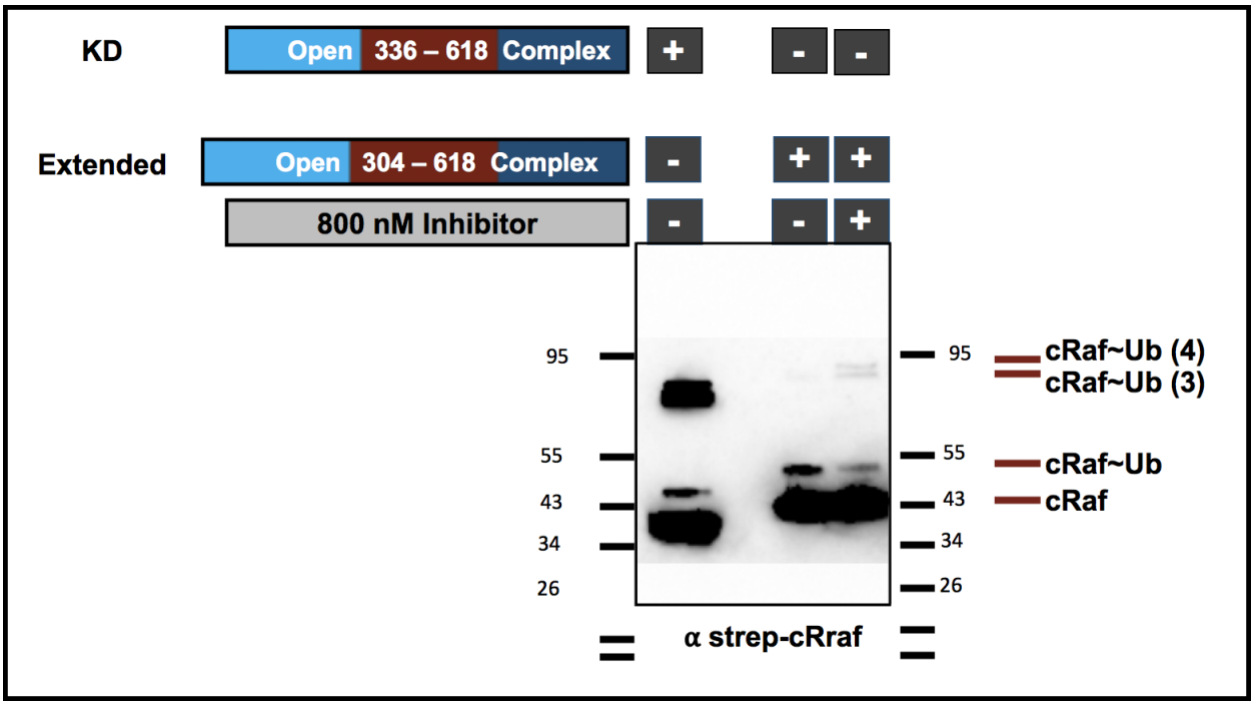

Figure 46 Extended Kinase more stable than KD

Western Blot Analysis of Cdc37:Raf1$_{KD}$:Hsp90 ubiquitination assay. 5μM of Cdc37:Raf1$_{KD}$:Hsp90 is incubated with 1μM E1, 1μM E2, 20μM Ubiquitin, 5 mM ATP and 2μM Hectd3 for 1 hour at varying incubation temperatures.

It is entirely possible that another co-factors exist that assists in the opening of Hsp90, or poises Hectd3 in such a way to polyubiquitinate Raf exists. It is also plausible that mono ubiquitination by Hectd3 also is sufficient to bias the kinase toward a degradative end. With other E3 ligases adding the K68 polyubiquitin chains on the mono ubiquitin first placed by Hectd3.

In-Vitro Unnatural Amino Acid Crosslinking

The transient nature of Hectd3's interactions with the Raf Hsp90 complex makes it difficult to study structurally. Our non-specific crosslinking allowed us to visualize additional density that we could assign to Hectd3 but not to the resolution where we could build a model of Hectd3 to understand what part of the ligase was interacting with the kinase chaperone module. In an attempt to validate as well as further stabilize Hectd3's interactions with Hsp90:Cdc37:Raf1 complex we utilized the incorporation of photoactivatable unnatural amino acids. Their incorporation into proteins have been used to capture interactions that are transient and of moderate affinity both in vivo and in vitro. Unnatural amino acids have been used both in many studies of chaperones and their substrates. Photoactivated crosslinkers have been used to identify catalytically important interactions of the Hectd3 ligase E6AP[67]. Similar strategies were used to develop E2-SUMO probes to capture adaptor like SUMO E3 ligases[68]. The structures of RING domains bound to stable mimics of E2-Ub and Ub-Ubl intermediates have shown consensus noncovalent interaction between E3,E2 and Ub[69–74]. The unnatural amino acid BPA (p-benzoyl-L-phenylalanine) was incorporated into ubiquitin in order to stabilize E2~Ub intermediates on RING domains. The BPA-Ub probe reacted with purified RNF4 in vitro and with CBL in cell lysates under conditions known to stimulate native interactions[75].

pBPA is activated from crosslinking through the formations of a diradical species generated by the exposure of UV light (350-365 nm). If a C-H bond of amino acid side

chains or back bones are within proximity, hydrogen atom abstraction followed by radical recombination will yield a covalent crosslink. The reactivity radius of pBPA crosslinking is generally between 3 to 5 angstroms[76].

pBPA replacement for the purpose of crosslinking an interface must also be optimized experimentally. pBPA is a bulky amino acid and has the power to disrupt an interface if replacing an amino acid that is nestled in a tight interface. Before we probed potential interfaces involving Hectd3 we wanted to validate that our crosslinking worked in the Hsp90-Cdc37-Kinase system. We utilized $Hsp90_{pBPA451}$ to ensure the formation of a closed Hsp90:Cdc37 sbRaf complex.

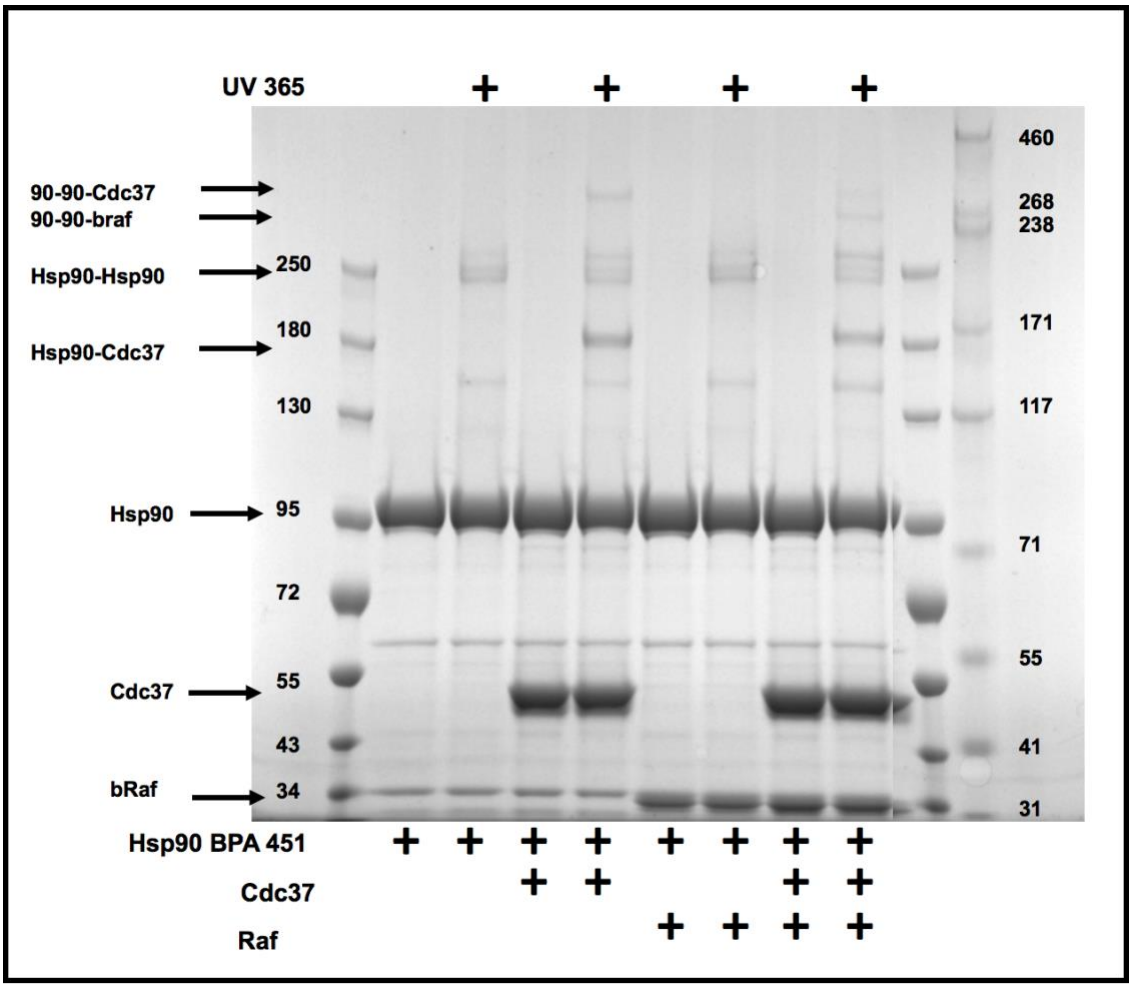

Figure 47 Hsp90 BPA 451 Validates Formation of HCRaf Complex

Coomassie Stained SDS-PAGE gel of pBPA crosslink products. 10μM Hsp90, 10μM Phosphorylated Cdc37 and 10μM sbRaf were incubated at RT for 1 hour in 50 mM HEPES 7.5, 50mM KCl, 5% Glycerol, 1 mM TCEP, 5 mM ATP, 5 mM $MgCl_2$ for 1 hour at 26C and then exposed to UV 365 nm for crosslinking for 1 hour at 4C.

The pBPA placement at 451 of Hsp90 puts the crosslinking amino acid in a great position to interact with clients or co-chaperones. Satisfying here we see the formation of Hsp90-Cdc37-Hsp90 and Hsp90-bRaf-Hsp90 crosslinks indicating the formation of a closed Hsp90:Cdc37:bRaf Complex (Fig 47). Additionally crosslinking with HOP shows

a robust interaction (Fig 48). Although not as robust of an interaction as with HOP, Hsp90 crosslinks with Hectd3 as it is a known client. With our crosslinking protocol established we moved to stabilizing novel Hectd3:Cdc37 and Hectd3:sbRaf interfaces.

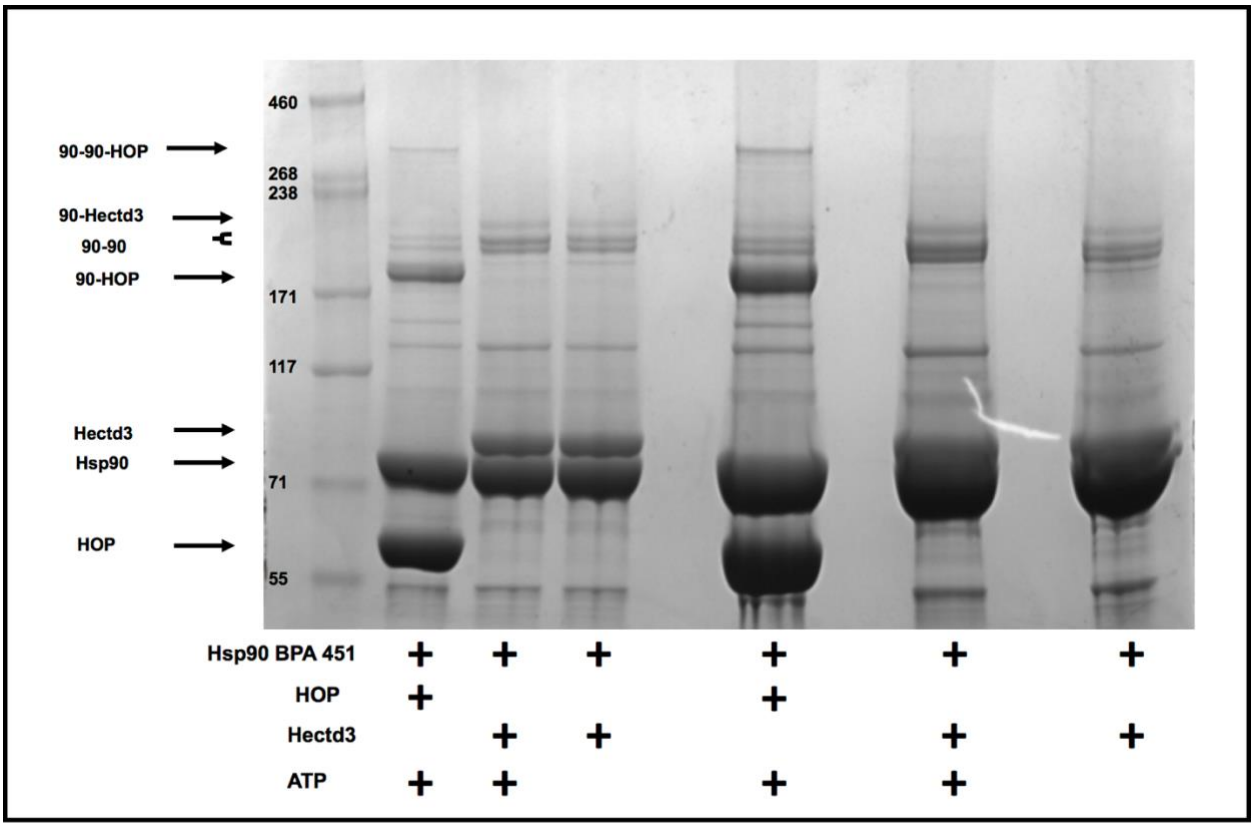

Figure 48 Hsp90 BPA 451 validates the association with HOP and Hectd3

Coomassie Stained SDS-PAGE gel of pBPA crosslink products. 10μM Hsp90, 5μM Hectd3 or 10μM HOP were incubated at RT for 1 hour in 50 mM HEPES 7.5, 50mM KCl, 5% Glycerol, 1 mM TCEP, 5 mM ATP, 5 mM $MgCl_2$ for 1 hour at 26C and then exposed to UV 365 nm for crosslinking for 1 hour at 4C.

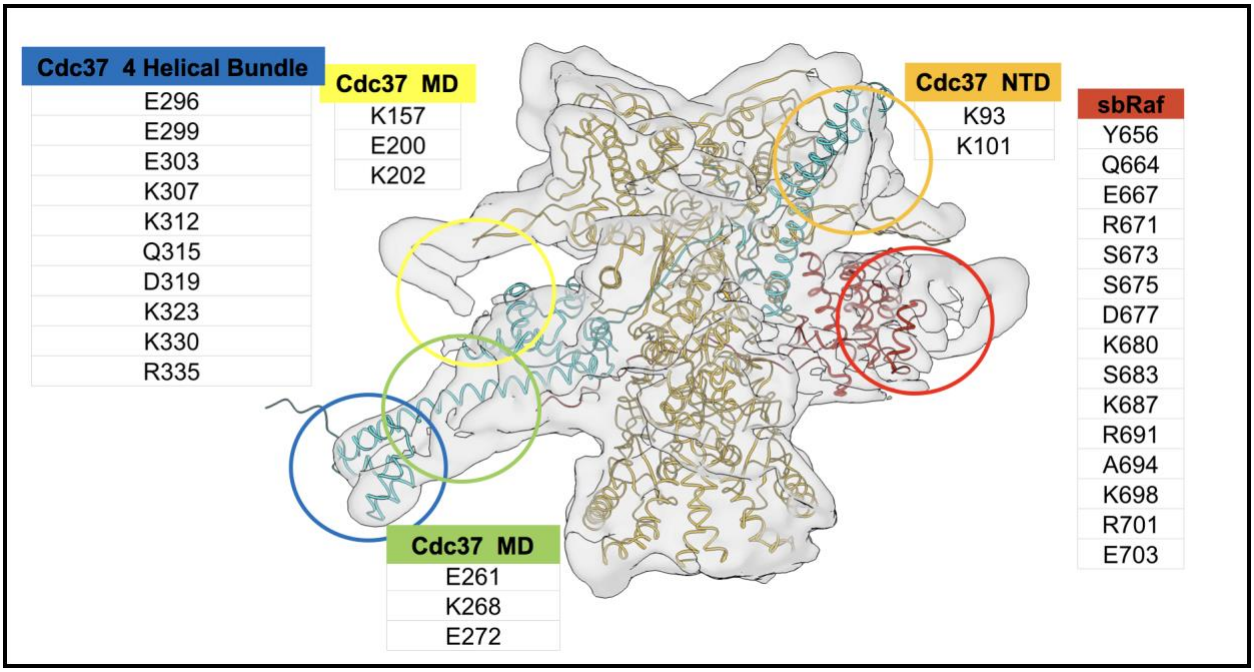

Figure 49 pBPA Mutants Designed at Interfaces of New Density

Model of Cdc37:Raf1$_{KD}$:Hsp90:Hectd3$_{X}$ was used to identify residues that could potentially crosslink with the novel EM density. 15 pBPA mutants were design on the C-lobe of sbRaf (circled in red). 18 mutants were designed in Cdc37, 2 on the N-terminal helixes (circled in orange), 3 at the Middle Domain (MD) extending toward the Hsp90 charged linker (circled in yellow), 3 at the MD extending toward sbRaf or Hectd3, and 10 at Cdc37's C-Terminal 4 helical bundle (circled in blue) which seems to be stabilized by Hectd3.

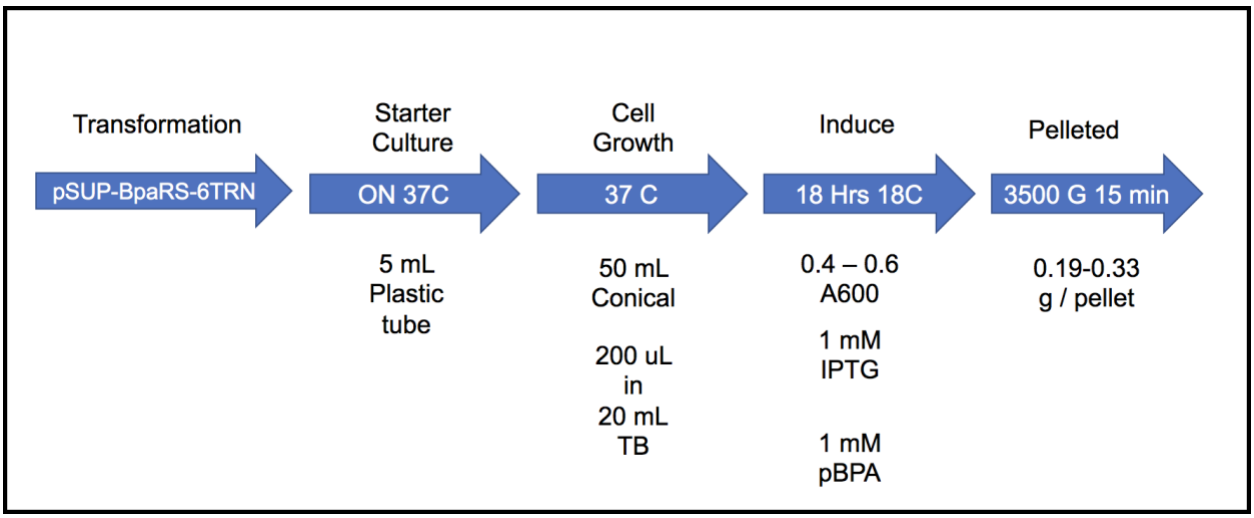

Figure 50 Work Flow for Expression of Cdc37 and sbRaf pBPA Mutants

pSUP-BpaRS-6TRN bacterial cells were transformed and a smear of colonies was collected to inoculate a 5mL starter culture to grown overnight. 200 uL of the started culture was added to 20 mL of TB and shaken at 37C in a 50 mL falcon tube. At A600 0.4 – 0.6, 1 mM IPTG, 1 mM pBPA and .02% galactose as added and cultures was grown for 18 hours at 18C. Media was pelleted at 3500 G and yielded between 0.19 and 0.3 g.

We set about designing a protocol where we would be able to test a vast amount of pBPA mutants. Utilizing the model we built into the EM density of our Cd37:Hsp90:Raf1$_{KD}$:Hectd3$_{x}$ data set. Looking at potentially interesting interfaces we designed 15 sbRAf mutants and 18 Cdc37 mutants (Fig 49). We chose to move to sbRaf as it as comparable kinase that can be relatively easily depressed in bacterial cells.

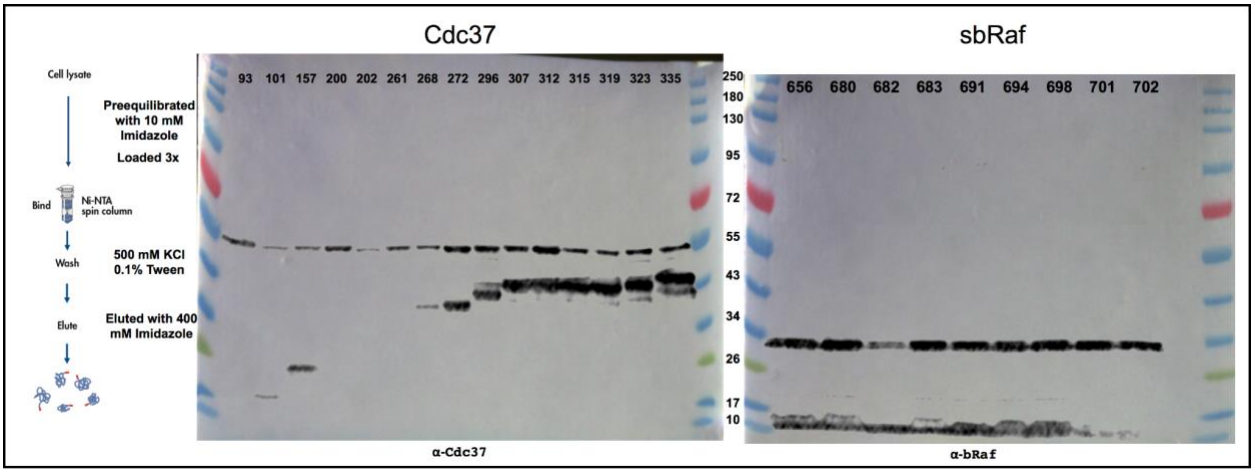

Figure 51 pBPA mutants of Cdc37 and sbRAf can be batch expressed and purified

Western blot analysis of protein elution after purification through quick Ni-NTA columns. Cell lysates incubated with B-PER lysis reagent for 15 min at 24C. Lysate was spun and soluble fraction was loaded onto a preequilibrated Ni-NTA column. Column was washed with 500 mM KCl with 0.1% Tween and eluted with 400 mM Imidazole.

Growth in small 25 mL cultures allowed for the expression of several constructs at a time (Fig 50). Utilizing nickel spin clowns allowed for the quick purification of several constructs at a time (Fig 51). After the elution of our constructs from the nickel columns we continued by adding the necessary components to the eluate in order to form and stabilize a closed complex (Fig 52). This complex would mimic the complex from our Cryo-EM data sets in order to validate our hypothesized Hectd3 interaction interfaces.

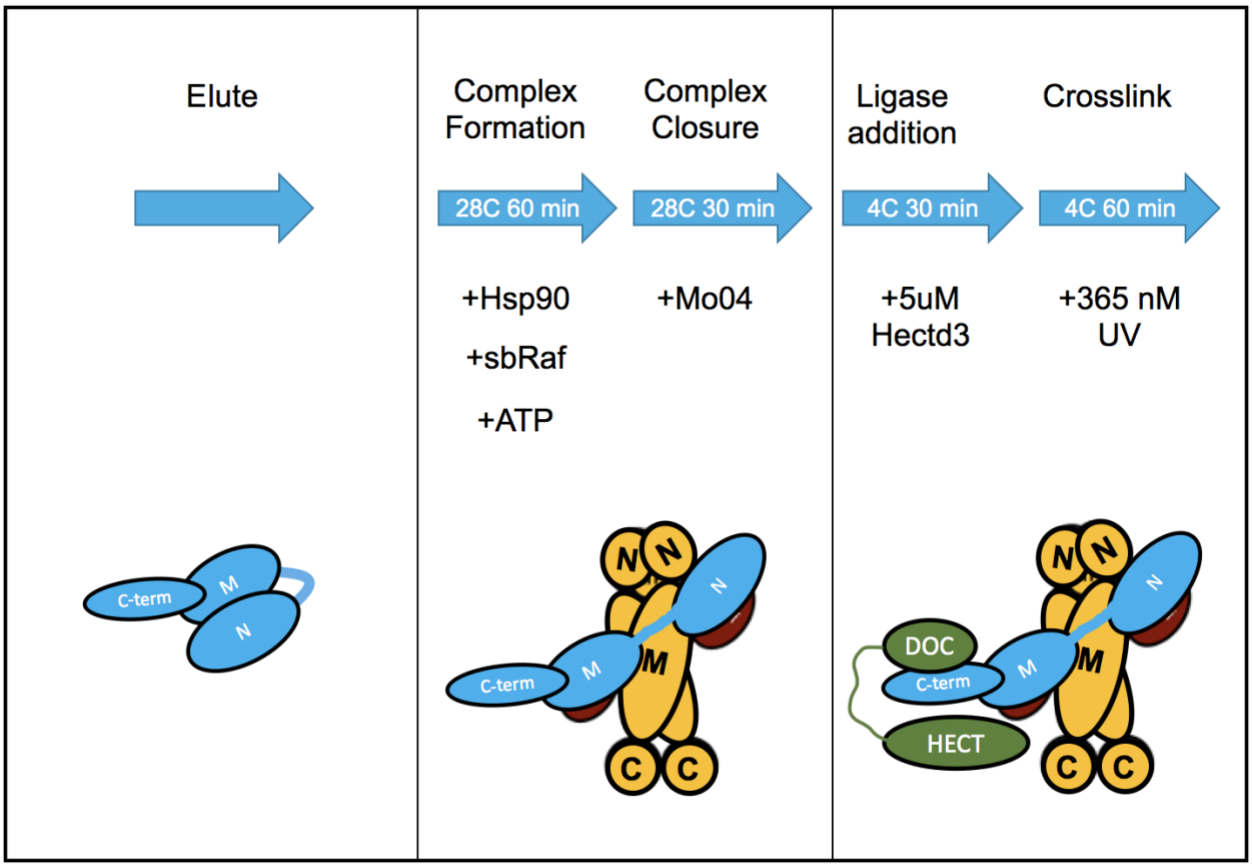

Figure 52 Purified Component Can Make a Hsp90 Cdc37 Complex

Schematic of how to make Hsp90:Cdc37:Kinase complexes from purified components. Phosphorylated Cdc37 can be incubated with Hsp90, sbRaf and 5 mM ATP to form a 3 component complex. Molybdate can then ensure the closure of Hsp90. Hectd3 can then be incubated with the closed complex and exposed to UV light to activate the crosslinker on the pPBA Cdc37 mutants.

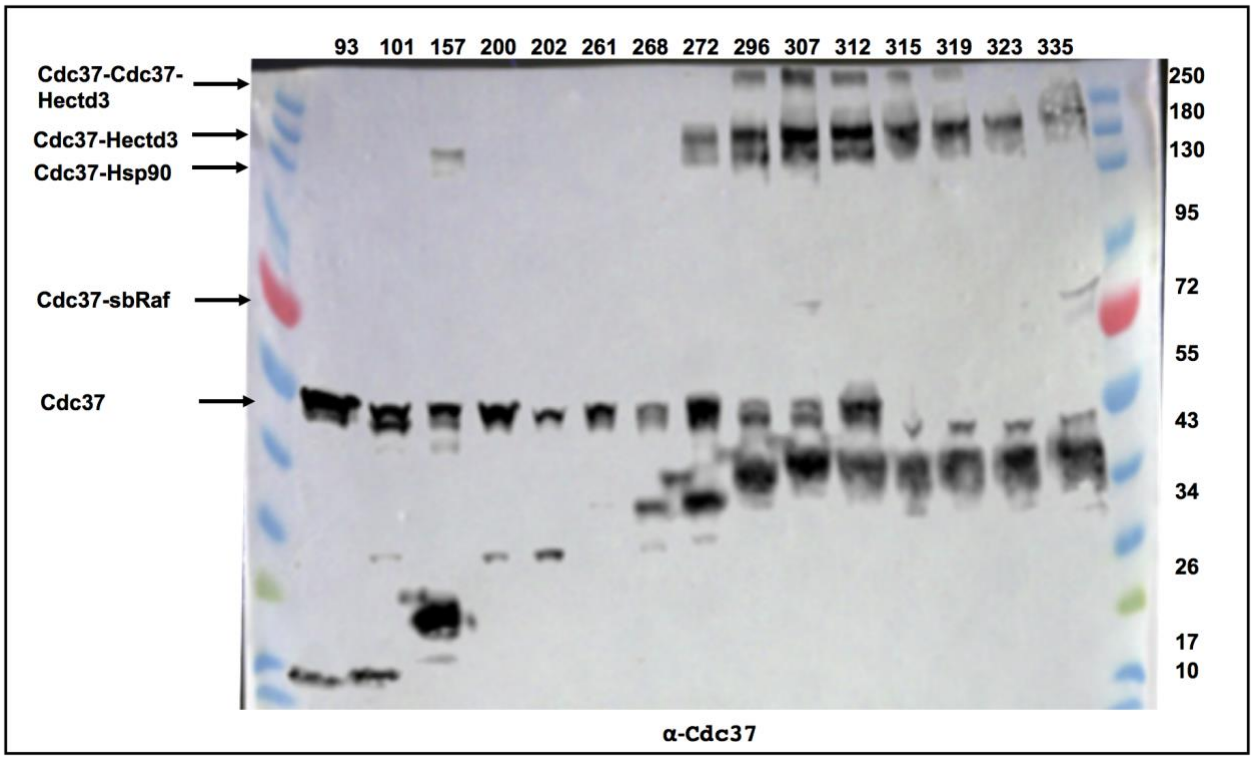

Figure 53 pBPA Cdc37 exhibits robust crosslinking

Western Blot Analysis of pBPA crosslinking reactions. Cdc37 elution fractions are phosphorylated and incubated with Hsp90 and sbRaf for 1 hour at 28C. Hectd3 is added and then incubated at 4C for one hour before exposure to UV light at 4C for 1 hour.

I tested a panel of 15 Cdc37 pBPA mutants and after crosslinking we saw quite a variety of crosslinking patterns. The pBPA mutants on the middle and C-terminal domains of Cdc37 exhibited the most crosslinking (Fig 53). A coomassie stained SDS gel informed us that the nickel spin columns were quick but produced protein dirty enough to muddle results. We decided to take a handful of Cdc37 mutants that exhibited different crosslinking patterns and scale up for a full expression and

purification. Having more and cleaner protein allowed us to draw more conclusive results.

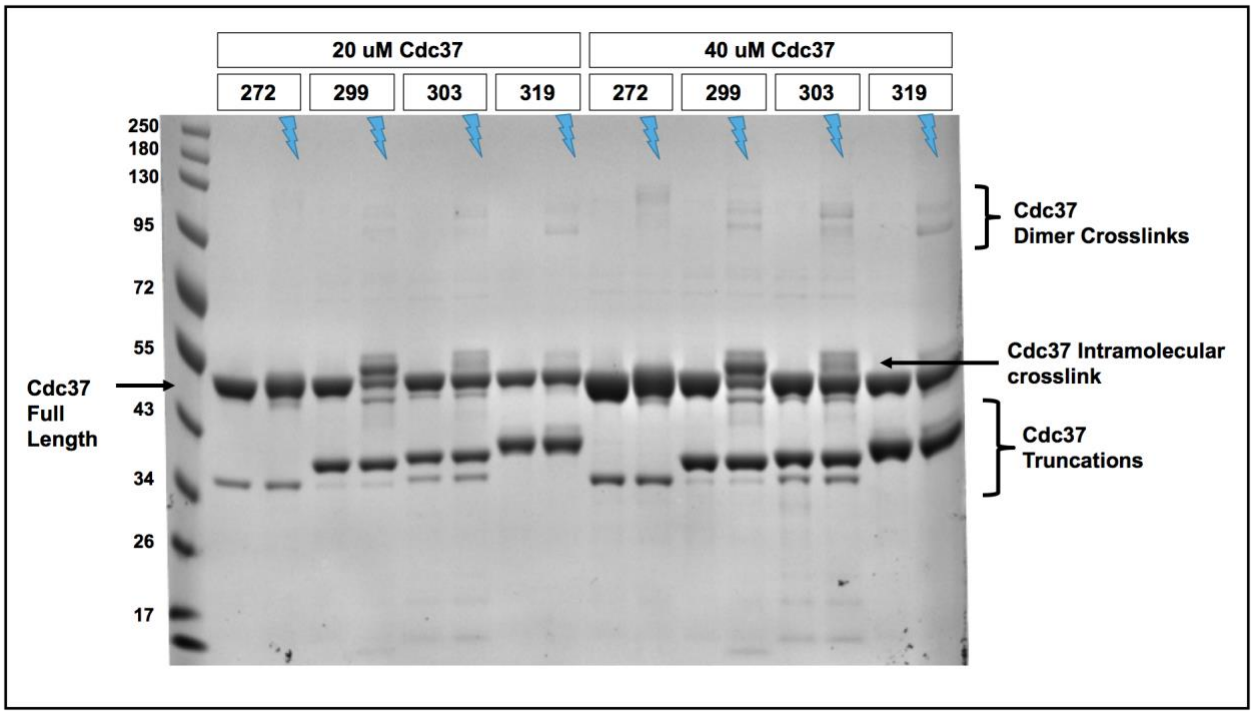

Figure 54 pBPA Cdc37 Exhibits Intra and Intermolecular crosslinking

Coomassie stained SDS-PAGE gel of pBPA crosslinking experiments for Cdc37 select mutants. 10μM Cdc37 pBPA mutants are incubated for 1 hour at 28C before being crosslinked at 4C for 1 hour.

In vitro Cdc37 was observed to form intra and intermolecular crosslinks (Fig 54). Cdc37 dimerization has been previously observed to occur via Cdc37's middle domain. When incubated with sbRaf, Hsp90 and Hectd3, $Cdc37_{pBPA272}$ was observed to make strong crosslinks with Raf1 (Fig 55).

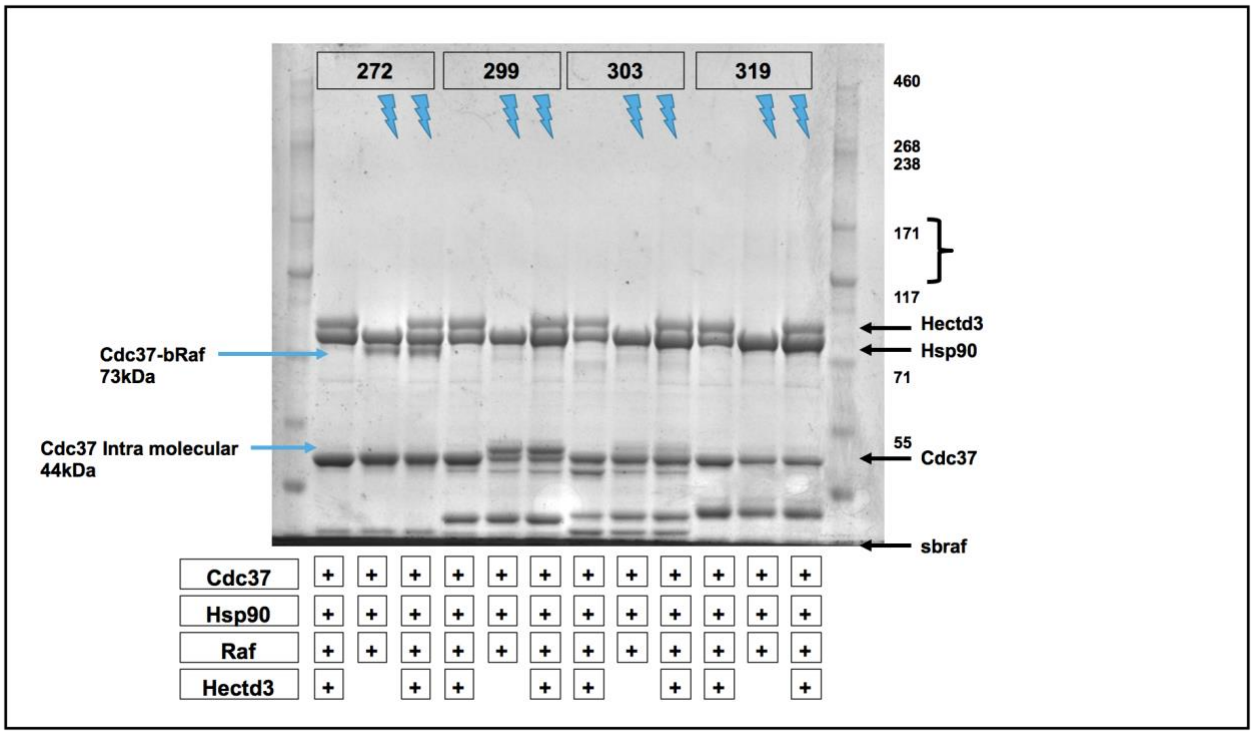

Figure 55 pBPA Cdc37 Exhibits Crosslinking to sbRaf

Coomassie stained SDS-PAGE gel of Cdc37 pBPA complex crosslinking. 10μM Cdc37 pBPA mutants are incubated for 1 hour at 28C before being crosslinked at 4C for 1 hour. 4μM phosphorylated Cdc37 pBPA mutants are incubated with 4μM Hsp90, 4μM sbRaf and 4μM Hectd3 at 28 C for 1 hour before closing at 4C for 1 hour.

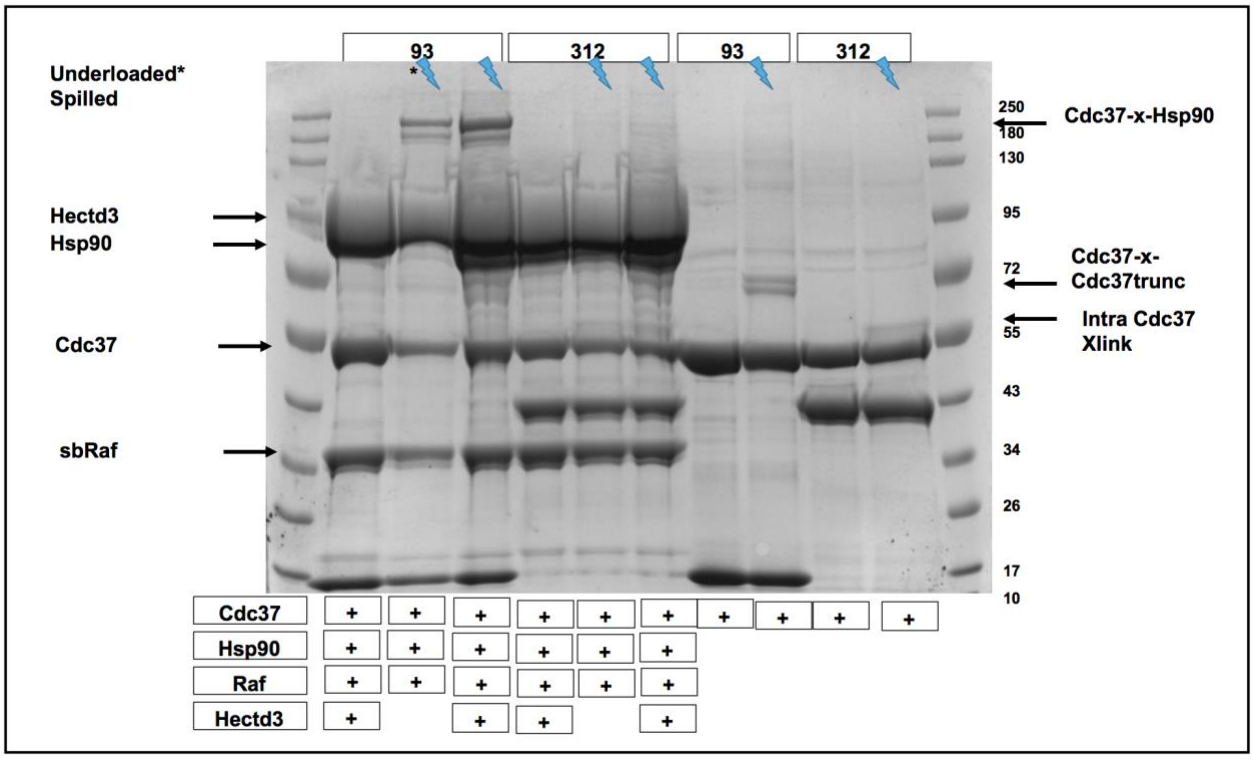

Figure 56 pBPA Cdc37 Exhibits Crosslinking to Hsp90

Coomassie stained SDS-PAGE gel of Cdc37 pBPA complex crosslinking. 10μM Cdc37 pBPA mutants are incubated for 1 hour at 28C before being crosslinked at 4C for 1 hour. 4μM phosphorylated Cdc37 pBPA mutants are incubated with 4μM Hsp90, 4μM sbRaf and 4μM Hectd3 at 28 C for 1 hour before crosslinking at 4C for 1 hour.

To absolutely ensure that all crosslinks are occurring in a closed complex that mimic our Cryo-EM data set we set about to further purify our complex before any crosslinking occurs. We set out to form Hsp90:Cd37$_{pBPA}$:Raf complex and purify any excess Cdc37 that could potentially confound the crosslinking results. Incubating our phosphorylated pBPA Cdc37 with Hsp90 and sbRaf at 28C for 1hour in the presence of ATP formed a 3 component complex. Cdc37 $_{pBPA344}$ and Cdc37 pBPA322 both formed complexes with Hsp90 and sbRaf that gave identical SEC traces when compared to WT Cdc37 (Fig 57).

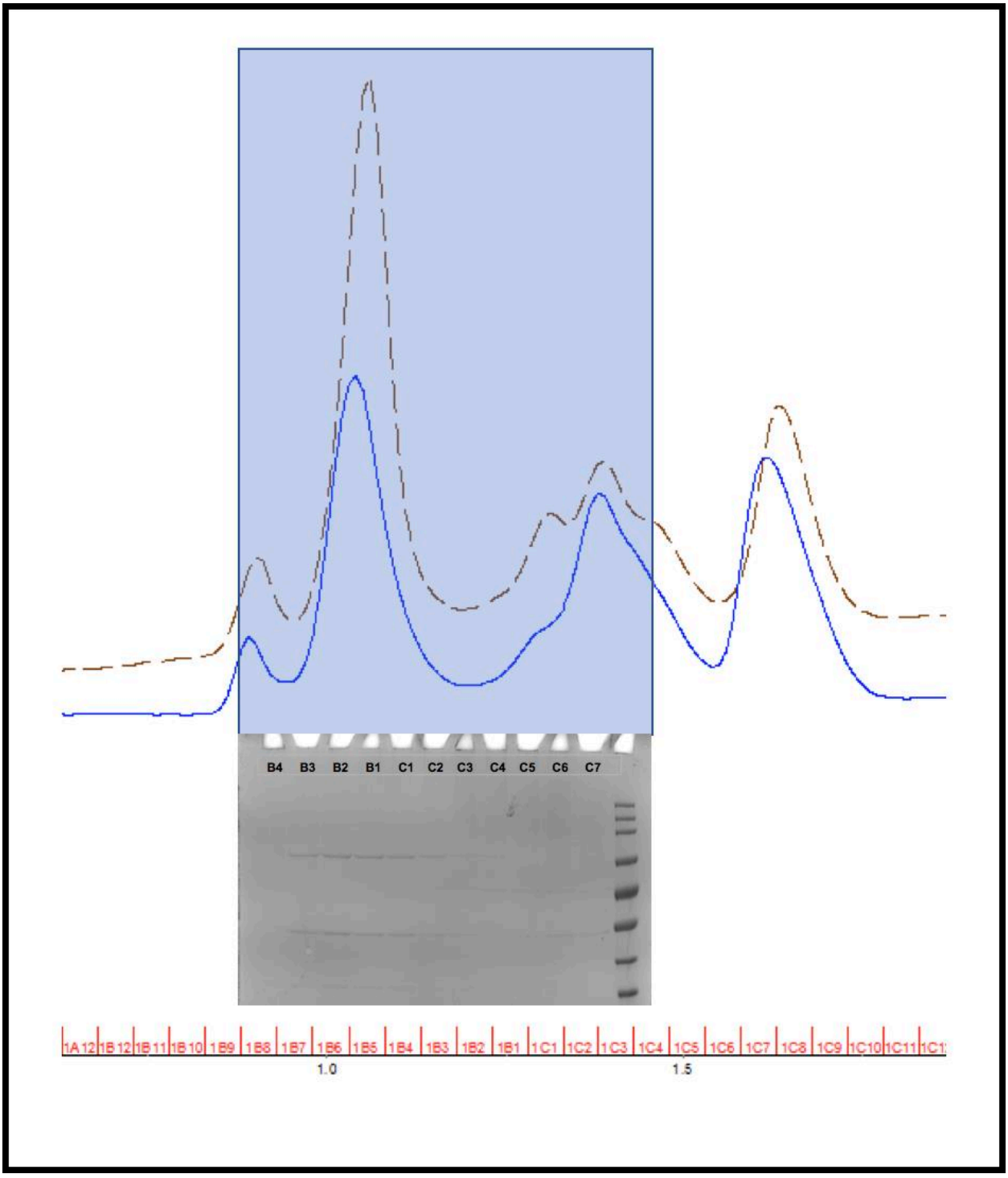

Figure 57 Cdc37 344 and 322 Form a complex with Hsp90 and sbRaf

A. SEC Chromograph showing Complex formation of WT (blue) and Mutant (dotted brown) Cdc37 with HSp90 and bRaf. 5μM Hsp90 is incubated with 5μM sbRaf and 5μM phosphorylated Cdc37

Hsp90 sbRaf and phosphorylated Cdc37 $_{pBPA\ 344}$ were incubated with 5 mM ATP in 50 mM KCl, 5% glycerol, 1 mM TCEP and 5 mM $MgCl_2$ for 1 hour at RT. 5 mM Sodium Molybdate was added and allowed to incubate at RT for 30 min. Samples was filtered through a 0.1 micron spin filter and run through a 3.2 s200 analytical column.

Alexa 488 fluorescently labeled Hectd3 was added to fractions that contained the Hsp90-:Cdc37:sbRaf tertiary complex. Hectd3 fluorescently labeled with Alex 488 was incubated with the complex at RT for 1 hour and then exposed to UV light for 20 min at 4C.

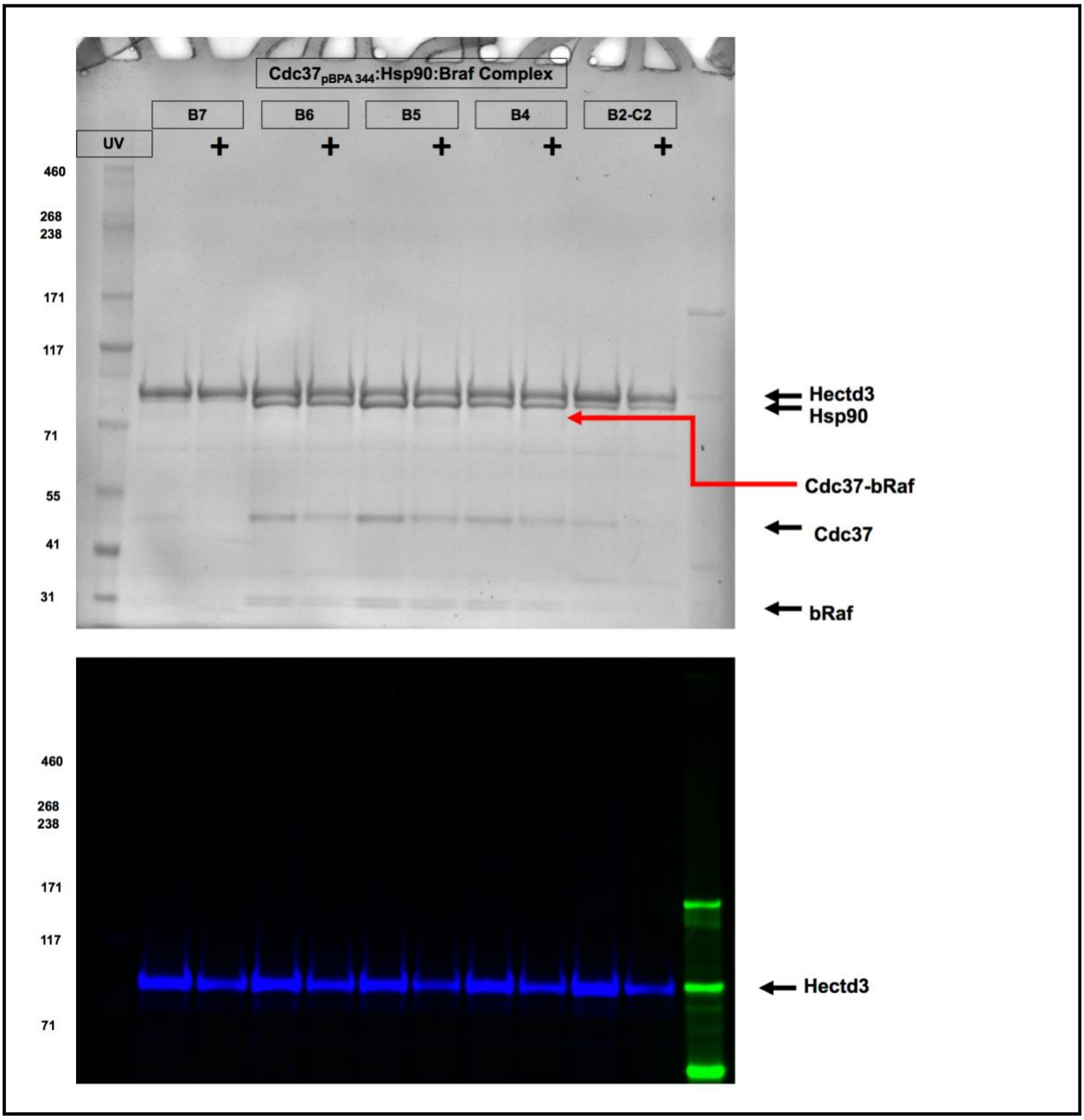

Figure 58 Cdc37 trapped in complex with Hsp90 and bRaf crosslinks

A. Coomassie stained gel loaded with the fractions that contained 3 component complex of Hsp90:Cdc37:and bRaf
B. Visualization of fluorescently labeled Hectd3

Interestingly the Cdc37 band appears to dissipate in intensity when exposed to ultraviolet light, signifying the formation of Cdc37 crosslinked species. While there is not

a single distinct and strong band visible a faint Cdc37-bRaf band appears. Visualizing just the fluorescent single of the Hectd3, a dissipation in signal intensity in UV treated samples is observed (Fig 58). Even with heavy exposure no distinct band of Hectd3 could be observed (Fig 59).

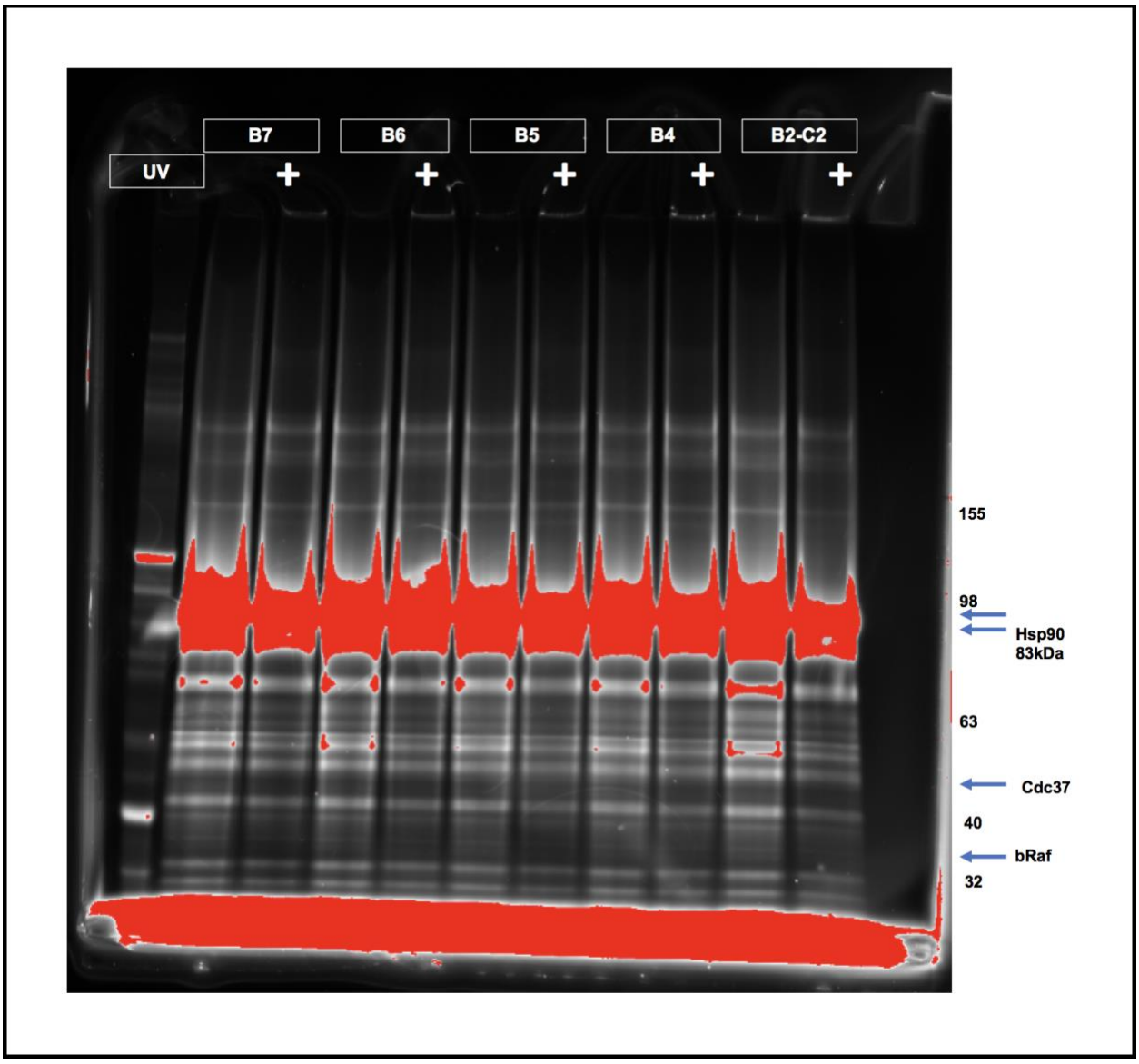

Figure 59 Cdc37 trapped in complex with Hsp90 and bRaf crosslinks
Hight exposure visualization of fluorescently labeled Hectd3

Two bands appear in the crosslinked vs the non crosslinked control On a bit below the 155 kDa marker. This could signify a faint Cdc37-Hectd3 crosslink. Notably there is a population of crosslinked Hectd3-Cdc37 that gets caught in the wells of the gel. Protein aggregation can cause this, perhaps the crosslinking of Cdc37 destabilizes Hectd3 to the point of aggregating.

When $Cdc37_{pBPA334}$ is incubated with itself, no robust crosslinking from dimerization is observed. Incubating with sbRaf yields a robust Cdc37-bRaf crosslink to the point where the normal Cdc37 band shifts up in a coomassie gel. When $Cdc37_{pBPA334}$ is incubated with bRaf and excess Hsp90 Cdc37 crosslinks with Hsp90. When $Cdc37_{pBPA334}$ is incubate with bRaf and excess Hsp90 and Hectd3 it crosslinks with Hsp90 and Hectd3. The Hectd3 crosslink profile is extremely broad, suggesting that Hectd3 interacts with Cdc37 interacts with $Cdc37_{pBPA334}$ in a myriad of ways (Fig 61). There is an extreme excess of Hsp90 and Hectd3, which means that a these crosslinks are more than likely coming from a state that is different from the one we seen in our structure. These crosslinks satisfyingly disappear if we perform the same reaction with a Hectd3 that lacks its recognition domain (Fig 60). Work that follows continue to attempt to quantify the crosslink efficiency at all relevant interfaces of the structure.

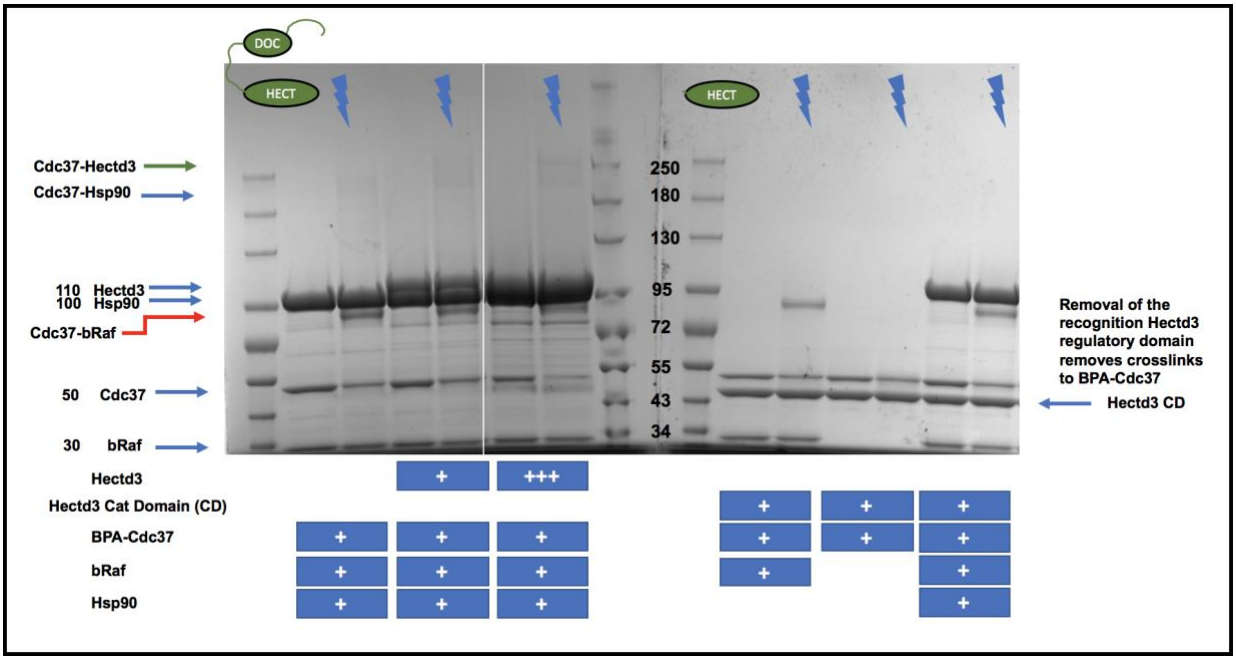

Figure 60 Cdc37 $_{pBPA\ 344}$ Crosslinks to bRaf and Hectd3

Coomassie stained SDS-PAGE gel of Cdc37 pBPA complex crosslinking. 10μM Cdc37 pBPA mutants are incubated for 1 hour at 28C before being crosslinked at 4C for 1 hour. 4μM phosphorylated Cdc37 pBPA mutants are incubated with 4μM Hsp90, 4μM sbRaf and 4μM Hectd3 at 28 C for 1 hour before closing at 4C for 1 hour.

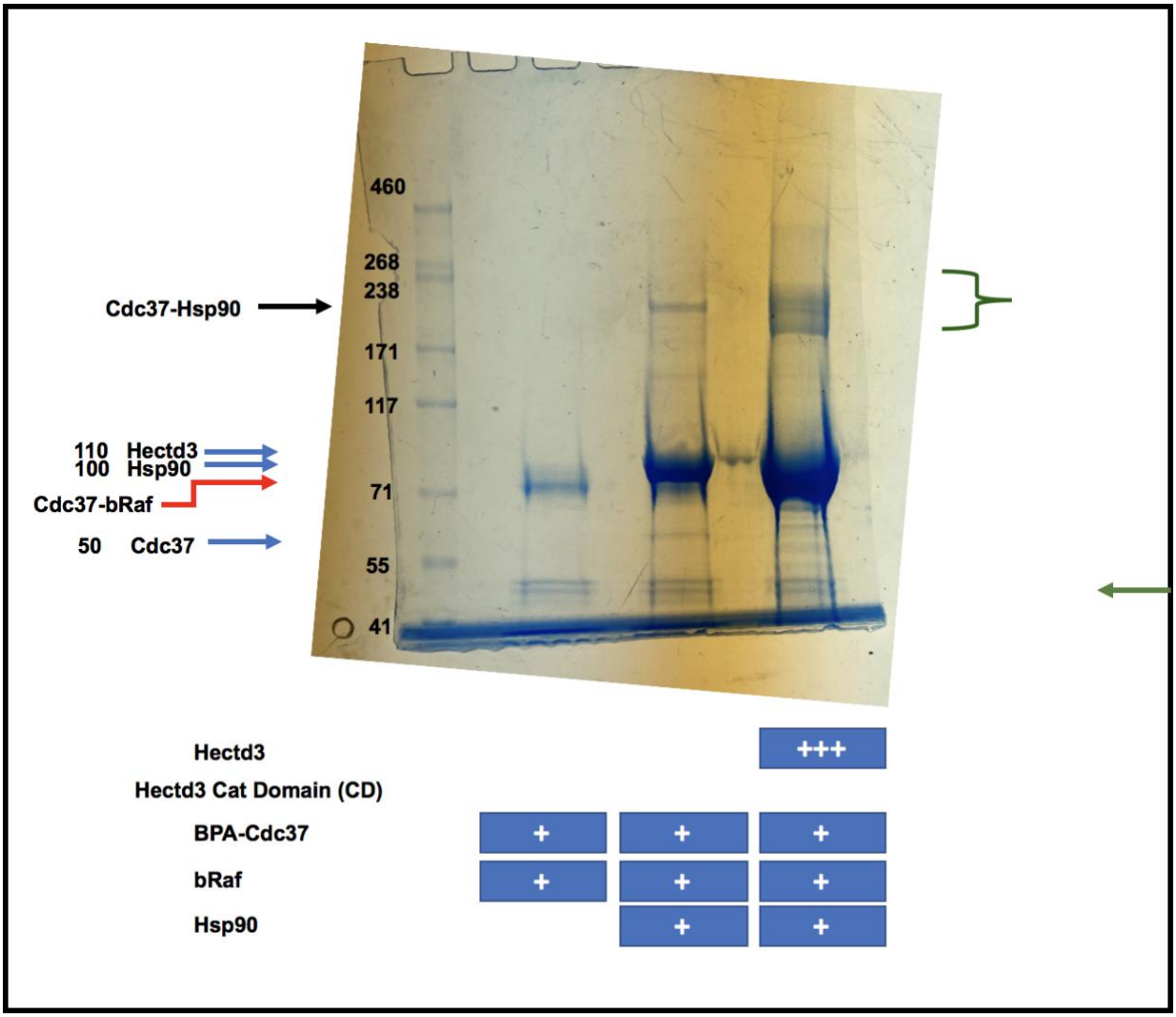

Figure 61 Broad banding of Hectd3 crosslinks and crosslinks to Hsp90

Coomassie stained SDS-PAGE gel of Cdc37 pBPA complex crosslinking. 10μM Cdc37 pBPA mutants are incubated for 1 hour at 28C before being crosslinked at 4C for 1 hour. 4μM phosphorylated Cdc37 pBPA mutants are incubated with 4μM Hsp90, 4μM sbRaf and 4μM Hectd3 at 28 C for 1 hour before closing at 4C for 1 hour.

Concluding Remarks

Biochemistry shows that Hectd3 transiently interacts with a Hsp90:Cdc37:Raf1 complex.. The interactions are too weak and transient to survive an analytical column and a pulldown assay is the only way to create a stoichiometric 4 component complex. Surprisingly there is not much difference between pull down efficiency when comparing 3 Raf constructs of differing length. From our structural work we were able to determine that Hsp90:Cdc37:Raf complexes purified in the absence of molybdate adopt a “closed” ADP state of Hsp90. This is a post hydrolysis state before opening. This Raf complex is very similar to previously solved structures. Hsp90 splits both kinase lobes with the disordered N-terminus of the kinase domain being threaded through the Hsp90 lumen and being stabilized on the other side by the middle domain of Cdc37. This N-terminus is extremely dynamic and further focused classification was unsuccessful in allowing the visualization of additional portions of the kinase N-lobe or any of the recognition domains of the kinase. Hectd3 does not survive the vitrification process. Glutaraldehyde crosslinking after pulldown allows us to visualize additional density. Hectd3 stabilizes Cdcc37’s C terminal platform. This C-terminal portion of Cdc37 has been identified in NMR experiments as important for kinase stabilization during loading as well as docking site for tyrosine kinases that facilitates phosphorylation of Hsp90 on Y197, which results in the dissociation of Cdc37. Here we propose that this C terminal platform could serve as a docking site for Heectd3. Our in vitro ubiquitination experiments show that Hectd3 has the ability to mono ubiquitinate the kinase domain of Raf1 at multiple sites. This ubiquitination only occurs when Hsp90 opens, a molybdate closed Hsp90 does not open and does not allow the ubiquitination of Raf1. When Hsp90:Cdc37:Raf1 complex

is incubated at higher temperatures, which would allow further opening of Hsp90, Hectd3 mono ubiquitinated Raf a several lysine positions. It is possible that Hectd3 mono ubiquitination of Raf1 kinase domain is the initial step that biases Raf toward further ubiquitination.

Works Cited

1. Baker, D. & Agard, D. A. Kinetics versus Thermodynamics in Protein Folding. *Biochemistry* **33**, 7505–7509 (1994).
2. Verma, K., Verma, M., Chaphalkar, A. & Chakraborty, K. Recent advances in understanding the role of proteostasis. *Fac. Rev.* **10**, 72 (2021).
3. Damgaard, R. B. The ubiquitin system: from cell signalling to disease biology and new therapeutic opportunities. *Cell Death Differ.* **28**, 423–426 (2021).
4. Taipale, M., Jarosz, D. F. & Lindquist, S. HSP90 at the hub of protein homeostasis: emerging mechanistic insights. *Nat. Rev. Mol. Cell Biol.* **11**, 515–528 (2010).
5. Biebl, M. M. & Buchner, J. p23 and Aha1: Distinct Functions Promote Client Maturation. in *The Networking of Chaperones by Co-Chaperones* (eds Edkins, A. L. & Blatch, G. L.) 159–187 (Springer International Publishing, Cham, 2023). doi:10.1007/978-3-031-14740-1_6.
6. M, T. *et al.* Quantitative analysis of HSP90-client interactions reveals principles of substrate recognition. *Cell* **150**, (2012).
7. Buljan, M. *et al.* Kinase Interaction Network Expands Functional and Disease Roles of Human Kinases. *Mol. Cell* **79**, 504-520.e9 (2020).
8. Keramisanou, D., Vasantha Kumar, M. V., Boose, N., Abzalimov, R. R. & Gelis, I. Assembly mechanism of early Hsp90-Cdc37-kinase complexes. *Sci. Adv.* **8**, eabm9294 (2022).
9. Smith, J. R. *et al.* Restricting direct interaction of CDC37 with HSP90 does not compromise chaperoning of client proteins. *Oncogene* **34**, 15–26 (2015).
10. Shao, J., Prince, T., Hartson, S. D. & Matts, R. L. Phosphorylation of Serine 13 Is Required for the Proper Function of the Hsp90 Co-chaperone, Cdc37 *. *J. Biol. Chem.* **278**, 38117–38120 (2003).
11. Vaughan, C. K. *et al.* Hsp90-Dependent Activation of Protein Kinases Is Regulated by Chaperone-Targeted Dephosphorylation of Cdc37. *Mol. Cell* **31**, 886–895 (2008).

12. Verba, K. A. *et al.* Atomic structure of Hsp90:Cdc37:Cdk4 reveals Hsp90 regulates kinase via dramatic unfolding. *Science* **352**, 1542 (2016).
13. S, G.-A. *et al.* Structure of the RAF1-HSP90-CDC37 complex reveals the basis of RAF1 regulation. *Mol. Cell* **82**, (2022).
14. Finci, L. I. *et al.* Structural dynamics of RAF1-HSP90-CDC37 and HSP90 complexes reveal asymmetric client interactions and key structural elements. *Commun. Biol.* **7**, 260 (2024).
15. Prince, T., Sun, L. & Matts, R. L. Cdk2: A Genuine Protein Kinase Client of Hsp90 and Cdc37. *Biochemistry* **44**, 15287–15295 (2005).
16. Roe, S. M. *et al.* The Mechanism of Hsp90 Regulation by the Protein Kinase-Specific Cochaperone p50cdc37. *Cell* **116**, 87–98 (2004).
17. Roiniotis, J., Masendycz, P., Ho, S. & Scholz, G. M. Domain-Mediated Dimerization of the Hsp90 Cochaperones Harc and Cdc37. *Biochemistry* **44**, 6662–6669 (2005).
18. Scholz, G. M., Cartledge, K. & Hall, N. E. Identification and Characterization of Harc, a Novel Hsp90-associating Relative of Cdc37. *J. Biol. Chem.* **276**, 30971–30979 (2001).
19. Eckl, J. M. & Richter, K. Functions of the Hsp90 chaperone system: lifting client proteins to new heights. *Int. J. Biochem. Mol. Biol.* **4**, 157–165 (2013).
20. Xu, W. *et al.* Dynamic Tyrosine Phosphorylation Modulates Cycling of the HSP90-P50CDC37-AHA1 Chaperone Machine. *Mol. Cell* **47**, 434–443 (2012).
21. Bachman, A. B. *et al.* Phosphorylation induced cochaperone unfolding promotes kinase recruitment and client class-specific Hsp90 phosphorylation. *Nat. Commun.* **9**, 265 (2018).
22. Avruch, J., Zhang, X. & Kyriakis, J. M. Raf meets Ras: completing the framework of a signal transduction pathway. *Trends Biochem. Sci.* **19**, 279–283 (1994).
23. Lavoie, H. & Therrien, M. Regulation of RAF protein kinases in ERK signalling. *Nat. Rev. Mol. Cell Biol.* **16**, 281–298 (2015).
24. Van Aelst, L., Barr, M., Marcus, S., Polverino, A. & Wigler, M. Complex formation between RAS and RAF and other protein kinases. *Proc. Natl. Acad. Sci.* **90**, 6213–6217 (1993).

25. Kyriakis, J. M. & Avruch, J. Mammalian mitogen-activated protein kinase signal transduction pathways activated by stress and inflammation. *Physiol. Rev.* **81**, 807–869 (2001).
26. Stokoe, D., Macdonald, S. G., Cadwallader, K., Symons, M. & Hancock, J. F. Activation of Raf as a Result of Recruitment to the Plasma Membrane. *Science* **264**, 1463–1467 (1994).
27. Mott, H. R. *et al.* The solution structure of the Raf-1 cysteine-rich domain: a novel ras and phospholipid binding site. *Proc. Natl. Acad. Sci.* **93**, 8312–8317 (1996).
28. Tartaglia, M., Gelb, B. D. & Zenker, M. Noonan syndrome and clinically related disorders. *Best Pract. Res. Clin. Endocrinol. Metab.* **25**, 161–179 (2011).
29. Allanson, J. E. *et al.* Cardio-facio-cutaneous syndrome: Does genotype predict phenotype? *Am. J. Med. Genet. C Semin. Med. Genet.* **157**, 129–135 (2011).
30. Roring, M. & Brummer, T. Aberrant B-Raf Signaling in Human Cancer − 10 Years from Bench to Bedside. *Crit. Rev. Oncog.* **17**, (2012).
31. Flaherty, K. T. *et al.* Improved Survival with MEK Inhibition in BRAF-Mutated Melanoma. *N. Engl. J. Med.* **367**, 107–114 (2012).
32. Schulte, T. W., Blagosklonny, M. V., Ingui, C. & Neckers, L. Disruption of the Raf-1-Hsp90 Molecular Complex Results in Destabilization of Raf-1 and Loss of Raf-1-Ras Association (∗). *J. Biol. Chem.* **270**, 24585–24588 (1995).
33. Grammatikakis, N., Lin, J.-H., Grammatikakis, A., Tsichlis, P. N. & Cochran, B. H. p50cdc37 Acting in Concert with Hsp90 Is Required for Raf-1 Function. *Mol. Cell. Biol.* **19**, 1661 (1999).
34. Kondo, Y. *et al.* Cryo-EM structure of a dimeric B-Raf:14-3-3 complex reveals asymmetry in the active sites of B-Raf kinases. *Science* **366**, 109–115 (2019).
35. Park, E. *et al.* Architecture of autoinhibited and active BRAF–MEK1–14-3-3 complexes. *Nature* **575**, 545–550 (2019).
36. Liau, N. P. D. *et al.* Negative regulation of RAF kinase activity by ATP is overcome by 14-3-3-induced dimerization. *Nat. Struct. Mol. Biol.* **27**, 134–141 (2020).

37. Martinez Fiesco, J. A., Durrant, D. E., Morrison, D. K. & Zhang, P. Structural insights into the BRAF monomer-to-dimer transition mediated by RAS binding. *Nat. Commun.* **13**, 486 (2022).
38. Oberoi, J. *et al.* HSP90-CDC37-PP5 forms a structural platform for kinase dephosphorylation. *Nat. Commun.* **13**, 7343 (2022).
39. Jaime-Garza, M. *et al.* Hsp90 provides a platform for kinase dephosphorylation by PP5. *Nat. Commun.* **14**, 2197 (2023).
40. Mitra, S., Ghosh, B., Gayen, N., Roy, J. & Mandal, A. K. Bipartite Role of Heat Shock Protein 90 (Hsp90) Keeps CRAF Kinase Poised for Activation. *J. Biol. Chem.* **291**, 24579 (2016).
41. Li, Z., Zhou, L., Prodromou, C., Savic, V. & Pearl, L. H. HECTD3 Mediates an HSP90-Dependent Degradation Pathway for Protein Kinase Clients. *Cell Rep.* **19**, 2515–2528 (2017).
42. Damgaard, R. B. The ubiquitin system: from cell signalling to disease biology and new therapeutic opportunities. *Cell Death Differ.* **28**, 423–426 (2021).
43. Wang, Y., Argiles-Castillo, D., Kane, E. I., Zhou, A. & Spratt, D. E. HECT E3 ubiquitin ligases – emerging insights into their biological roles and disease relevance. *J. Cell Sci.* **133**, jcs228072 (2020).
44. Carroll, C. W. & Morgan, D. O. The Doc1 subunit is a processivity factor for the anaphase-promoting complex. *Nat. Cell Biol.* **4**, 880–887 (2002).
45. Shah, S. S. & Kumar, S. Adaptors as the regulators of HECT ubiquitin ligases. *Cell Death Differ.* **28**, 455–472 (2021).
46. Yu, J. *et al.* The E3 ubiquitin ligase HECTD3 regulates ubiquitination and degradation of Tara. *Biochem. Biophys. Res. Commun.* **367**, 805–812 (2008).

47. Li, Y. *et al.* The E3 ligase HECTD3 promotes esophageal squamous cell carcinoma (ESCC) growth and cell survival through targeting and inhibiting caspase-9 activation. *Cancer Lett.* **404**, 44–52 (2017).
48. Zhang, L., Kang, L., Bond, W. & Zhang, N. Interaction Between Syntaxin 8 and HECTd3, a HECT Domain Ligase. *Cell. Mol. Neurobiol.* **29**, 115–121 (2008).
49. Li, Y. *et al.* The HECTD3 E3 Ubiquitin Ligase Suppresses Cisplatin-Induced Apoptosis via Stabilizing MALT1. *Neoplasia* **15**, 39-IN15 (2013).
50. Li, Y. *et al.* The HECTD3 E3 ubiquitin ligase facilitates cancer cell survival by promoting K63-linked polyubiquitination of caspase-8. *Cell Death Dis.* **4**, e935 (2013).
51. Li, F. *et al.* HECTD3 mediates TRAF3 polyubiquitination and type I interferon induction during bacterial infection. *J. Clin. Invest.* **128**, 4148–4162.
52. Cho, J. J. *et al.* Hectd3 promotes pathogenic Th17 lineage through Stat3 activation and Malt1 signaling in neuroinflammation. *Nat. Commun.* **10**, 701 (2019).
53. Liu, Z. *et al.* Systematic comparison of 2A peptides for cloning multi-genes in a polycistronic vector. *Sci. Rep.* **7**, 2193 (2017).
54. Gibson, D. G. *et al.* Creation of a bacterial cell controlled by a chemically synthesized genome. *Science* **329**, 52–56 (2010).
55. Asor, R., Loewenthal, D., Wee, R. van, Benesch, J. L. P. & Kukura, P. Mass Photometry. *Annu. Rev. Biophys.* **54**, 379–399 (2025).
56. Zheng, S. Q. *et al.* MotionCor2: anisotropic correction of beam-induced motion for improved cryo-electron microscopy. *Nat. Methods* **14**, 331–332 (2017).
57. Scheres, S. H. W. RELION: Implementation of a Bayesian approach to cryo-EM structure determination. *J. Struct. Biol.* **180**, 519–530 (2012).
58. Sander, B., Xu, W., Eilers, M., Popov, N. & Lorenz, S. A conformational switch regulates the ubiquitin ligase HUWE1. *eLife* **6**, e21036.

59. Noddings, C. M., Wang, R. Y.-R., Johnson, J. L. & Agard, D. A. Structure of Hsp90–p23–GR reveals the Hsp90 client-remodelling mechanism. *Nature* **601**, 465–469 (2022).
60. Hayat, M. A. Glutaraldehyde: Role in electron microscopy. *Micron Microsc. Acta* **17**, 115–135 (1986).
61. Adams, P. D. *et al.* PHENIX: a comprehensive Python-based system for macromolecular structure solution. *Acta Crystallogr. D Biol. Crystallogr.* **66**, 213–221 (2010).
62. Cutforth, T. Mutations in Hsp83 and cdc37 impair signaling by the sevenless receptor tyrosine kinase in Drosophila. *Cell* **77**, 1027–1036 (1994).
63. Panaretou, B. *et al.* ATP binding and hydrolysis are essential to the function of the Hsp90 molecular chaperone in vivo. *EMBO J.* **17**, 4829–4836 (1998).
64. Noble, C. *et al.* CRAF Autophosphorylation of Serine 621 Is Required to Prevent Its Proteasome-Mediated Degradation. *Mol. Cell* **31**, 862–872 (2008).
65. Dhillon, A. S. *et al.* The C-terminus of Raf-1 acts as a 14-3-3-dependent activation switch. *Cell. Signal.* **21**, 1645–1651 (2009).
66. Schneider, C. *et al.* Pharmacologic shifting of a balance between protein refolding and degradation mediated by Hsp90. *Proc. Natl. Acad. Sci. U. S. A.* **93**, 14536–14541 (1996).
67. Krist, D. T. & Statsyuk, A. V. Catalytically Important Residues of E6AP Ubiquitin Ligase Identified Using Acid-Cleavable Photo-Cross-Linkers. *Biochemistry* **54**, 4411–4414 (2015).
68. Zhang, Y. *et al.* Chemical Synthesis of Atomically Tailored SUMO E2 Conjugating Enzymes for the Formation of Covalently Linked SUMO-E2-E3 Ligase Ternary Complexes. *J. Am. Chem. Soc.* **141**, 14742–14751 (2019).
69. Dou, H. *et al.* Structural basis for autoinhibition and phosphorylation-dependent activation of c-Cbl. *Nat. Struct. Mol. Biol.* **19**, 184–192 (2012).
70. Plechanovová, A., Jaffray, E. G., Tatham, M. H., Naismith, J. H. & Hay, R. T. Structure of a RING E3 ligase and ubiquitin-loaded E2 primed for catalysis. *Nature* **489**, 115–120 (2012).

71. Pruneda, J. N. *et al.* Structure of an E3:E2~Ub Complex Reveals an Allosteric Mechanism Shared among RING/U-box Ligases. *Mol. Cell* **47**, 933–942 (2012).
72. Scott, D. C. *et al.* Structure of a RING E3 Trapped in Action Reveals Ligation Mechanism for the Ubiquitin-like Protein NEDD8. *Cell* **157**, 1671–1684 (2014).
73. Streich, F. C. & Lima, C. D. Structural and Functional Insights to Ubiquitin-Like Protein Conjugation. *Annu. Rev. Biophys.* **43**, 357–379 (2014).
74. Streich, F. C. & Lima, C. D. Capturing a substrate in an activated RING E3/E2-SUMO complex. *Nature* **536**, 304–308 (2016).
75. Mathur, S., Fletcher, A. J., Branigan, E., Hay, R. T. & Virdee, S. Photocrosslinking Activity-Based Probes for Ubiquitin RING E3 Ligases. *Cell Chem. Biol.* **27**, 74-82.e6 (2020).
76. Farrell, I. S., Toroney, R., Hazen, J. L., Mehl, R. A. & Chin, J. W. Photo-cross-linking interacting proteins with a genetically encoded benzophenone. *Nat. Methods* **2**, 377–384 (2005).

Publishing Agreement

It is the policy of the University to encourage open access and broad distribution of all theses, dissertations, and manuscripts. The Graduate Division will facilitate the distribution of UCSF theses, dissertations, and manuscripts to the UCSF Library for open access and distribution. UCSF will make such theses, dissertations, and manuscripts accessible to the public and will take reasonable steps to preserve these works in perpetuity.

I hereby grant the non-exclusive, perpetual right to The Regents of the University of California to reproduce, publicly display, distribute, preserve, and publish copies of my thesis, dissertation, or manuscript in any form or media, now existing or later derived, including access online for teaching, research, and public service purposes.

DocuSigned by:
Carlos Nowotny
9096321F8820499...
Author Signature

9/2/2025
Date